

Electronic Thesis and Dissertation Repository

9-24-2019 10:00 AM

Strategies for the Preparation of Functional Pendant Group Polymer Materials via Click Chemistry

Rajeshwar Vasdev, *The University of Western Ontario*

Supervisor: Workentin, Mark S., *The University of Western Ontario*

Joint Supervisor: Gilroy, Joseph B., *The University of Western Ontario*

A thesis submitted in partial fulfillment of the requirements for the Master of Science degree in Chemistry

© Rajeshwar Vasdev 2019

Follow this and additional works at: <https://ir.lib.uwo.ca/etd>

 Part of the [Organic Chemistry Commons](#)

Recommended Citation

Vasdev, Rajeshwar, "Strategies for the Preparation of Functional Pendant Group Polymer Materials via Click Chemistry" (2019). *Electronic Thesis and Dissertation Repository*. 6578.
<https://ir.lib.uwo.ca/etd/6578>

This Dissertation/Thesis is brought to you for free and open access by Scholarship@Western. It has been accepted for inclusion in Electronic Thesis and Dissertation Repository by an authorized administrator of Scholarship@Western. For more information, please contact wlsadmin@uwo.ca.

Abstract

This thesis describes the development of a polymer via a unique masking-unmasking strategy allowing for physical and chemical modification as desired. Modifiable polymers may lead to improved applications in drug delivery, photo-patterning and emissive materials design. In recent years, these potential traits have motivated the search for efficient protocols for the synthetic modification of polymers. Accordingly, click chemistry, characterized by fast, clean and high yielding reactions represents an effective tool for the modification of polymers. To achieve this goal, an efficient methodology is created to incorporate a highly reactive strained alkyne functional group as a modification site to expand the post polymerization modification of polymers.

A desirable family of functional groups for click chemistry are the highly reactive strained alkynes, which can undergo strain promoted alkyne-azide cycloaddition in the absence of a transition metal catalyst. Although the reactivity of the strained alkyne is desirable, it can be susceptible to side reactivity due to the highly reactive carbon-carbon triple bond. To circumvent this problem, a cyclopropenone masking group, which can undergo a decarbonylation by UV irradiation to afford the strained alkyne, can be employed. The advantage of this unmasking strategy is the fact that only CO gas is evolved, no purification is required, there is spatial and temporal control and due to the high atom economy of the polymer, and every repeating unit of the polymer backbone can be functionalized.

The photochemical decarbonylation which proceeds cleanly and efficiently, liberates the strained alkyne functional group, which can form covalent bonds with azides reactions bearing substituents with specific functionality such as redox-active or emissive properties. Thus, the

liberation of the strained alkyne and the subsequent reaction with a variety of azide reaction partners provides a robust route towards post-polymerization modification of polymers and generating a library of polymers.

This thesis outlines the synthesis and characterization of a masked strained alkyne dibenzocyclooctyne-monomer, its polymerization, polymerization kinetics study and post-polymerization modification of the resulting polymer.

Keywords

Modifiable polymers, redox-active polymers, emissive polymers, click chemistry, strained alkyne, strain-promoted alkyne-azide cycloaddition, reactive carbon-carbon triple bond, polymer synthesis, post-polymerization modification and masking strategy.

Summary for Lay Audience

Materials such as plastic bags and Styrofoam cups are used in our everyday lives. These materials are called polymers, and are made up of small building blocks called monomers and produced via a process known as polymerization. Most bulk polymers are designed for one specific role, which requires the physical and chemical properties to remain constant. Modifiable polymers on the other hand, allow the physical and chemical properties to be altered as desired. The goal of my thesis research was to synthesize a polymer that has the ability to be altered post polymerization. To incorporate functionality such as emissive properties for dyes or redox properties for batteries. The functional group of choice for my project was a strained alkyne, which is a highly reactive group allowing for fast and efficient reactivity. The reactivity of the strained alkyne is desired; however, it can also undergo undesirable side reactions and thus we also incorporated a masking strategy so the strained alkyne will not interfere with the polymerization process and only react when needed. The masked strained alkyne can be unmasked by treatment with UV light limiting the need for purification. Herein, I report a novel monomer, its unique masking-unmasking, polymerization and synthetic modification. The new monomer and polymers were identified using state-of-the-art analytical techniques such as nuclear magnetic resonance, UV-Visible absorption spectroscopy and mass spectrometry.

Co-Authorship Statement

The work discussed in this thesis contains contributions from the author and my supervisors Profs. Mark S. Workentin and Joe B. Gilroy and colleagues Dr Wilson Luo, Jasveer Dhindsa and Micheal Anghel. The contributions of each are described below.

Chapter 1 was written by the author and edited by Profs. Mark S. Workentin and Joe B. Gilroy.

Chapter 2 describes the experimental monomer and polymer syntheses that were completed by the author and Dr. Wilson Luo. Micheal Anghel assisted with the thermal analysis of the polymer samples. The chapter was written by the author and edited by Profs. Mark S. Workentin and Joe B. Gilroy.

Chapter 3 describes the post-polymerization functionalization of the monomer and polymer where all the experimental work and characterization was completed by the author. Jasveer Dhindsa conducted the cyclic voltammetry studies on the monomer and polymer samples. Micheal Anghel assisted with the thermal analysis of the polymer samples. The chapter was written by the author and edited by Profs. Mark S. Workentin and Joe B. Gilroy.

Chapter 4 was written by the author and edited by Profs. Mark S. Workentin and Joe B. Gilroy.

Acknowledgments

First and foremost, I would like to thank Prof. Mark S. Workentin for his constant support and mentorship; thank you for giving me the opportunity to work in your lab and for pushing me to do my best. I would also like to thank Prof. Joe B. Gilroy for his support and mentorship as well. I know I have an unorthodox way of doing things, but I want to thank you for having the patience of putting up with me. I can say that I've become a better chemist and a better man with your guidance. From the bottom of my heart, thank you both for everything, I will never forget what you guys have done for me.

I would also like to thank my lab mates for always being there for me and being the funniest bunch to work with. More specifically, I would like to thank Dr. Wilson Luo/Wong for not only helping me in the lab but for looking out for me and giving great life advice during our "TLC" talks. I would also like to thank Samantha, Praveen, Alex, Kyle, Jun, Petrozza, Andy, Daniella, Ryan, Francis, Frank and Michael for their help and support. Last but not least, thank you to our lab volunteers Komal and Grace for helping out in the lab.

The Department of Chemistry was essential to complete my degree. I want to thank Dr. Matt Willans for advice and assistance with NMR spectroscopy, Master Aneta Borecki for running my GPC samples, Doug Hairsine for running my mass spectroscopy experiments. I would also like to thank the administrative staff and the ChemBio stores staff.

Finally, I would like to thank my friends and family for their constant support. Firstly, I would like to thank my mother; Anita, for all the sacrifices she made and trying her best to make sure I had everything I needed. It's time for you take a break and relax, it's my turn to make sure *you're good*. I want to thank my uncle; Raman, I will never forget everything that you've done

for me, I love you. My aunt; Preeti, you are one of the kindest souls and I can always talk to you about anything. My cousins Armaan and Ishaan who are always there to make me laugh. Lastly, I'd like to thank my good friend Sarb for always motivating me to do great things and playing NHL as an excuse to have deep life talks. I love you all.

Table of Contents

Abstract	ii
Summary for Lay Audience	iv
Co-Authorship Statement.....	v
Acknowledgments.....	vi
Table of Contents	viii
List of Tables	x
List of Figures	xi
List of Schemes.....	xiv
List of Appendices	xvii
List of Abbreviations	xviii
Chapter 1	1
1 Introduction	1
1.1 Polymers: A Brief Introduction	1
1.2 Synthetic Routes for Polymers.....	4
1.3 Click Chemistry used in Polymer Functionalization	16
1.4 Polymer Characterization.....	23
1.5 Scope of Thesis	25
1.6 References.....	28
Chapter 2.....	33
2 Synthesis of a Masked Strained Alkyne Polymer	33
2.1 Introduction.....	33
2.2 Results and Discussion	35
2.2.1 Synthesis and characterization of the photoDIBO-monomer	35
2.2.2 Polymerization strategy for the photoDIBO-monomer 2.13	38

2.2.3	Kinetic study of the photoDIBO-polymer 2.14	43
2.3	Conclusion	48
2.4	References	53
3	Polymer Post-Polymerization Functionalization	54
3.1	Introduction.....	54
3.2	Photo-unmasking and SPAAC reaction involving the photoDIBO-monomer 2.13 and photoDIBO-polymer 2.14	56
3.2.1	Photo-unmasking and SPAAC with benzyl azide as a model reaction	56
3.2.2	SPAAC with azidomethyl pyrene and fluorescence study	62
3.2.3	SPAAC with azidomethyl ferrocene and Cyclic Voltammetry study	68
3.3	Conclusion	73
3.4	Experimental	74
3.5	References	81
Chapter 4	83
4	Conclusions and Future Work.....	83
4.1	Conclusions.....	83
4.2	Future Work	88
4.3	References.....	90
Appendices	91
Appendix A1	– Permission to Reuse Copyright Material.....	91
Appendix A2	– Supporting Information for Chapter 2.....	93
Appendix A3	– Supporting Information for Chapter 3.....	100
Curriculum Vitae	124

List of Tables

Table 2-1. Summary of GPC analysis for aliquots of photoDIBO-polymers 2.14 conducted at room temperature and using 1 mol % of 3-bromopyridine of Grubbs III.	44
---	----

List of Figures

Figure 1.1. General figure of monomer, oligomer and polymer.....	1
Figure 1.2. High packing efficiency of low degree branching of polyethylene chains (A). The low packing efficiency of highly branched polyethylene (B).....	3
Figure 1.3. Relationship between molecular weight and monomer conversion for "living" chain growth and step growth.	6
Figure 1.4. Examples of ruthenium- and molybdenum-based catalysts used for ROMP.....	15
Figure 1.5. Cyclic six-membered ring formed highlighted in the black box as result of a side reaction formed in thiol-ene addition modification of poly(1,2-butadiene).	17
Figure 2.1. Comparison of the ^1H NMR spectra of compounds 2.9 , 2.12 and 2.13 . The coloured dots represent aromatic protons and the box indicates the alkene protons.	38
Figure 2.2. Comparison of the ^1H NMR spectra of the monomer 2.13 (blue) and 1 h polymer 2.14 (orange) aliquot showing shift of alkene peaks to the backbone of the polymer 2.14 . ..	40
Figure 2.3. TGA plot (A) and DSC plot (B) of polymer 2.14	41
Figure 2.4. ^1H NMR spectra of the photoDIBO-monomer 2.13 and photoDIBO-polymer 2.14	42
Figure 2.5. IR spectra of the photoDIBO-monomer 2.13 and photoDIBO-polymer 2.14	43
Figure 2.6. GPC traces for aliquots of photoDIBO-polymer 2.14 at various aliquot times from 1-8 h.	44
Figure 2.7. Semi-logarithmic plot of initial monomer concentration vs monomer concentration over time.....	46
Figure 2.8. Kinetic study of the molecular weight vs conversion percent for polymer 2.14 where the plotted data represents different aliquot intervals (A). Kinetic study of feed molar ratio vs degree of polymerization of polymer 2.14 (B).	47

Figure 3.1. UV-Vis Spectra for the photoDIBO-monomer **2.13** (blue), DIBO-monomer **3.1** (green) and benzyltriazole-monomer **3.2** (purple) to highlight unmasking and SPAAC. 57

Figure 3.2. ¹H NMR spectra for the photoDIBO-monomer **2.13** (A), DIBO-monomer **3.1** (B) and benzyltriazole-monomer **3.2** (C) to highlight unmasking and SPAAC. The black box represents the addition of phenyl peaks from the benzyl azide and DIBO-monomer **3.5**. The red box indicates the benzylic CH₂ peaks from the benzyltriazole-monomer **3.2**..... 58

Figure 3.3. UV-Vis (A) spectra of the photoDIBO-polymer **2.13** (orange), DIBO-polymer **3.5** (blue) and BzN₃ yielding the benzyltriazole-clicked-polymer **3.6** (light purple) to highlight unmasking and SPAAC. ¹H NMR spectra (B) for the DIBO-polymer **3.5** (blue) and benzyltriazole-clicked-polymer **3.6** (light purple). GPC traces (C) of the photoDIBO-polymer **2.13** (orange) with benzyltriazole-clicked-polymer **3.6** (light purple). 61

Figure 3.4. UV-Vis spectra (A) and ¹H NMR spectra (B) for the DIBO-monomer **3.1** (green) and pyrene-clicked-monomer **3.7** (light brown) to highlight SPAAC. The black and red boxes are discussed in the text. 63

Figure 3.5. UV-Vis spectra (A) of the DIBO-polymer **3.5** (blue) and pyrene-clicked-polymer **3.8** (light brown) to highlight the click reaction with azidomethyl pyrene. ¹H NMR spectra (B) for the DIBO-polymer **3.5** (blue) and pyrene-clicked-polymer **3.8** (light brown). GPC traces (C) of the photoDIBO-polymer **2.14** (orange) and pyrene-clicked-polymer **3.7** (light brown). 65

Figure 3.6. UV-Vis absorption spectra (solid line) and emission spectra (dashed line) of the pyrene-clicked-monomer **3.7** (A) and pyrene-clicked-polymer **3.8** (B), recorded in degassed CH₂Cl₂ at a concentration of 10⁻⁶ M. 67

Figure 3.7. UV-Vis spectra (A) and ¹H NMR spectra (B) for the DIBO-monomer **3.1** (green) and the ferrocene-clicked-monomer **3.9** (light blue) to highlight SPAAC. The inset is a zoom in of the ferrocene-clicked-monomer **3.9** (light blue) at a higher concentration of 7.00E-4 M representing the d → d transition of Ferrocene. 69

Figure 3.8. UV-Vis spectra (A) of the DIBO-polymer **3.5** (blue), ferrocene-clicked-polymer **3.10** (turquoise) to highlight deprotection and SPAAC. The inset is a zoom in of the

ferrocene-clicked-polymer **3.10** (light blue) representing the d → d transition of Ferrocene. ¹H NMR spectra (**B**) of the DIBO-polymer **3.5** (blue) and ferrocene-clicked-polymer **3.10** (turquoise). GPC traces (**C**) of the photoDIBO-polymer **2.13** (orange) and ferrocene-clicked-polymer **3.10** (turquoise)..... 71

Figure 3.9 CVs of compounds **3.9** and **3.10** recorded in dry, degassed CH₂Cl₂ containing ~ 1 mM analyte and 0.1 M [*n*Bu₄N][PF₆] as a supporting electrolyte at a scan rate of 250 mV/s. The arrows indicate the scan direction. 73

List of Schemes

Scheme 1.1. General scheme for polymerization of polyethylene.....	3
Scheme 1.2. General Scheme for synthesis of nylon-6,6 where the box highlights the intermediate salt.....	6
Scheme 1.3. General Sonogashira coupling mechanism pathway.....	7
Scheme 1.4. General scheme of inter- and intramolecular chain transfer in FRP.....	10
Scheme 1.5. The two main equilibrium steps during the propagation step of RAFT, the growing polymer chains, P_n and P_m , showing how the "dormant species" circumvents side reactivity.....	11
Scheme 1.6. Propagation of ATRP mediated by dormant species.....	12
Scheme 1.7. General reaction mechanism for anionic polymerization.....	13
Scheme 1.8. General reaction mechanism for cationic polymerization.....	13
Scheme 1.9. General scheme for initiation by a Ziegler-Natta Catalyst.....	14
Scheme 1.10. General reaction scheme of ROMP including initiation and propagation.....	16
Scheme 1.11. General reaction scheme for the thiol-ene addition.....	17
Scheme 1.12. Scheme for PMMA-maleimide and PS-anthracene polymers and their block copolymers by a Diels-Alder cycloaddition.....	18
Scheme 1.13. Scheme for PVA-azide and PS-acetylene polymers and their block copolymers by CuAAC.....	19
Scheme 1.14. SPAAC with substituted cyclooctynes.....	20
Scheme 1.15. Preparation of PEG brushes via solvent-free, catalyst free click reaction. Image reproduced with permission from Ref. 80.....	21

Scheme 1.16. Schematic illustration of "click" coupling between appropriately functionalized "inner" and "outer" dendrons to produce a high-generation dendrimer. Image partially reproduced with permission from Ref. 82.	22
Scheme 1.17. Dicobalt-hexacarbonyl protection-deprotection strategy for a cyclooctyne....	22
Scheme 1.18. Adronov and co-workers scheme for step growth synthesis of a strained alkyne polymer. ⁸⁷	26
Scheme 1.19. General cartoon scheme showing polymerization with a masked monomer and post-polymerization modification (A). General scheme showing polymerization with masked monomer and post-polymerization modification with a click partner (B).	27
Scheme 2.1. General cartoon scheme showing polymerization with masked monomer and post polymerization modification (A). General scheme showing polymerization with the masked monomer (B).....	34
Scheme 2.2. General scheme for the synthesis of the photoDIBO-monomer 2.13	36
Scheme 2.3. Reaction scheme for ROMP of monomer 2.13	40
Scheme 2.4. General cartoon scheme showing polymerization with masked monomer in the orange box and post-polymerization modification in the blue box which is discussed in chapter 3.....	48
Scheme 3.1. General cartoon scheme showing polymerization with masked monomer and post-polymerization modification (A). General scheme for the different click partners with DIBO-polymer 3.5 to highlight PPM introduction of different functionalities (B).....	55
Scheme 3.2. Photo-unmasking of the photoDIBO-monomer 2.13 (blue) and SPAAC reaction between DIBO-monomer 3.1 (green) and BzN ₃ yielding benzyltriazole-monomer 3.2 (purple).....	57
Scheme 3.3. Photo-unmasking of the photoDIBO-polymer 2.14 (orange) and SPAAC reaction between DIBO-polymer 3.5 (blue) and BzN ₃ yielding benzyltriazole-DIBO-polymer 3.6 (light purple).	61

Scheme 3.4. SPAAC reaction between DIBO-monomer 3.1 (green) and azidomethyl pyrene yielding the pyrene-clicked-monomer 3.7 (light brown).....	63
Scheme 3.5. SPAAC reaction between DIBO-polymer 3.5 (blue) and azidomethyl pyrene yielding the pyrene-clicked-polymer 3.8 (dark brown).	65
Scheme 3.6. SPAAC reaction between DIBO-monomer 3.1 (green) and azidomethyl ferrocene yielding the ferrocene-clicked-monomer 3.9 (light blue).	69
Scheme 3.7 SPAAC reaction between the DIBO-polymer 3.5 (blue) and azidomethyl ferrocene yielding ferrocene-clicked-polymer 3.10 (turquoise).	71
Scheme 4.1. General scheme of monomer 2.13 synthesis and ROMP.	85
Scheme 4.2. General scheme for the different click partners with DIBO-polymer 3.5 to highlight PPM introduction of different functionalities.....	87
Scheme 4.3. General scheme for a biological polymer. The grey polymer represents polymer 3.5 and the green partner represents a biological azide to perform SPAAC (A). Scheme for polymer 3.5 undergoing SPAAC to generate biological polymers and a phenylalanine azide derivative 4.1 and biotin azide 4.2 (B).....	88
Scheme 4.4. General scheme for a ‘grafting to’ polymer. The grey polymer represents polymer 3.5 and the pink polymer represents an azide or nitron end functionalized polystyrene chain to perform SPAAC or SPANC, respectively (A). Scheme for polymer 3.5 undergoing SPAAC and SPANC to generate graft polymers with polystyrene (B).....	89

List of Appendices

Appendix A1 – Permission to Reuse Copyright Material.....	91
Appendix A2 – Supporting Information for Chapter 2.....	94
Appendix A3 – Supporting Information for Chapter 3.....	101

List of Abbreviations

°C	Degree Celsius
¹³ C	Carbon-13
¹ H	Proton
ATR	Attenuated total reflectance
BCN	Bicyclononyne
BnN ₃	Benzyl azide
BUNA	Butadiene styrene copolymer
cm ⁻¹	Wavenumber
CuAAC	Copper (I)-assisted alkyne-azide cycloaddition
CV	Cyclic Voltammetry
DIBO	Dibenzocyclooctyne
DSC	Differential scanning calorimetry
EI	Electron impact ionization
ESI-HRMS	Electrospray ionization-high resolution mass spectrometry
ESI-LRMS	Electrospray ionization-low resolution mass spectrometry
Eq.	Equivalence
GPC	Gel permeation chromatography
h	hours
HDPE	High density polyethylene
<i>hν</i>	Light

Hz	Hertz
IR	Infrared
L	Liter
min	minutes
mL	Milliliter
mol	Mole
NHS	<i>n</i> -Hydroxysuccinimide
nm	Nanometer
NMR	Nuclear magnetic resonance
Ph	Phenyl
PPM	Post-polymerization modification
ppm	Parts per million
TGA	Thermogravimetric analysis
UV	Ultraviolet
V	Volts
λ_{\max}	Wavelength of maximum absorption
μM	micromolar
δ	Chemical shift

Chapter 1

1 Introduction

1.1 Polymers: A Brief Introduction

Polymers are ubiquitous materials that have been studied for decades because of the unique physical and chemical properties that arise once atoms are arranged into long chains. Historically, it was thought that polymers were small molecules bound together by enigmatic secondary forces, and it was not until the 1920s when Hermann Staudinger established the term ‘macromolecule’ and provided a clear understanding of polymerization.¹ Staudinger’s theory was not widely accepted until Wallace Carothers from Dupont synthesized polymers with high commercial importance such as neoprene rubber and nylon, demonstrating the relationship between their structure and physiochemical properties.² In that respect, polymers are defined as macromolecules, composed of repeating units called monomers. Several monomers are bound together, in most cases via a covalent bond, to form an oligomer which is a short chain. As more monomer is added a polymer is formed (Figure 1.1).³

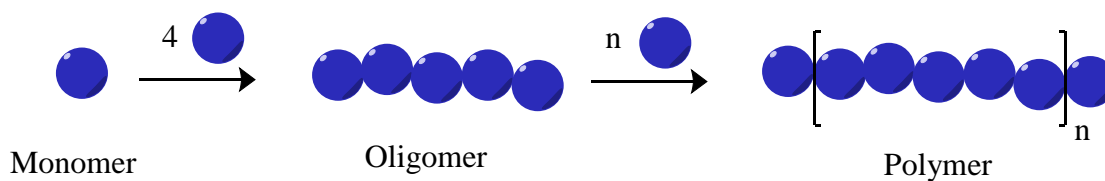
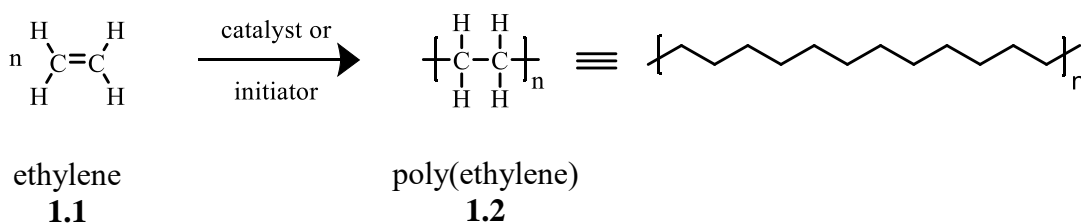


Figure 1.1. General figure of monomer, oligomer and polymer.

Oligomers do not interact with themselves or other short chains, which gives discrete physical properties such as well-defined melting and boiling points. Once enough monomers are joined to form a long chain, a phenomenon called chain entanglement⁴ occurs which leads to broad melting and boiling points, drastically different from the respective monomer and oligomers.

In general, most commercial polymers have an organic makeup consisting of carbon-carbon and carbon-hydrogen covalent linkages. Other common elements involved in organic synthetic polymers are oxygen,⁵ nitrogen,⁶ fluorine,⁷ phosphorus,⁸ and sulfur.⁹ Despite the primary covalent interactions of the polymer backbone and functional groups, the integrity of a polymer also relies on the secondary intermolecular forces present. These secondary intermolecular forces¹⁰ include: dipole-dipole interactions (between opposite ends of polar bonds), London dispersion forces (which are the interaction of electron clouds of individual atoms within the polymer) and hydrogen bonding (which is an electrostatic force of attraction between a hydrogen atom on one molecule with an electronegative atom on another molecule. An example where London dispersion forces plays a significant role in polymer properties is in an important, versatile and possibly the simplest polymer; polyethylene. Polyethylene is composed of ethylene repeating units shown in Scheme 1.1. Ethylene itself is a gas that is colourless, but once incorporated into a long chain is a solid versatile material. The reason for polyethylene's versatility arises from the way the polymer can be packed. In one instance, long linear chains of polyethylene with a low degree of branching (HDPE) facilitates high packing efficiency with strong intermolecular interaction (Figure 1.2A). Allowing it to be used as strenuous materials such as plumbing¹¹ and prosthetics.¹² In another instance, polyethylene can form highly branched polymers

which in turn have weaker intermolecular interactions present and thus a lower packing efficiency (LDPE) shown in Figure 1.2B. Thus LDPE is used as a less strenuous material such as plastic bags and food containers.¹³



Scheme 1.1. General scheme for polymerization of polyethylene.

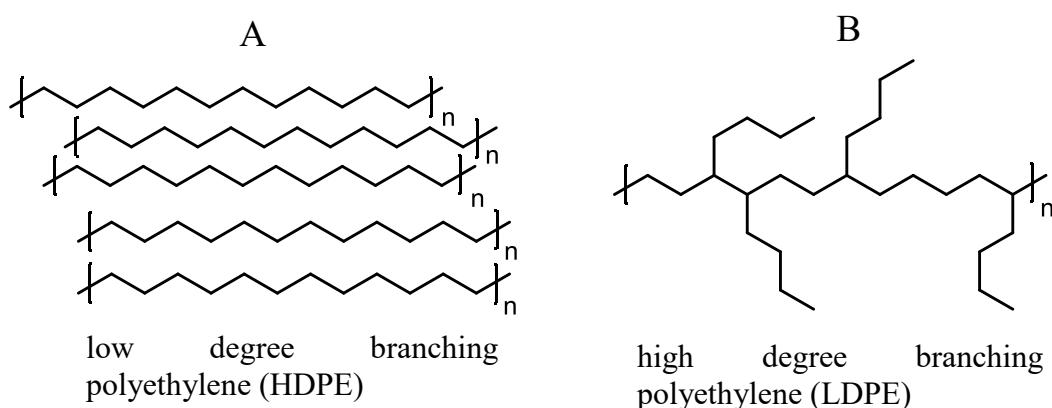


Figure 1.2. High packing efficiency of low degree branching of polyethylene chains (**A**). The low packing efficiency of highly branched polyethylene (**B**).

Alongside synthetic polymers, it is important to note that secondary forces also play a role in natural polymers such as proteins, which are composed of amino acid repeating units. Although the primary forces are covalent linkages between amino acid repeating units, H-bonding positions the protein in a specific orientation for the desired function in cellular processes.¹⁴

The covalent and intermolecular forces that govern the polymer integrity play a vital role in their applications, but when polymers are prepared, they result in a mixture of molecular weights which is governed by statistics¹⁰ and understanding the molecular weight distribution can be crucial for their application. To quantify molecular weight, there are three main parameters evaluated¹⁵:

1. The mean or number average molecular weight (M_n) of the polymer chains. The statistical formula for $M_n = \sum \frac{M_i N_i}{N_i}$, where M_i is the molar mass of the polymer chain and N_i is the number of polymer chains with mass M_i .
2. The weighted average molecular weight (M_w), represented by $M_w = \sum \frac{M_i^2 N_i}{M_i N_i}$, which places a higher weighting average on larger molecular weight species.
3. The dispersity (\mathcal{D}), which is a ratio of M_w/M_n , is used as a measure of the breadth of the molecular weight distribution. A value of $\mathcal{D} = 1$ is achieved for a sample of perfectly monodisperse polymers.

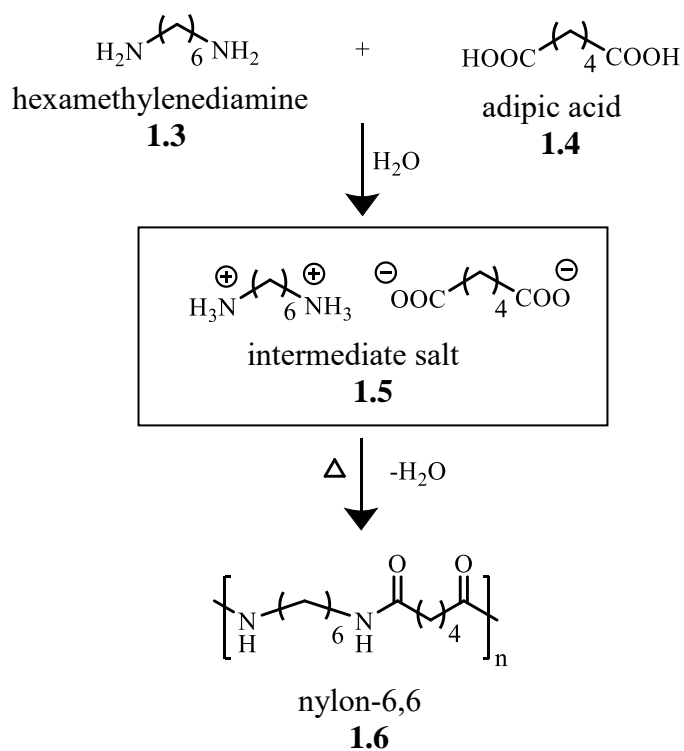
These parameters are crucial to evaluate the molecular weight distribution of a polymer.

The evaluation of these parameters will be discussed further on in the introduction.

1.2 Synthetic Routes for Polymers

Over the past few decades, many polymerization methods have been developed. They generally fall into two main classes of polymerization techniques; step growth¹⁶ or chain growth polymerization.¹⁷ The synthetic routes involved differ by the mechanism by which they proceed and by the reaction kinetics.

Step growth polymerization is defined as the reaction between functional groups on the monomers with the loss of a small molecule such as water, methanol, or hydrochloric acid, as each unit joins to form the chain,¹⁸ but there are a few exceptions where step growth can proceed without the loss of a small molecule when catalysts are employed.¹⁹ There are three main types of step growth monomers: bifunctional monomers are used to form the chain, monofunctional monomers are used to control chain length and trifunctional species are used to give branched or cross-linked polymers.²⁰ In practice, no appreciable high molecular weight polymer is seen until conversion above 95%²¹ shown in Figure 1.3, thus high purity monomers are required for efficient reactions. During the late 1920s, Carothers and coworkers were looking for alternatives to polyester materials because of its low melting point so they delved into reactions between dibasic acids and diamines and came across a high melting point product called nylon-6,6.²² The production of nylon-6,6 involves an important step where the intermediate product **1.5** of hexamethylenediamine and adipic acid is a salt, which is recrystallized to ensure a high-purity intermediate for a high molecular weight product shown in Scheme 1.2. The synthesis of nylon-6,6 proceeds by the removal of water from the system which drives the polymerization forward.



Scheme 1.2. General Scheme for synthesis of nylon-6,6 where the box highlights the intermediate salt.

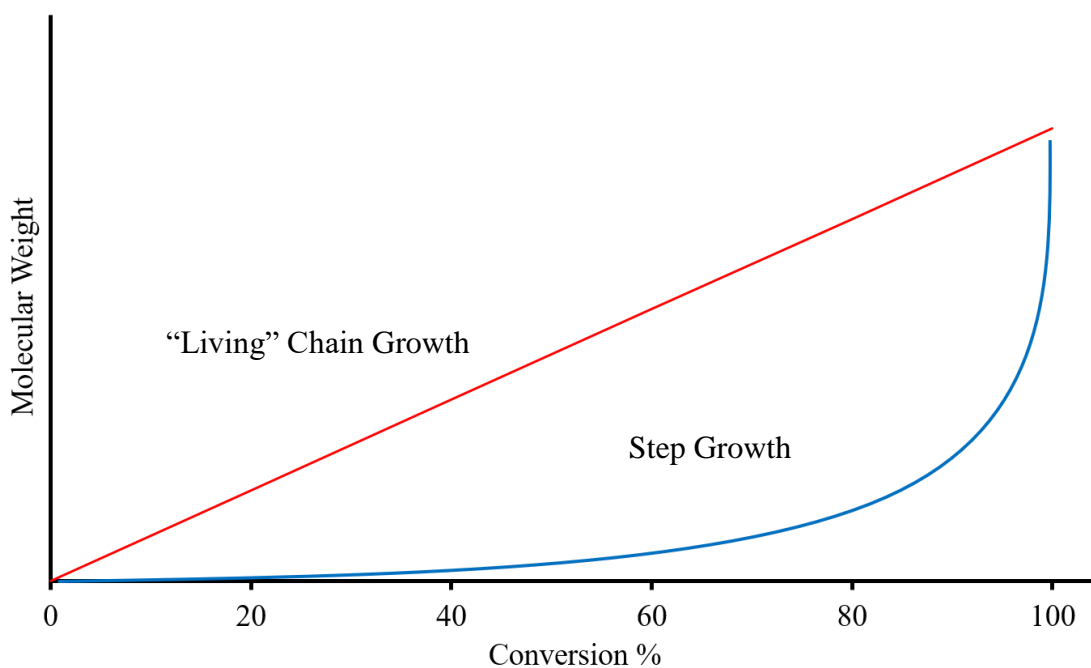
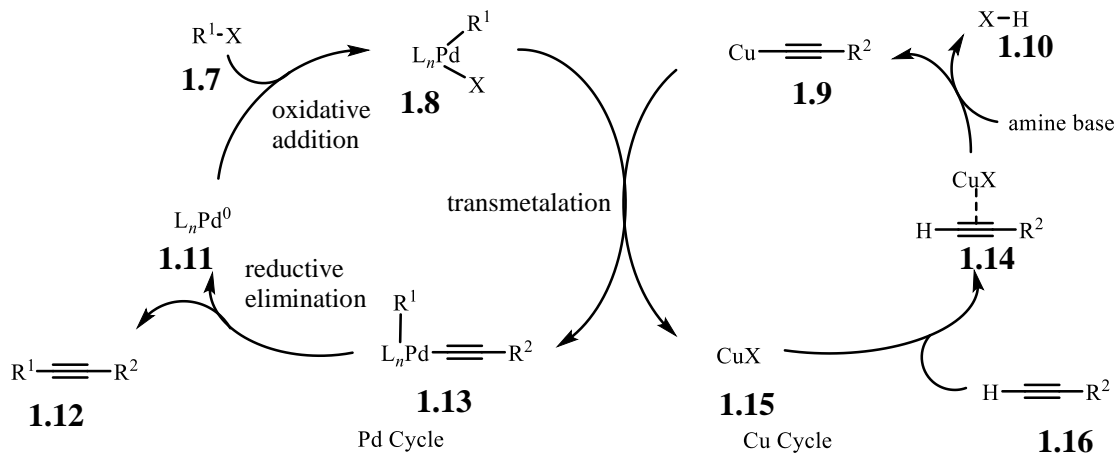


Figure 1.3. Relationship between molecular weight and monomer conversion for "living" chain growth and step growth.

Step growth polymerization can also proceed without the loss of a small molecule via a transition metal catalyzed reactions, and a popular method is through Sonogashira coupling. The Sonogashira coupling method couples a terminal alkyne with an aryl or vinyl halide via palladium catalyst, copper (I) co-catalyst and amine base. The palladium catalyst coordinates with the aryl or vinyl halide and the copper(I) co-catalyst coordinates with the alkyne, which then undergoes a transmetalation reaction to coordinate the terminal alkyne to the palladium catalyst. Finally, the palladium catalyst performs a reductive elimination conjoining the terminal alkyne with the vinyl or aryl group shown in Scheme 1.3.²⁴ In one instance, Kuehne and co-workers synthesized conjugated polymers with bifunctional monomers; 9,9-dioctyl-2,7-diiodofluorene and 1,3-diethylenebenzene.²⁵ The resulting conjugated polymer had accessible acetylene moieties which were functionalized via thiol-yne click chemistry and used as fluorescent probes for imaging of activated endothelial cells.



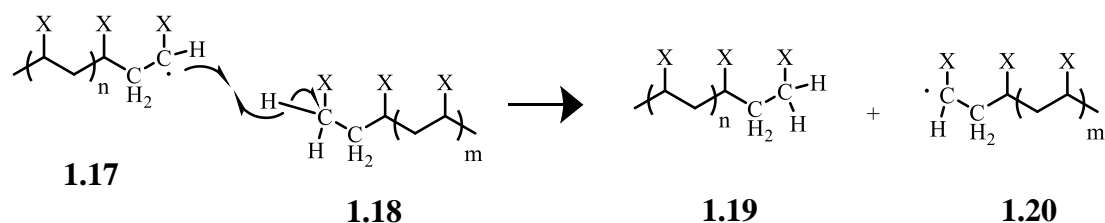
Scheme 1.3. General Sonogashira coupling mechanism pathway.

The second class of synthetic routes for polymers is chain growth polymerization defined as a reaction with a distinct initiation process through an initiator or catalyst, propagation process where growth of the chain is from one end and a termination event from consumption of all the monomer, a terminating agent or simply by cooling the reaction. The “living” chain growth polymerization is a subclass which must adhere to the following criterion:²⁶

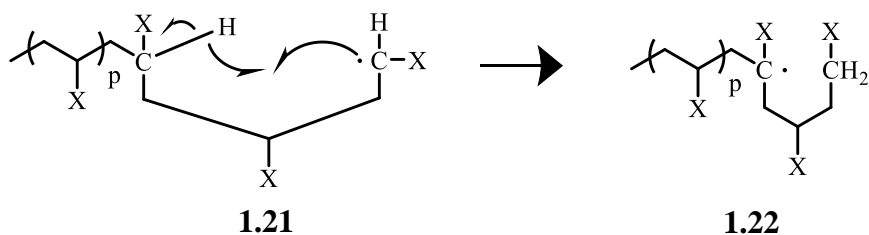
1. The logarithm of initial monomer concentration over monomer concentration vs time is a linear function that obeys first order reactions kinetics.
2. The number average molecular weight can be controlled by stoichiometry
3. Narrow molecular weight distributions if rate of initiation is greater than rate of propagation, limited side reactivity and the rate of de-propagation is lower than the rate of propagation
4. Propagation proceeds until all the monomer is consumed or until intentionally terminated.

In typical cases, free radical polymerization (FRP) is a common type of polymerization used industrially to produce a range of polymers including low density polyethylene (LDPE).²⁷ The FRP technique is not very technically demanding but oxygen must be strictly excluded because it will quench radical species.²⁸ Initiation is done by selecting an initiator, typically, benzoyl peroxide or azoisobutylnitrile (AIBN) and converting it into a radical species by a thermal or photolytic route. Propagation occurs when the radical initiator reacts with the unsaturated monomer such as styrene, ethylene, *tert*-butyl-methacrylate etc. It should be noted that, formation of the highly substituted radical is favoured in each step, introducing regiospecificity. During propagation, chain transfer²⁹ is

a problem because it introduces structural irregularities which result in the formation of polydispersed samples. Chain transfer can occur intermolecularly, where the propagating site can transfer the radical to a new chain (halting polymerization on the initial chain and initiating another chain) or intramolecularly by transferring the radical within the chain to introduce branching shown in Scheme 1.4. Finally, the termination of the polymerization is generally achieved by cooling the reaction, but complications also arise during this step. During the cooling stage, chain coupling³⁰ can occur, where two chains can meet at the radical ends and form a bond. Furthermore, disproportionation³¹ can occur where two radical species come into close proximity. The first species can act as an acceptor, abstracting an α hydrogen with the other species acting as a donor, which undergoes an elimination reaction forming a double bond, resulting in two non-radical products. In general, free radical polymerization is not a “living” method because it affords polydisperse products due to the complications of chain transfer, disproportionation and coupling side reactions. To circumvent the challenges of FRP, much effort was put into controlled radical polymerization (CRP) during the 90s.



Intermolecular Chain Transfer

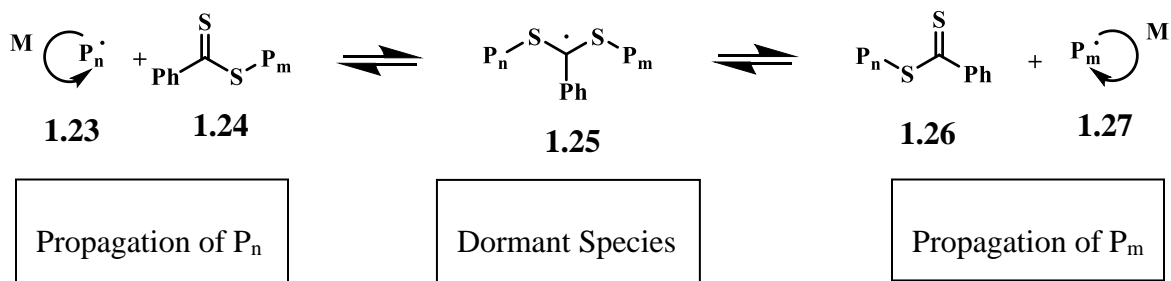


Intramolecular Chain Transfer

Scheme 1.4. General scheme of inter- and intramolecular chain transfer in FRP.

CRP is very similar to FRP, but a mediating agent is introduced to prevent the undesirable side reactions associated with the free radical technique. In 1998, the Commonwealth Scientific and Industrial Research Organization (CSIRO) discovered reversible addition fragmentation chain transfer (RAFT),³² which employs a thiocarbonyl or thioester mediating agent (also known as a RAFT agent) to protect the radical propagating site. The initiation process for RAFT is the same as FRP where an initiator such as AIBN is initiated via a thermal or photolytic route, but a RAFT agent³³ such as 2-phenyl-2-propyl benzodithioate is also present. The RAFT agent works by reacting with the propagating species to form a stable adduct radical (**1.25**) shown in Scheme 1.5 which is the key to preventing undesirable side reactivity. The stable radical then fragments forming a propagating polymer thiocarbonyl complex and a new propagating radical species. The reactions between the propagating radical polymers and polymer-thiocarbonyl species are

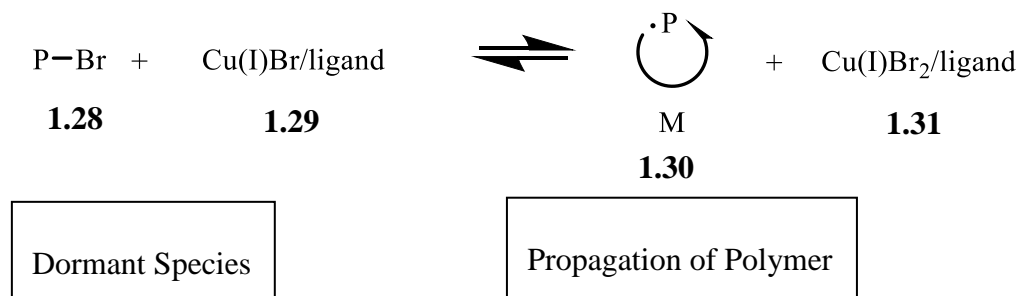
reversible which establishes an equilibrium, so it is important to use an excess of RAFT agent to ensure side reactions do not occur. Finally, termination of the polymer is done by cooling the reaction before the monomer runs out or coupling and disproportionation can occur and typically, polymerization is terminated at 80% conversion.



Scheme 1.5. The two main equilibrium steps during the propagation step of RAFT, the growing polymer chains, P_n and P_m , showing how the "dormant species" circumvents side reactivity.

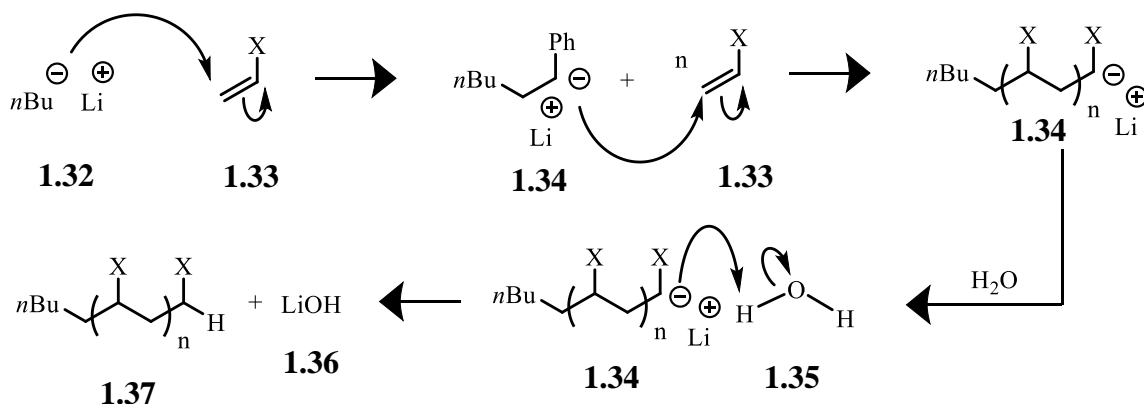
Another "living" radical technique is atom transfer radical polymerization (ATRP)³⁴ which was discovered by Mitsuo Sawamoto and Krzysztof Matyjaszewski in 1995. ATRP is comparable to the RAFT method in the sense that a dormant species is present to prevent any side reactivity. ATRP is a redox reaction that utilizes an alkyl halide initiated by a transition metal complex as the catalyst. The catalyst typically used is a Cu(I)Br with a 2,2-bipyridine ligand (bipy) allowing the catalyst to solubilize in solution. The mechanism for ATRP is a one electron transfer so the copper is oxidized, forming a Cu(II)Br_2 complex and thus generating the alkyl group into a radical species, allowing propagation with the unsaturated monomer of choice. The propagation is mediated by an equilibrium established between the propagating chain and the dormant species (Scheme 1.6) which results in monodisperse polymer chains. Although ATRP is considered a

remarkable “living” technique, it’s use is limited because of the challenge of removing the Cu(I)/Cu(II) species post polymerization.³⁵



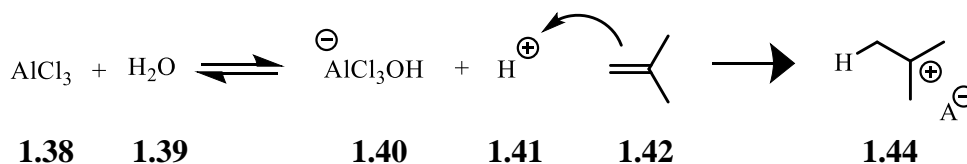
Scheme 1.6. Propagation of ATRP mediated by dormant species.

Radical “living” techniques are used as common practice for polymerization but another “living” technique is anionic polymerization (AP). AP is a great method for molecular weight control, but it is very technically demanding. The anionic species involved are air- and moisture-sensitive, so rigorous purification of monomer, solvent and reagents is required.³⁶ Another caveat of the anionic technique is the incompatibility with acidic and electrophilic functional groups such as alcohols, amines and aldehydes.³⁷ The initiation of AP utilizes reactive, negatively charged molecules such as *n*-butyllithium, potassium *tert*-butoxide and Grignard reagents reacting with an unsaturated monomer shown in Scheme 1.7. The anionic initiators are more reactive if the separation from the counter ion is greater. In some cases, crown ethers are employed³⁸ to increase ion pair separation, thus increasing the reaction rate. Propagation occurs from the chain end with consumption of the monomers and this process is highly exothermic, therefore it must be cooled to limit side reactions. Finally, termination occurs by introducing an acidic species to quench the reaction.



Scheme 1.7. General reaction mechanism for anionic polymerization.

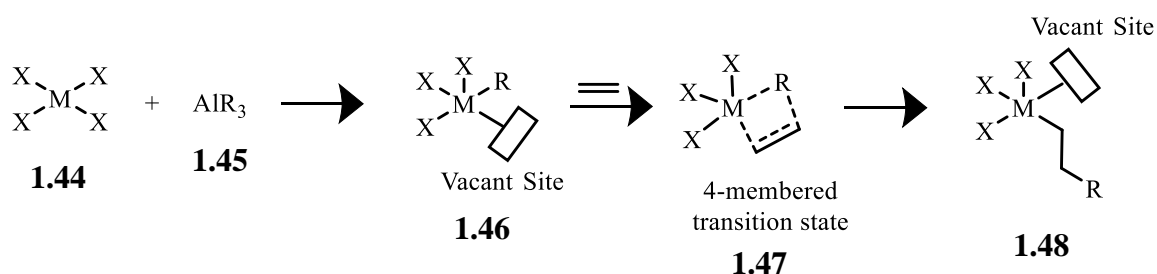
A complementary, less common, technique, cationic polymerization (CP), is also technically demanding and temperature dependent.³⁹ The initiation for CP⁴⁰ requires strong acids such as phosphoric or sulfuric acid or the addition of water to Lewis acids such as aluminum chloride (Scheme 1.8). The counter ion must be non-nucleophilic in nature to avoid side reactivity. Next, the propagation for CP is highly exothermic and must be cooled down. Finally, the termination process is done by bringing the reaction to room temperature.



Scheme 1.8. General reaction mechanism for cationic polymerization.

Transition metal catalyzed polymerization is another technique, which was first developed in the 1950s by Karl Ziegler and Giulio Natta using what are now known as the Ziegler-Natta catalysts (Z-N catalysts).⁴¹ The Z-N catalysts have two main components: an

organometallic complex comprised of an alkyl, aryl or hydrogen compound of aluminum, lithium, magnesium or zinc and a second component comprised of a transition metal co-catalyst, usually a halide or oxyhalide of titanium or vanadium. The mechanism for Ziegler-Natta polymerizations⁴² are not well known but it is thought to react with a Lewis acid to separate the halide from the metal centre opening a vacant coordination site for initiation and propagation of an olefin monomer (Scheme 1.9). Termination proceeds by an active hydrogen donor such as an acid or β -hydride elimination where a β -hydrogen is abstracted from the vacant metal centre. The class of Z-N catalysts have been used to produce plastics, elastomers and rubbers with high stereoselectivity with little to no side branching.⁴¹



Scheme 1.9. General scheme for initiation by a Ziegler-Natta Catalyst.

Alongside the Ziegler-Natta catalysts, other transition metals are also used in ring-opening metathesis polymerization (ROMP).⁴³ ROMP is an excellent “living” technique for the synthesis of unconventional polymers because this method allows for exceptional functional group tolerance with limited side reactivity,⁴⁴ the rate of initiation is greater than the rate of propagation⁴⁵ and the technique provides narrow molecular weight distributions. The ROMP technique uses cyclic monomers such as cyclopentene or norbornene, where the driving force is the relief of ring strain. The cyclic olefin of choice is polymerized using a metal carbene catalyst such as Grubbs I (**1.49**),⁴⁶ Grubbs II (**1.50**),⁴⁷ Grubbs III (**1.51**)⁴⁸

or Schrock catalyst (**1.52**)⁴⁹ which are complexes based on the transition metals molybdenum and ruthenium shown in Figure 1.4. In one instance, Grubbs and coworkers performed ROMP on functionalized low strain/high strain olefins using ruthenium-based catalysts, comparing the utility of the different catalysts under different reaction conditions for optimized molecular weight distributions.⁵⁰ The ruthenium based catalysts are used to synthesize “living” polymers because of their quick initiation⁵¹ and stability in a variety of solvents.⁵² The initiation for ROMP is through disassociation of the tricyclohexylphosphine ligands of GI and GII and pyridine ligands of GIII which opens a vacant sight for the cyclic olefins and propagation is driven by the relief of ring strain shown in Scheme 1.10. Finally, the termination of ROMP is done by adding excess ethyl vinyl ether which fills the vacant site and inactivates the catalyst.

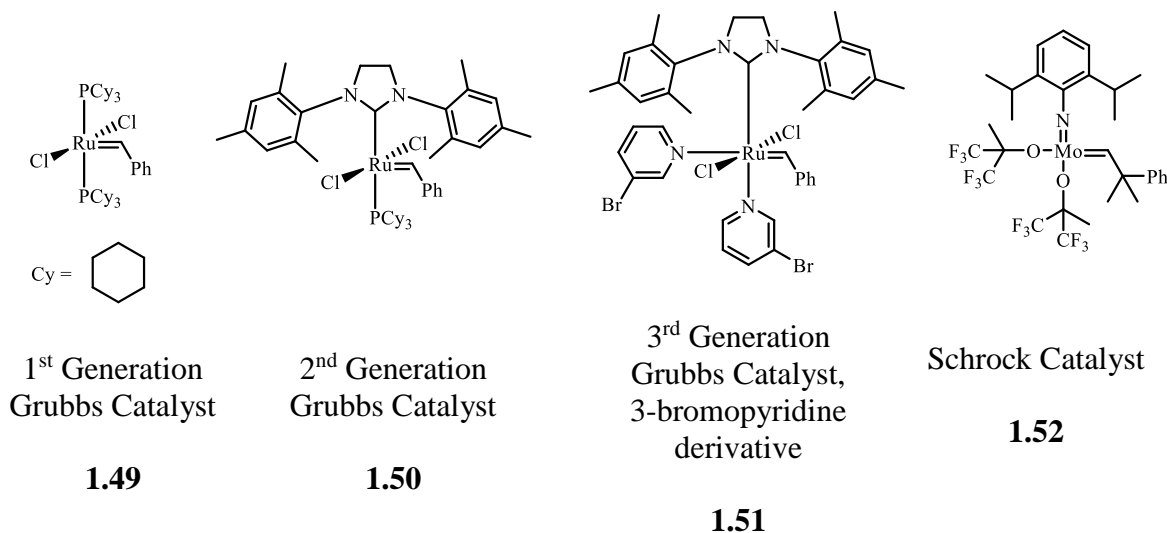
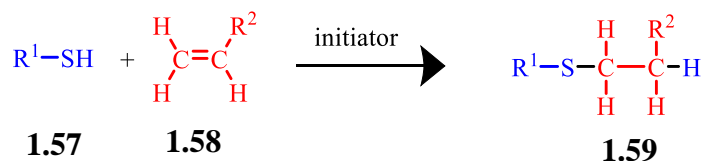


Figure 1.4. Examples of ruthenium- and molybdenum-based catalysts used for ROMP.

The thiol-ene addition is the reaction between a thiol and an alkene, initiated by light, heat or radical to form a thioether (Scheme 1.11).⁵⁸ The use of thiol-ene click chemistry has been used in the past for reaction of BUNA rubbers with aliphatic mercaptans⁵⁹, polymer-polymer conjugation for photopatterning and photolithography⁶⁰ and even as a method for polymerization.⁶¹



Scheme 1.11. General reaction scheme for the thiol-ene addition.

Also, the thiol-ene reaction has been used as a viable method for modifying polymers post-polymerization. The Schlad group synthesized a poly(1,2-butadiene) possessing an alkene on every repeating unit which was reacted with a variety of thiols bearing different R groups.⁶² These R groups included ethers, esters, carboxylic acids and amines to show the thiol-ene functionalization was compatible with acidic and nucleophilic groups. However, not all the thiol groups could be added to all the olefin repeating units because of a side reaction where addition of the thiol would add itself to another double bond in its vicinity, forming a six membered cyclic structure shown in Figure 1.5.

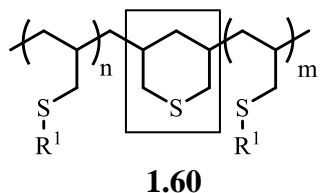
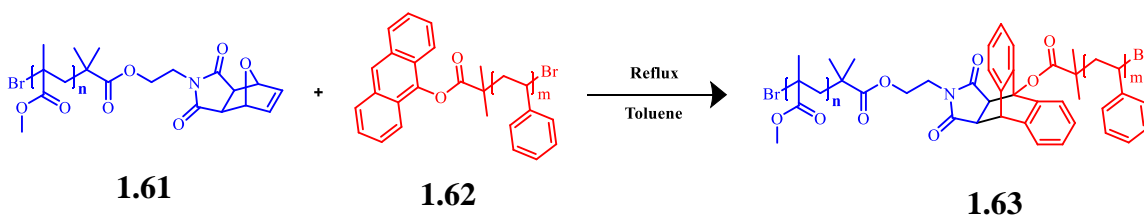


Figure 1.5. Cyclic six-membered ring formed highlighted in the black box as result of a side reaction formed in thiol-ene addition modification of poly(1,2-butadiene).

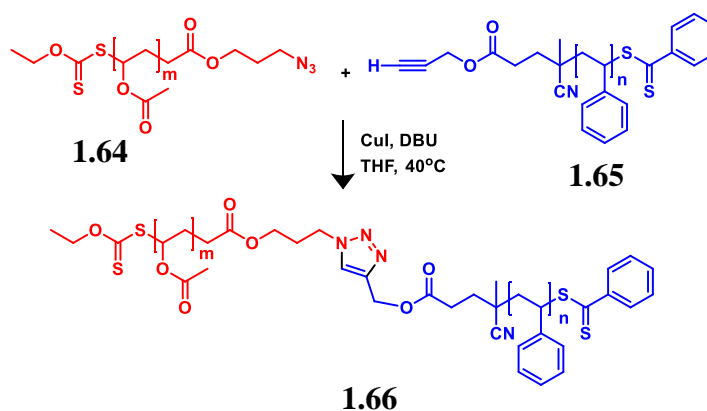
Another popular click reaction is the Diels-Alder cycloaddition, which is the reaction between a conjugated diene and a dienophile in the presence of heat to form a cyclohexene ring.⁶³ The diene or dienophile used usually bear some sort of functionality and the Diels-Alder reaction has been used extensively in organic synthesis⁶⁴ as well as polymer chemistry such as 3D photo fixation lithography,⁶⁵ formation of cross-linked polymers⁶⁶ and as self-healing materials.⁶⁷ The cycloaddition reaction has also been used as a tool for block copolymer synthesis. The Hiral group showed an effective technique for preparation of block copolymers with maleimide-and anthracene-end functionalized polymers (Scheme 1.12).⁶⁸ The group synthesized polystyrene end functionalized with an anthracene group and polyethylene glycol end functionalized with a maleimide group, refluxed in toluene to form to form the block copolymer without further purification and with great dispersity.



Scheme 1.12. Scheme for PMMA-maleimide and PS-anthracene polymers and their block copolymers by a Diels-Alder cycloaddition.

Perhaps the most well-known click reaction is the copper(I) assisted alkyne-azide cycloaddition (CuAAC). The CuAAC reaction produces a 1,2,3-triazole ring from the reaction between a linear alkyne and an azide⁶⁹. The triazole ring acts as a bridge between the two species that have been covalently connected indicated as R₁ and R₂ which bring function to the material. These R groups can include fluorescent probes for imaging, polar groups for solubility or any wide range of functional groups. “CuAAC” is used in a wide

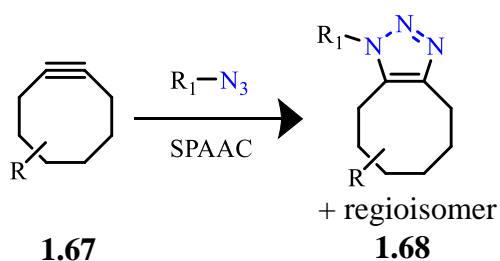
array of applications such as surface modification⁷⁰, micelle modification⁷¹ and block copolymer synthesis.⁷² In one instance, Barner-Kowollik and co-workers used reversible addition fragmentation chain transfer (RAFT) to synthesize polystyrene, end-functionalized with an acetylene functional group, and a polyvinyl acetate polymer, end-functionalized with an azide functional group. The polystyrene and polyvinyl acetate polymers were clicked together using the copper-assisted alkyne-azide cycloaddition method creating a block copolymer (Scheme 1.13).⁷³



Scheme 1.13. Scheme for PVA-azide and PS-acetylene polymers and their block copolymers by CuAAC.

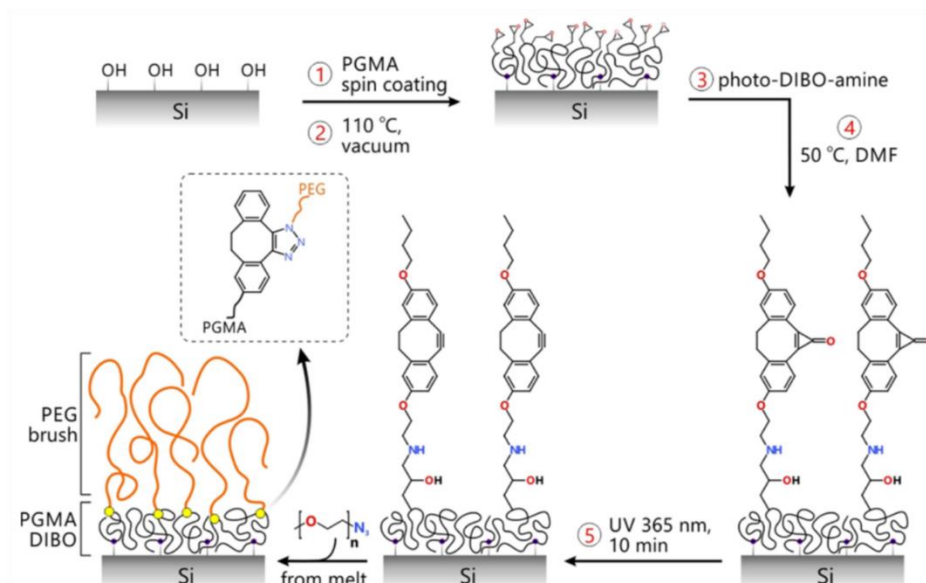
Although CuAAC is the most common click reaction, it does have some drawbacks. The Cu(I) catalyst is thermodynamically unstable and disproportionates to Cu(II) and Cu(0) which has harmful effects in biological applications.⁷⁴ Another drawback is the Cu(I) catalyst produces undesirable side products in organic solvents.⁷⁴ These limitations highlight the importance of exploring alternatives to the Cu(I) catalyzed alkyne-azide cycloaddition.

The strain-promoted alkyne-azide cycloaddition (SPAAC) reaction (Scheme 1.14) fits the criteria for click chemistry by producing compounds in high yields, occurring under mild conditions and producing stereoselective and chemoselective products.⁷⁵ In this case, the Cu(I) catalyst is not required because the reaction makes use of the highly reactive strained alkyne.^{76, 77, 78} The strain comes from the incorporation of the alkyne in a ring system. The SPAAC reaction is a versatile reaction that can be used in micelle labeling, material surface modification⁷⁹ and polymer modification.



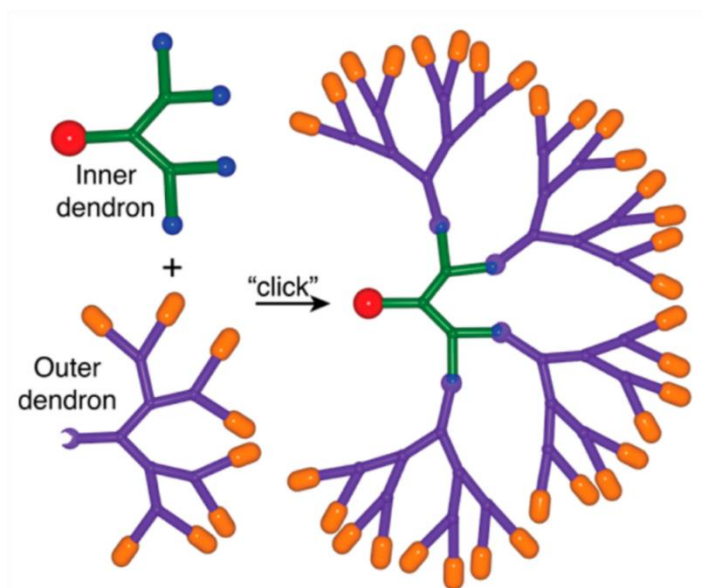
Scheme 1.14. SPAAC with substituted cyclooctynes.

In some cases, polymers can be tethered onto a substrate generating polymer brushes. Minko and co-workers synthesized poly(ethylene glycol) (PEG) polymer brushes on silicon substrates via a solvent-free and catalyst-free SPAAC reaction shown in Scheme 1.15.⁸⁰ They grafted poly(glycidyl methacrylate) onto a silicon substrate end functionalized with cyclopropenone-caged dibenzocyclooctyne-amine (DIBO-amine). Finally, they performed SPAAC with end functionalized azide PEGs and grafted to the DIBO-modified silicon substrates.



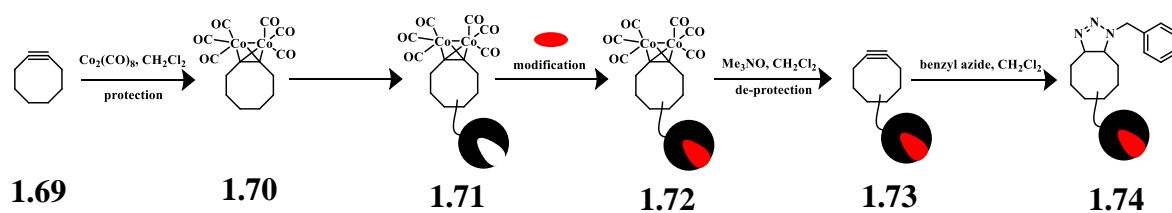
Scheme 1.15. Preparation of PEG brushes via solvent-free, catalyst free click reaction. Image reproduced with permission from Ref. 80.

Polymers are not limited to linear conformations, they also have the ability to take on branching, tree-like structures called dendrimers.⁸¹ In one instance, Adronov and co-workers synthesized a third generation polyester dendron based on the bisMPA monomer structure, having eight peripheral azide functionalities shown in Scheme 1.16.⁸² The “blue spheres” on the inner dendron represented azides, the hook at the end of the outer dendron represented a strained alkyne so they could perform SPAAC to connect the inner and outer dendron. They were able to generate a library of dendrimers by preparing various peripheral groups of the outer dendron including aromatic, aliphatic and polar structures.



Scheme 1.16. Schematic illustration of "click" coupling between appropriately functionalized "inner" and "outer" dendrons to produce a high-generation dendrimer. Image partially reproduced with permission from Ref. 82.

Although the reactivity of the strained alkyne is desired, it is susceptible to side reactivity such as nucleophilic attack leading to undesired side reactions,⁸³ making the development of orthogonal reaction chemistry a difficult challenge. To overcome this problem, a protection-deprotection or masking-unmasking strategy is required. Workentin and co-workers devised a strategy where they used a dicobalt-hexacarbonyl complex to protect bicyclononyne (Scheme 1.17) and performed modifications on the molecule.⁸⁴



Scheme 1.17. Dicobalt-hexacarbonyl protection-deprotection strategy for a cyclooctyne.

Once the modifications were complete they were able to deprotect the BCN with trimethyl amine oxide for further modification.⁸⁴ However, when the dicobalt-hexacarbonyl complex protection strategy was incorporated into polymers there were undesired side products. In another example, Adronov and co-workers incorporated a strained alkyne functional group in a dibenzocyclooctyne-containing conjugated polyimine and performed SPAAC on the resulting polymer.⁸⁵ Remarkably, Adronov and co-workers were able to circumvent the side reactivity of the strained alkyne by using the relatively mild condensation polymerization. However, the reported method lacks general compatibility with living polymerization methods due to the reactivity of the strained alkyne, therefore, there remains the need to investigate alternative pathways towards incorporating strained alkynes into polymers for further modification.

1.4 Polymer Characterization

The spectroscopic and chromatographic analysis of polymers is important because polymerization is a random process governed by statistics, so determining the average molecular weight, molecular weight distribution and atomic makeup is important for its applications. ¹H NMR spectroscopy can be used as a tool for molecular weight determination by comparing the integration values for a signal unique to an end group and a signal unique to the repeating unit of the polymer backbone.⁸⁶ Also, ¹H NMR spectroscopy is not limited to analysis of molecular weight parameters, it is used as a spectroscopic method to determine the atomic makeup of a polymer. The most well-known method for determining molecular weight and molecular weight distribution is gel permeation chromatography (GPC)⁸⁷ also known as size exclusion chromatography (SEC), which involves the separation of polymers based solely on size and not polarity. SEC works

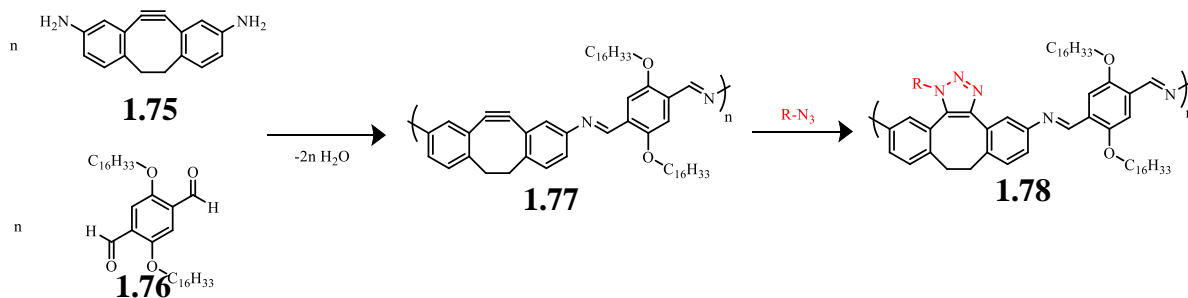
by running a sample through a column which has porous beads. Oligomers or small molecules are retained in the porous material and large molecules are not retained and elute more quickly. The technique most commonly employed is conventional calibration, which uses commercially available monodisperse standards such as polystyrene or poly (methyl methacrylate) to generate a calibration curve based on their maximum refractive index response. For the conventional calibration method, if the polymer being analyzed is structurally different compared to the standard being used, the data obtained can be misleading. Therefore, multi-detection GPC/SEC can be used for absolute molecular weight determination independent of the standard used.⁸⁸ The multi-detection method uses a refractive index detector and a static light scattering detector simultaneously allowing for direct measure of the weight average molecular weight. Matrix assisted laser desorption ionization time of flight (MALDI-TOF) analysis is another method that can accurately determine molecular weight parameters under the postulation that all polymer chains are equally volatile.⁸⁹ In MALDI-TOF analysis, the polymer is co-crystallized with a matrix capable of absorbing the incident beam by a laser, which ionizes the matrix and the polymer. Then, the ionized samples pass through the TOF detector separated on their mass to charge (m/z) values.

Aside from determining the average molecular weight and molecular weight distributions of a polymer, thermal analysis is also important to measure the physical properties as a function of temperature. Thermal gravimetric analysis (TGA) is a method used to assess the thermal stability of a polymer by mass loss with increasing temperature.⁹⁰ As the temperature increases, the corresponding mass loss can indicate which parts of the polymer are lost upon decomposition. Alongside TGA, differential scanning calorimetry (DSC) is

another technique of thermal analysis, which measures changes in heat flow, capable of determining phase changes in bulk polymer samples.⁹¹ The DSC analysis measures the difference in heat flow between the reference and sample with a defined temperature range, which can be used to determine the glass transition and crystallization/melting temperatures of a polymer sample. TGA and DSC can both provide very important physical characteristics of a polymer dependent on temperature versus time, important for the use of polymers in temperature sensitive applications.

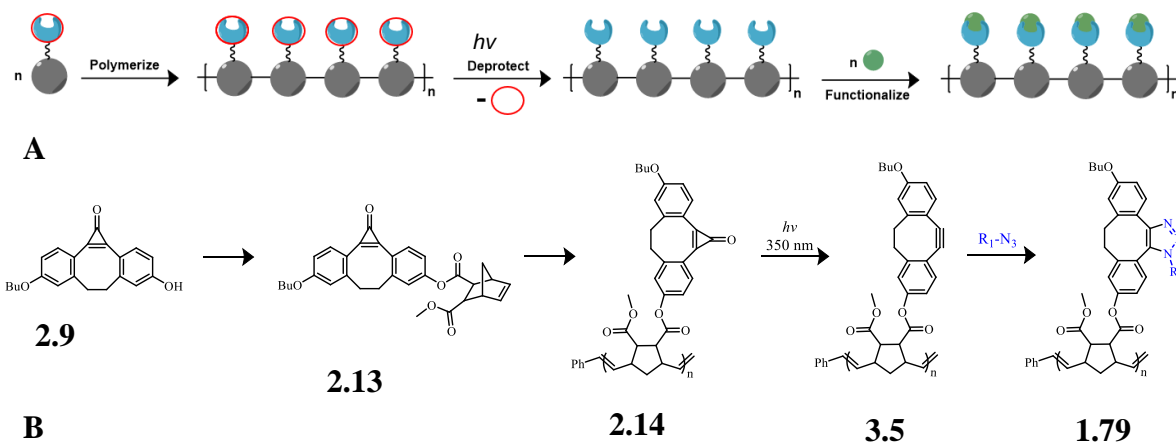
1.5 Scope of Thesis

This thesis will focus on the synthesis of a novel monomer with a unique strategy to unmask a strained alkyne, polymerization of the monomer via ROMP and subsequent photounmasking of the polymer to liberate the strained alkyne to facilitate SPAAC reactions with various azides. For this strategy, a cyclopropanone will be used as a precursor to the strained alkyne which can be decarbonylated by UV irradiation, with loss of CO, to afford the strained alkyne for post-polymerization modification. The advantages of the photo-unmasking are that only CO gas is evolved, no purification is required and there is spatial and temporal control. Previously, Popik and co-workers have successfully shown this strategy of strained alkynes in brush polymers.⁸⁰ The interest in these studies lies in synthesizing a “living”/“well-behaved” polymer where every repeating unit bears a pendant group that can be functionalized. Previously, Adronov and co-workers synthesized a polymer with the strained alkyne functional group on every repeating unit incorporated in the backbone of the polymer shown in Scheme 1.18, but the reported method lacks compatibility with living polymerization methods due to the reactivity of the strained alkyne.



Scheme 1.18. Adronov and co-workers scheme for step growth synthesis of a strained alkyne polymer.⁸⁷

Therefore, there remains a need to investigate alternative pathways towards incorporating strained alkynes into polymers. My work focuses on the synthesis of a novel polymer with a strained alkyne on every repeating group as pendant group, which can be modified via SPAAC where the general Scheme is shown in Scheme 1.19A. The monomer will incorporate the cyclopropenone masking group for side reactions to be avoided with the strained alkyne during polymerization with the Grubbs 3rd generation catalyst. The resulting polymer will be unmasked via UV irradiation to expose the strained alkyne for SPAAC with various azides represented by “R₁” that have electrochemical or emissive properties as shown in Scheme 1.19B.



Scheme 1.19. General cartoon scheme showing polymerization with a masked monomer and post-polymerization modification (**A**). General scheme showing polymerization with masked monomer and post-polymerization modification with a click partner (**B**).

Chapter 2 will focus on the synthesis and characterization of the photo-DIBO monomer, homopolymerization of the photo-DIBO monomer and a kinetics study to show that the polymerization is a well-behaved process.

Chapter 3 will focus on the comparison of SPAAC click reactions with the monomer and polymer with benzyl azide, azidomethyl ferrocene and azidomethyl pyrene and their characterization.

1.6 References

1. Mülhaupt, R., *Angew. Chem. Int. Ed.* **2004**, *43*, 1054-1063.
2. Carothers, W. H., *J. Chem. Soc., Faraday Trans.* **1936**, *32*, 39.
3. Stepto, R.; Chang, T.; Kratochvíl, P.; Hess, M.; Horie, K.; Sato, T.; Vohlídal, J., *Pure Appl. Chem.* **2015**, *87*, 71-120.
4. Likhtman, A. E.; Ponmurugan, M., *Macromolecules* **2014**, *47*, 1470-1481.
5. Kroonblawd, M. P.; Goldman, N.; Lewicki, J. P.; Lawrence Livermore National Lab, L. C. A., *J. Phys. Chem. B* **2018**, *122*, 12201-12210.
6. Zhao, Y.; Watanabe, K.; Hashimoto, K., *J. Am. Chem. Soc.* **2012**, *134*, 19528-19531.
7. Wang, J.-P.; Wang, J.-K.; Zhou, Q.; Yang, S.; Li, G. L., *Colloids Surf. A* **2019**, *569*, 52-58.
8. Watson, B. M.; Kasper, F. K.; Mikos, A. G., *Biomed. Mater.* **2014**, *9*, 025014.
9. Kausar, A.; Zulfiqar, S.; Sarwar, M. I., *Polym. Rev.* **2014**, *54*, 185-267.
10. Nicholson, J. W., *The chemistry of polymers*. 5th ed.; Royal Society of Chemistry: London, UK, 2017.
11. Poduška, J.; Hutař, P.; Kučera, J.; Frank, A.; Sadílek, J.; Pinter, G.; Náhlík, L., *Polym. Test.* **2016**, *54*, 288-295.
12. Galo Silva, G.; Valente, M. L. d. C.; Bachmann, L.; dos Reis, A. C., *Mater. Sci. Eng. C* **2019**, *99*, 1341-1349.
13. Ke, A.-Y.; Chen, J.; Chen, M.; Zhu, J.; Wang, Y.-H.; Hu, Y.; Fan, Z.-L.; Peng, P.; Jiang, S.-W.; Xu, X.-R.; Li, H.-X., *Mar. Pollut. Bull.* **2019**, *142*, 54-57.
14. Yesselman, J. D.; Horowitz, S.; Brooks, C. L.; Trievel, R. C., *Proteins* **2015**, *83*, 403-410.
15. Fetters, L. J.; Lohse, D. J.; Richter, D.; Witten, T. A.; Zirkel, A., *Macromolecules* **1994**, *27*, 4639-4647.
16. Billiet, L.; Fournier, D.; Du Prez, F., *Polymer* **2009**, *50*, 3877-3886.
17. Gao, H.; Matyjaszewski, K., *Prog. Polym. Sci.* **2009**, *34*, 317-350.
18. Flory, P. J., *Chem. Rev.* **1946**, *39*, 137-197.

19. Lee, S. M.; Park, K. H.; Jung, S.; Park, H.; Yang, C., *Nat. Commun.* **2018**, *9*, 1867-1867.
20. Slavko, E.; Taylor, M. S., *Chem. Sci.* **2017**, *8*, 7106-7111.
21. Aplan, M. P.; Gomez, E. D., *Ind. Eng. Chem. Res.* **2017**, *56*, 7888-7901.
22. Viswanathan, A., *World Patent Information* **2010**, *32*, 300-305.
23. Thomas, A. M.; Sujatha, A.; Anilkumar, G., *RSC Adv* **2014**, *4*, 21688-21698.
24. Wang, X.; Song, Y.; Qu, J.; Luo, Y., *Organometallics* **2017**, *36*, 1042-1048.
25. Anwar, N.; Rix, A.; Lederle, W.; Kuehne, A. J. C., *Chem. Commun.* **2015**, *51*, 9358-9361.
26. Qiu, J.; Charluex, B.; Matyjaszewski, K., *Polimery* **2001**, 453-574.
27. Dai, S.; Chen, C., *Macromolecules* **2018**, *51*, 4040-4048.
28. Bozzelli, J. W.; Dean, A. M., *J. Phys. Chem* **1993**, *97*, 4427-4441.
29. Gridnev, A. A.; Ittel, S. D., *Chem. Rev.* **2001**, *101*, 3611-3660.
30. Pyun, J.; Rees, I.; Jean, M. J. F., *Aust. J. Chem.* **2003**, *56*, 775-782.
31. Nakamura, Y.; Ogihara, T.; Hatano, S.; Abe, M.; Yamago, S., *Chem. Eur. J.* **2017**, *23*, 1299-1305.
32. Chiefari, J.; Chong, Y. K.; Ercole, F.; Krstina, J.; Jeffery, J.; Le, T. P. T.; Mayadunne, R. T. A.; Meijs, G. F.; Moad, C. L.; Moad, G.; Rizzardo, E.; Thang, S. H., *Macromolecules* **1998**, *31*, 5559-5562.
33. Mayadunne, R. T. A.; Rizzardo, E.; Chiefari, J.; Krstina, J.; Moad, G.; Postma, A.; Thang, S. H., *Macromolecules* **2000**, *33*, 243-245.
34. Patten, T. E.; Matyjaszewski, K., *Acc. Chem. Res.* **1999**, *32*, 895-903.
35. Matyjaszewski, K.; Pintauer, T.; Gaynor, S., *Macromolecules* **2000**, *33*, 1476-1478.
36. Hadjichristidis, N.; Iatrou, H.; Pispas, S.; Pitsikalis, M., *J. Polym. Sci., Part A: Polym. Chem.* **2000**, *38*, 3211-3234.
37. Webster, O. W., *Science* **1991**, *251*, 887-893.
38. Ding, J.; Heatley, F.; Price, C.; Booth, C., *Eur. Polym. J.* **1991**, *27*, 895-899.
39. Shimomoto, H.; Fukami, D.; Kanaoka, S.; Aoshima, S., *J. Polym. Sci., Part A: Polym. Chem.* **2011**, *49*, 2051-2058.

40. Higashimura, T.; Aoshima, S.; Sawamoto, M., *Macromol. Chem. Phys.* **1988**, *13-14*, 457-471.
41. Cossee, P., *J. Catal.* **1964**, *3*, 80-88.
42. Ewen, J. A., *J. Mol. Catal. A:Chem.* **1998**, *128*, 103-109.
43. Schrock, R. R., *Acc. Chem. Res.* **1990**, *23*, 158-165.
44. Binder, W. H.; Kluger, C., *Macromolecules* **2004**, *37*, 9321-9330.
45. Bielawski, C. W.; Grubbs, R. H., *Macromolecules* **2001**, *34*, 8838-8840.
46. Krause, J. O.; Lubbad, S.; Nuyken, O.; Buchmeiser, M. R., *Adv. Synth. Catal.* **2003**, *345*, 996-1004.
47. Allaert, B.; Dieltiens, N.; Ledoux, N.; Vercaemst, C.; Van Der Voort, P.; Stevens, C. V.; Linden, A.; Verpoort, F., *J. Mol. Catal. A:Chem.* **2006**, *260*, 221-226.
48. Ji-xing Yang Li-xia Ren Yue-sheng, L., *Chinese. J. Polym. Sci.* **2017**, *35*, 36-45.
49. Hultsch, K. C.; Jernelius, J. A.; Hoveyda, A. H.; Schrock, R. R., *Angew. Chem. Int. Ed.* **2002**, *41*, 589-593.
50. Bielawski, C. W.; Grubbs, R. H., *Angew. Chem. Int. Ed.* **2000**, *39*, 2903-2906.
51. Walsh, D. J.; Lau, S. H.; Hyatt, M. G.; Guironnet, D., *J. Am. Chem. Soc.* **2017**, *139*, 13644-13647.
52. Ashworth, I. W.; Nelson, D. J.; Percy, J. M., *Dalton Trans.* **2013**, *42*, 4110-4113.
53. Kolb, H. C.; Finn, M. G.; Sharpless, K. B., *Angew. Chem. Int. Ed.* **2001**, *40*, 2004-2021.
54. Hoyle, C. E.; Bowman, C. N., *Angew. Chem. Int. Ed.* **2010**, *49*, 1540-1573.
55. Liu, Y. L.; Chuo, T. W., *Polym. Chem.* **2013**, *4*, 2194-225.
56. (a) Meldal, M.; Tornøe, C. W., *Chem. Rev.* **2008**, *108*, 2952-3015; (b) Xi, W.; Scott, T. F.; Kloxin, C. J.; Bowman, C. N., *Adv. Funct. Mater.* **2014**, *24*, 2572-2590.
57. Sutton, D. A.; Yu, S.-H.; Steet, R.; Popik, V. V., *Chem. Commun.* **2016**, *52*, 553-556.
58. Kade, M. J.; Burke, D. J.; Hawker, C. J., *J. Polym. Sci., Part A: Polym. Chem.* **2010**, *48*, 743-750.
59. Serniuk, G. E.; Banes, F. W.; Swaney, M. W., *J. Am. Chem. Soc.* **1948**, *70*, 1804-1808.

60. Fairbanks, B. D.; Love, D. M.; Bowman, C. N., *Macromol. Chem. Phys.* **2017**, *218*, 1700073-1700083.
61. Cramer, N. B.; Scott, J. P.; Bowman, C. N., *Macromolecules* **2002**, *35*, 5361-5365.
62. Brummelhuis, N. T.; Diehl, C.; Schlaad, H., *Macromolecules* **2008**, *41*, 9946-9947.
63. Bouacha, S.; Nacereddine, A. K.; Djerourou, A., *Tetrahedron Lett.* **2013**, *54*, 4030-4033.
64. Takao, K. I.; Munakata, R.; Tadano, K. I., *Chem. Rev.* **2005**, *105*, 4779-4807.
65. Adzima, B. J.; Kloxin, C. J.; DeForest, C. A.; Anseth, K. S.; Bowman, C. N., *Macromol. Rapid Commun.* **2012**, *33*, 2092-2096.
66. Adzima, B. J.; Aguirre, H. A.; Kloxin, C. J.; Scott, T. F.; Bowman, C. N., *Macromolecules* **2008**, *41*, 9112-9117.
67. Chen, X.; Dam, M. A.; Ono, K.; Mal, A.; Shen, H.; Nutt, S. R.; Sheran, K.; Wudl, F., *Science* **2002**, *295*, 1698-1702.
68. Durmaz, H.; Colakoglu, B.; Tunca, U.; Hizal, G., *J. Polym. Sci., Part A: Polym. Chem.* **2006**, *44*, 1667-1675.
69. Haldón, E.; Nicasio, M. C.; Pérez, P. J., *Org. Biomol. Chem.* **2015**, *13*, 9528-955.
70. Chen, R. T.; Muir, B. W.; Such, G. K.; Postma, A.; Evans, R. A.; Pereira, S. M.; McLean, K. M.; Caruso, F., *Langmuir* **2010**, *26*, 3388.
71. Li, T. h.; Jing, X. b.; Huang, Y. b., *Polym. Adv. Technol.* **2011**, *22*, 1266-1271.
72. Cao, Y.; Lai, Z.; Feng, J.; Wu, P., *J. Mater. Chem.* **2011**, *21*, 9271.
73. Quémener, D.; Davis, T. P.; Barner-Kowollik, C.; Stenzel, M. H., *Chem. Commun.* **2006**, 5051-5053.
74. Siemsen, P.; Livingston, R. C.; Diederich, F., *Angew. Chem. Int. Ed.* **2000**, *39*, 2632-2657.
75. Manova, R. K.; Beek, V. T. A.; Zuilhof, H., *Angew. Chem. Int. Ed.* **2011**, *50*, 5428-5430.
76. Ramsubhag, R. R.; Dudley, G. B., *Org. Biomol. Chem.* **2016**, *14*, 5028-5031.
77. Trættemberg, M.; Lüttke, W.; Machinek, R.; Krebs, A.; Hohlt, H. J., *J. Mol. Struct.* **1985**, *128*, 217-232.
78. Debets, M. F.; Prins, J. S.; Merckx, D.; Berkel, S. S. v.; Delft, F. L. v.; Hest, J. C. M. v.; Rutjes, F. P. J. T., *Org. Biomol. Chem.* **2014**, *12*, 5031-5037.

79. Arumugam, S.; Orski, S. V.; Mbua, N. E.; McNitt, C.; Boons, G.-J.; Locklin, J.; Popik, V. V., *Pure Appl. Chem.* **2013**, *85*, 1499-1513.
80. Laradji, A. M.; McNitt, C. D.; Yadavalli, N. S.; Popik, V. V.; Minko, S., *Macromolecules* **2016**, *49*, 7625-7631.
81. Dykes, G. M., *J. Chem. Technol. Biotechnol.* **2001**, *76*, 903-918.
82. McNelles, S. A.; Adronov, A., *Macromolecules* **2017**, *50*, 7993-8001.
83. Arnold, R. M.; McNitt, C. D.; Popik, V. V.; Locklin, J., *Chem. Commun.* **2014**, *50*, 5307-5309.
84. Gobbo, P.; Romagnoli, T.; Barbon, S. M.; Price, J. T.; Keir, J.; Gilroy, J. B.; Workentin, M. S., *Chem. Commun.* **2015**, *51*, 6647-6650.
85. Kardelis, V.; Chadwick, R. C.; Adronov, A., *Angew. Chem. Int. Ed.* **2016**, *128*, 957.
86. Izunobi, J. U.; Higginbotham, C. L., *J. Chem. Educ.* **2011**, *88*, 1098.
87. Tennikov, M. B.; Gorbunov, A. A.; Skvortsov, A. M., *J. Chromatogr. A* **1990**, *509*, 219-226.
88. Clementi, L. A.; Vega, J. R.; Meira, G. R., *Macromol. Theory Simul.* **2014**, *23*, 90-100.
89. Wu, T.; Zhang, C.; Ren, H.; Xi, Y.; Du, Y.; Peng, Y., *Int. J. Polym. Anal. Charact.* **2017**, *22*, 160-168.
90. D. W. Levi, L. R., H. T. Lee, *Polym. Eng. Sci.* **1965**, *5*, 135-141.
91. Schick, C., *Anal. Bioanal. Chem.* **2009**, *395*, 1589-1611.

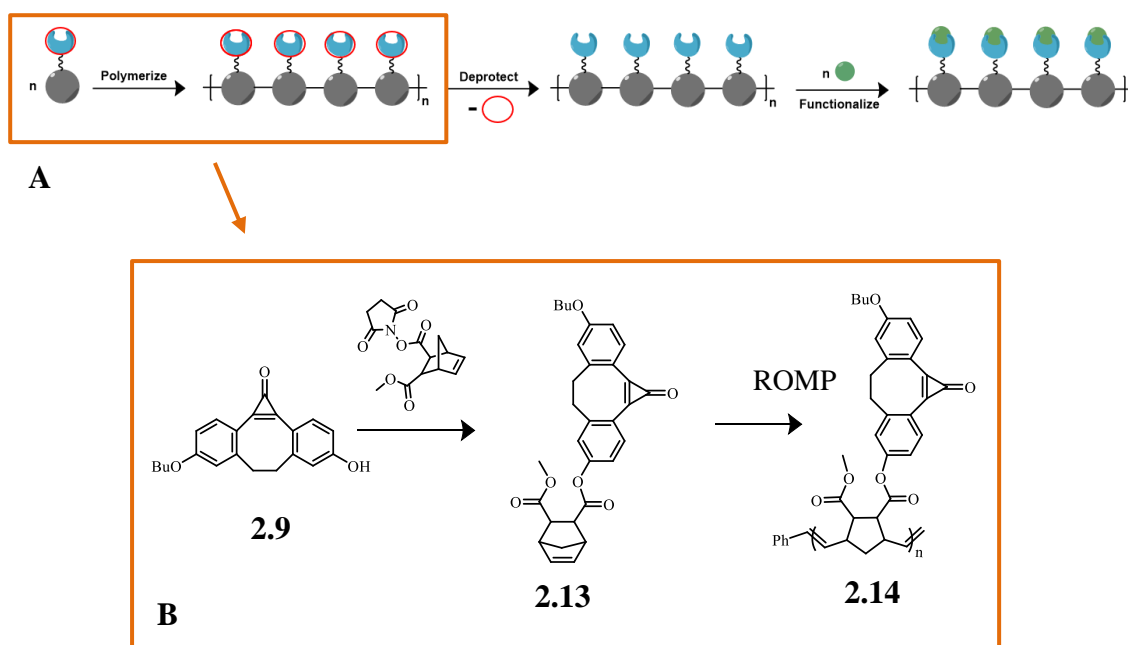
Chapter 2

2 Synthesis of a Masked Strained Alkyne Polymer

2.1 Introduction

Modifiable polymers have demonstrated promising applications in photo patterning,¹ biomedicine² and electrochemical processes.³ The “living” polymerization methods such as radical,⁴ anionic,⁵ cationic⁶ and metal-catalyzed polymerization⁷ have been optimized for traditional bulk polymers such as polystyrene and polyethylene, but show limitations for exotic monomers with reactive functional groups. Thus, traditional “living” methods pose a challenge for the production of polymers with controlled molecular weight distributions and low dispersity. Post-polymerization modification (PPM) is a potential way to allow functional/exotic monomers to be polymerized, enhancing functional group tolerance. However, some exotic monomers contain reactive functional groups,⁸ which can interfere with the polymerization, thus it is important to implement a protecting or masking strategy to make sure the monomer is successfully polymerized and does not undergo any side reactions. More specifically, chapter 2 presents the synthesis and characterization of a photoDIBO-monomer **2.13** with a unique masking/unmasking strategy of a strained alkyne via a cyclopropanone group. The cyclopropanone group masking the strained alkyne can be decarbonylated by UV irradiation to afford the strained alkyne for post-polymerization modification and the advantages of the photo-unmasking are that only CO gas is evolved, no purification is required and there is spatial and temporal control. Previously, Popik and co-workers have successfully shown the masking and unmasking of linear alkynes⁹ and graft polymers showing how effective and efficient the masking/unmasking strategy is for further modification.¹⁰ A well-behaved polymerization process and its purification is also

presented and will allow for a further modification as shown in Scheme 2.1. The method of polymerization for the monomer is ROMP via the bromopyridine Grubbs 3rd generation derivative catalyst. ROMP was chosen as the method of polymerization because of its functional group control, chain growth from one end and chain length control from stoichiometry.⁹ Also, a kinetics study was done where aliquots of the polymerization were taken at different times, proving that the polymerization of the photo-DIBO-monomer was a well-behaved process.



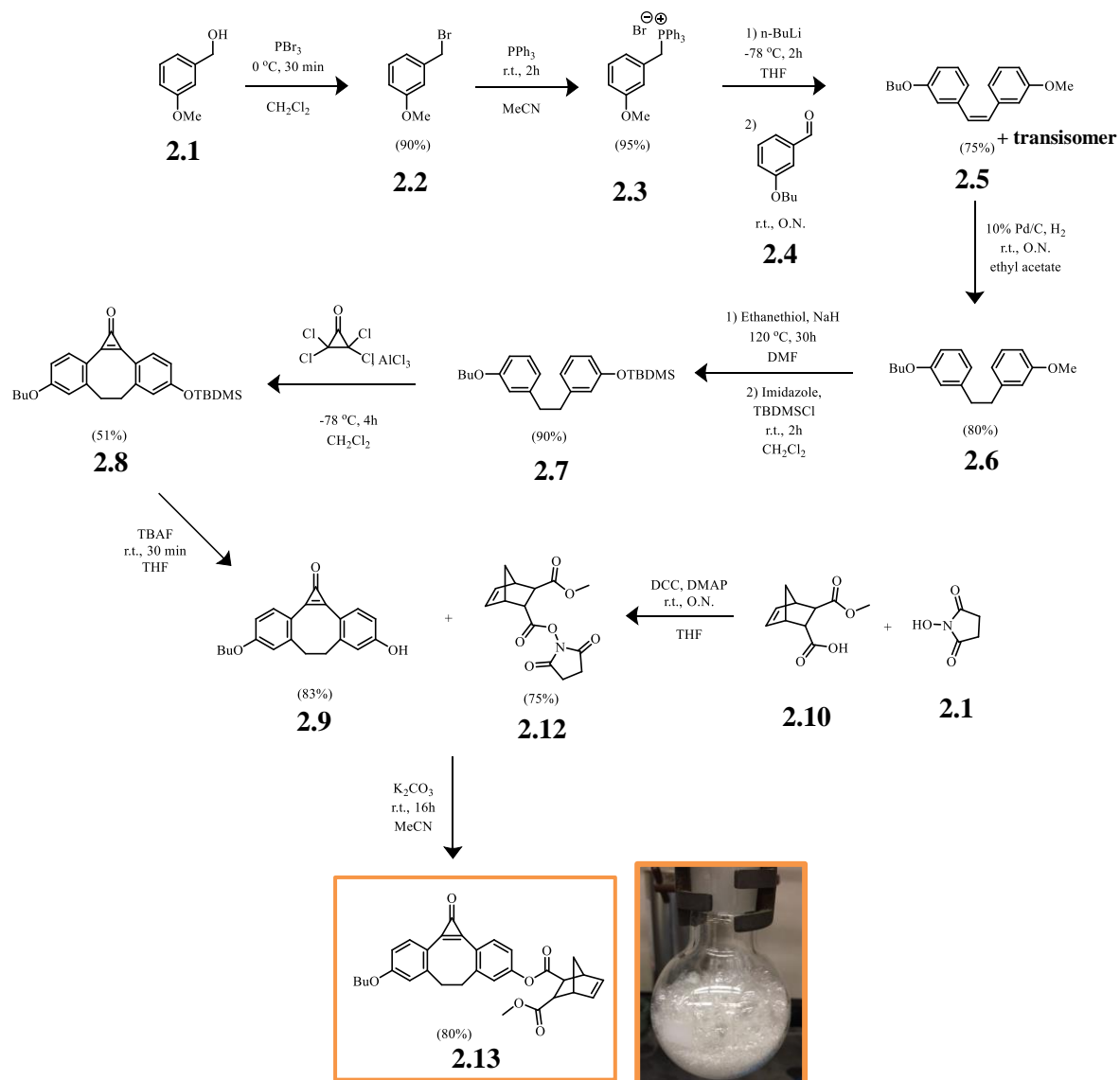
Scheme 2.1. General cartoon scheme showing polymerization with masked monomer and post polymerization modification (**A**). General scheme showing polymerization with the masked monomer (**B**).

2.2 Results and Discussion

2.2.1 Synthesis and characterization of the photoDIBO-monomer

The general scheme for the preparation of the photoDIBO-monomer **2.13** is shown in Scheme 2.2 and has three main synthetic parts. The first part is the synthesis of the cyclopropenone masked dibenzocyclooctyne (**2.9**) (photoDIBO-OH). The photoDIBO-OH **2.9** was synthesized using the procedure developed by Locklin and coworkers.¹⁰ Compound **2.9** was selected as a precursor because of its simple molecular structure, it is stable under -20 °C and allows for facile purification. Although the strained alkyne is relatively stable, it can be subject to nucleophilic attack¹¹ and for that reason has a cyclopropenone cage for the strained alkyne. The hydroxyl group on 3-methoxy benzyl alcohol **2.1** was substituted with bromine to generate a better leaving group. The bromine functional group on complex **2.2** was then substituted with triphenyl phosphine affording the phosphonium ylide **2.3** which was subsequently used to perform a Wittig reaction with the butoxy benzaldehyde (**2.4**), generating a carbon-carbon double bond to afford the phenyl cis/trans isomers **2.5**. The double bond of the phenyl product **2.5** was hydrogenated using palladium over carbon and purified via flash chromatography resulting in compound **2.6**. The final step for the synthesis of photoDIBO-OH (**2.9**) was the incorporation of the masked strained alkyne. The methoxy group of complex **2.6** was converted to a hydroxyl group and protected with *tert*-butyldimethylsilylchloride to prevent any side reactivity, constructing the protected phenyl product **2.7**. Subsequently, tetrachlorocyclopropenone was incorporated into compound (**2.7**) generating the masked cyclooctyne ring (**2.8**) followed by deprotection of the hydroxyl group with tetrabutylammonium fluoride (TBAF) to afford the photoDIBO-OH **2.9**. The second step involved generating the *n*-

hydroxysuccinimide activated norbornene carboxylate derivative **2.12** by reacting the substituted norbornene **2.10** and *n*-hydroxysuccinimide **2.11**. The third step was a nucleophilic acyl substitution of compounds **2.9** and **2.12** to generate the photoDIBO-monomer **2.13** with an overall yield of 15%.



Scheme 2.2. General scheme for the synthesis of the photoDIBO-monomer **2.13**.

The characterization of photo-DIBO-monomer **2.13** was completed using ^1H and ^{13}C NMR spectroscopy, high-resolution mass spectrometry as well as UV-Vis and IR spectroscopy (Figure A.2.7). The ^1H NMR spectrum showed preservation of the photoDIBO protons, where a triplet at 1.01 ppm, two multiplets at 1.56-1.52 and 1.83-1.80 ppm and a triplet at 4.08 ppm correspond to the $-\text{CH}_3$, $-\text{CH}_2 \times 2$ and $-\text{CH}_2\text{-O-}$ respectively of the butoxy group. Two multiplets at 2.63-2.61 and 3.51-3.29 ppm correspond to $-\text{CH}_2 \times 2$ protons of the cyclooctyne ring with the phenyl protons show up at 6.92 as a doublet of doublets, 7.23-7.21 and 8.01-7.96 ppm as multiplets. The alkene protons from the norbornene ring appear at 6.26-6.25 and 6.46-6.43 ppm as multiplets (Figure 2.1). The ^{13}C NMR spectrum (Figure A.2.6) showed diagnostic signals¹² of the $\text{C}=\text{O}$ and $\text{C}=\text{C}$ of the cyclopropenone group (162.3 ppm and 153.7 ppm, respectively) and additional peaks at 172.5 ppm and 170.6 ppm correspond to the ester groups of the norbornene portion of the molecule. The IR spectrum (Figure A.2.7) showed the appearance of a peak at 1842 cm^{-1} which is diagnostic of a cyclopropenone $\text{C}=\text{O}$. Also, signals at 1763 cm^{-1} and 1738 cm^{-1} are indications of the $\text{C}=\text{O}$ of the esters present on the norbornene portion of the photoDIBO-monomer **2.13**. The ESI-HRMS data for the photoDIBO-monomer, showed good agreement between the calculated m/z for $\text{C}_{31}\text{H}_{30}\text{O}_6^+ [\text{M}]^+$: 498.2042 and the 498.2032 m/z found. These characterization data confirm that the *n*-hydroxysuccinimide norbornene derivative **2.12** was successfully coupled to the photo-DIBO-OH **2.9** to yield monomer **2.13**.

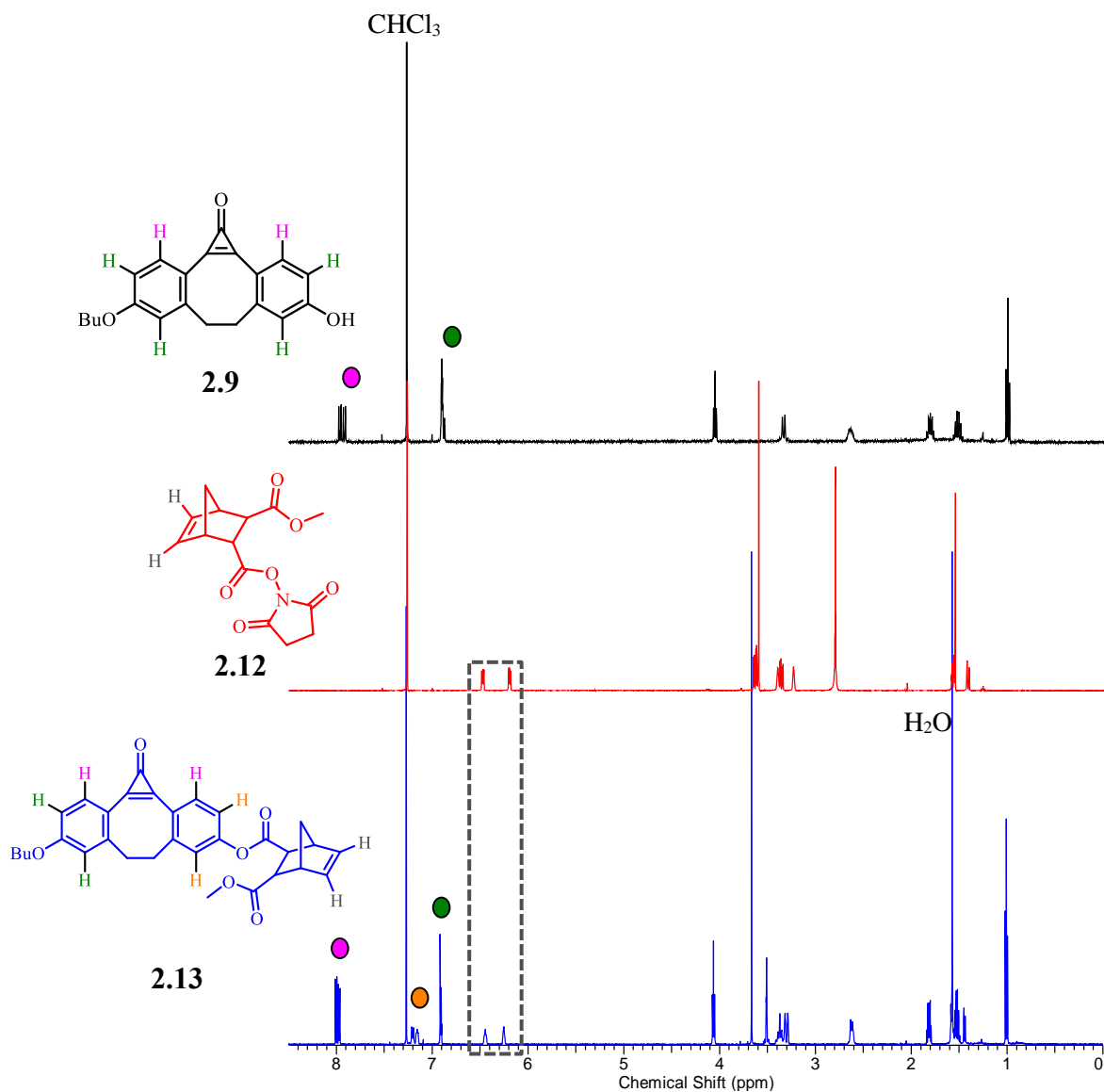


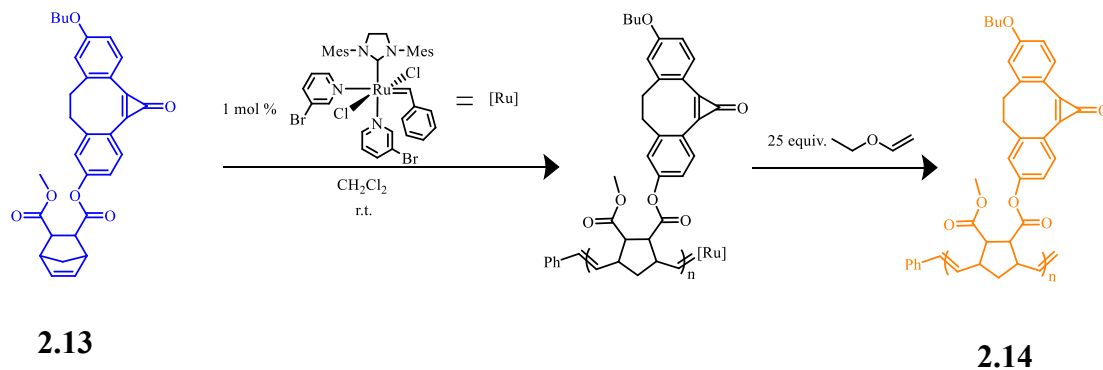
Figure 2.1. Comparison of the ^1H NMR spectra of compounds **2.9**, **2.12** and **2.13**. The coloured dots represent aromatic protons and the box indicates the alkene protons.

2.2.2 Polymerization strategy for the photoDIBO-monomer **2.13**

Chain growth polymerization by ROMP was chosen as the method of polymerization. The driving force of the polymerization involves the release of ring strain so bicyclic olefin monomers are commonly used as substrates.¹³ This type of

polymerization is functional group tolerant and the chain only grows from one end which affords molecular weight control.¹³ The polymerization occurs by metathesis of a bicyclic olefin complex, in this case a norbornene derivative with the R group equal to the photo-DIBO. Our ROMP reactions were catalyzed by the 3-bromopyridine derivative of Grubbs 3rd generation catalyst (GIII). This ruthenium-based catalyst initiates ROMP with the loss of the pyridine ligand. Grubbs III was selected as the catalyst because of its efficiency in creating high molecular weight polymers, solubility in CH₂Cl₂ and its tolerance of functional groups.¹⁴

Due to the presence of a highly reactive strained alkyne, a masking-unmasking strategy was implemented for the polymerization. The polymerization was done under a nitrogen atmosphere. The Grubbs III catalyst was dissolved in dry and degassed CH₂Cl₂, then 1 mol % of the catalyst was added to the solution of monomer. The polymerization was terminated after 1 h with 25 equivalents of ethyl vinyl ether where the oxygen coordinates with the ruthenium and terminates the polymerization (Scheme 2.3) which fills the vacant orbital and inactivates the catalyst. It is important to note that after 1 h of polymerization there was still monomer remaining shown in Figure 2.2, denoted by the red boxes showing the two multiplets of the monomer **2.13** olefin protons at 6.46-6.43 and 6.26-6.25 ppm still present with the appearance of a broad multiplet at 5.63 ppm corresponding to the polymer **2.14** olefin protons. The reason for stopping after 1 h was to gauge the behavior of the polymerization, to limit side reactions and crosslinking. Thus, a kinetic study was done to investigate how long it takes to polymerize, and this is discussed in section 2.2.3.



Scheme 2.3. Reaction scheme for ROMP of monomer **2.13**.

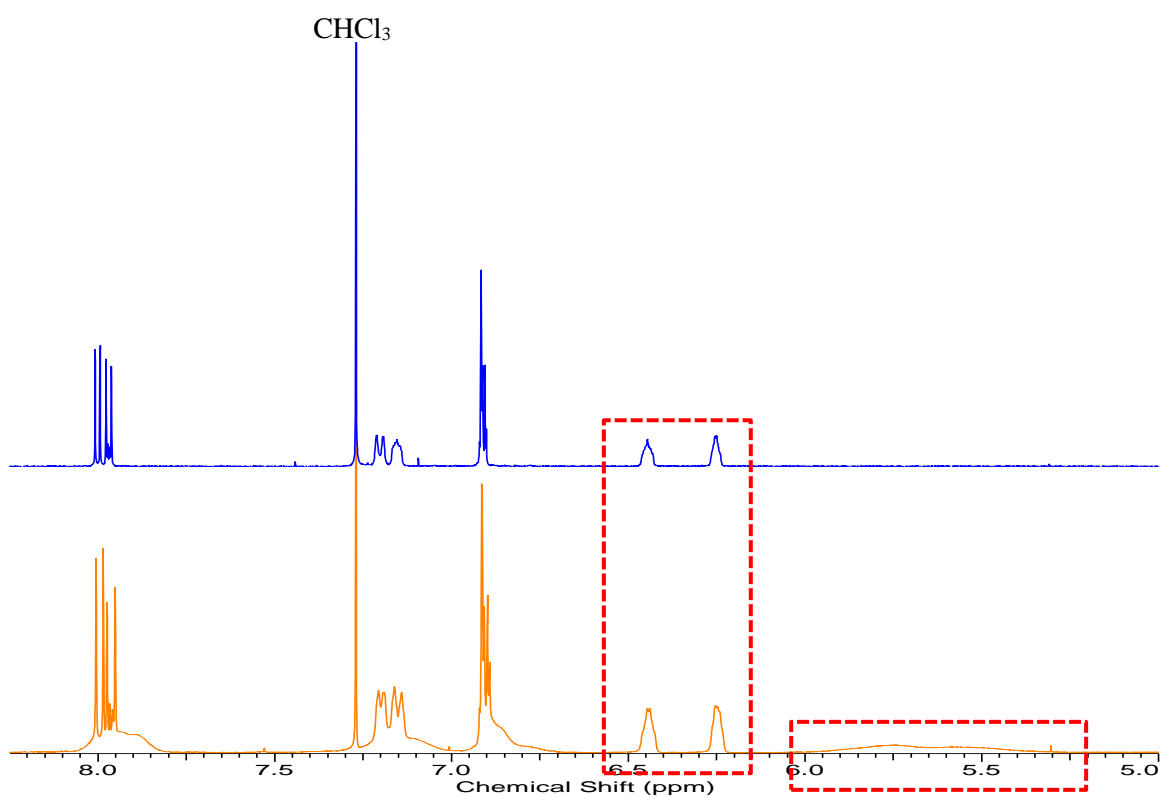


Figure 2.2. Comparison of the ^1H NMR spectra of the monomer **2.13** (blue) and 1 h polymer **2.14** (orange) aliquot showing shift of alkene peaks to the backbone of the polymer **2.14**.

The polymer **2.14** was purified via a neutral alumina plug to remove the Grubbs III catalyst, precipitated in rapidly stirred 0 °C pentane and isolated by centrifugation. Once the polymer **2.14** was purified, it was confirmed by ^1H NMR spectroscopy and gel permeation chromatography (GPC); Figure A.2.13. The broadening of the ^1H NMR spectrum shown in Figure 2.3 was the first indication a polymer was made and the second was the GPC trace that showed a unimodal distribution of high molecular weight species. Thermogravimetric analysis (TGA) and differential scanning calorimetry (DSC) were also conducted **2.14**. The TGA data (Figure 2.3A) showed that there were 4 steps involved in the decomposition of the polymer **2.14** and the initial step of decomposition was at 246 °C. The DSC (Figure 2.3B) data showed that the glass transition temperature (T_g) was 172 °C.

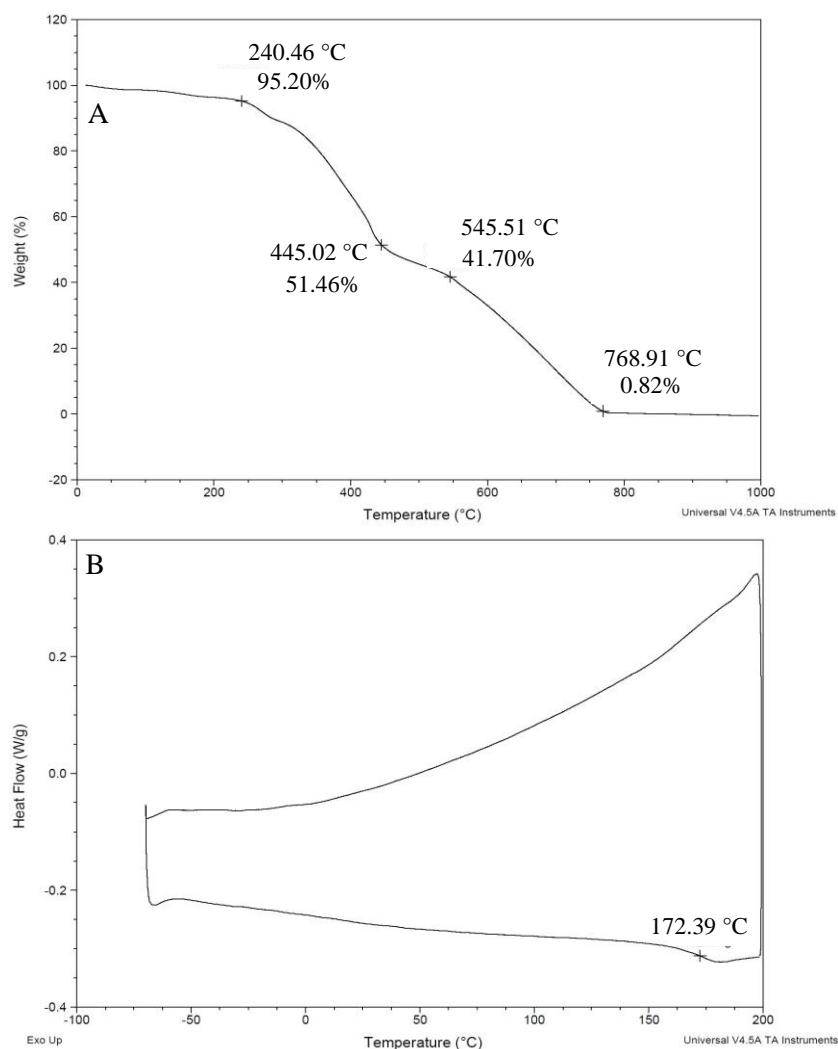


Figure 2.3. TGA plot (A) and DSC plot (B) of polymer **2.14**.

The ^1H NMR spectrum of the pure polymer suggests that the phenyl protons on the phenyl rings adjacent to the cyclopropanone group in the DIBO ring align with the same protons in the photoDIBO-monomer **2.13** 6.92 ppm, 7.21-7.15 ppm and 8.01-7.96 ppm shown in Figure 2.4 by the black dotted lines. The ^1H NMR spectrum of polymer **2.14** also shows the disappearance of the alkene protons in the photo-DIBO-monomer at 6.26-6.25 ppm and 6.46-6.43 ppm, and new alkene protons reappear in the backbone of the polymer at 5.63 ppm shown in Figure 2.3 by the pink box which are consistent with alkene proton signals of a norbornene backbone polymer. IR spectroscopy confirmed that the cyclopropanone group remained intact because the C=O bond at 1842 cm^{-1} and C=C bond at 1630 cm^{-1} both appear in the IR spectrum shown in Figure 2.5. Presence of the ester C=O bonds on the norbornene backbone were indicated by signals at 1763 cm^{-1} and 1738 cm^{-1}

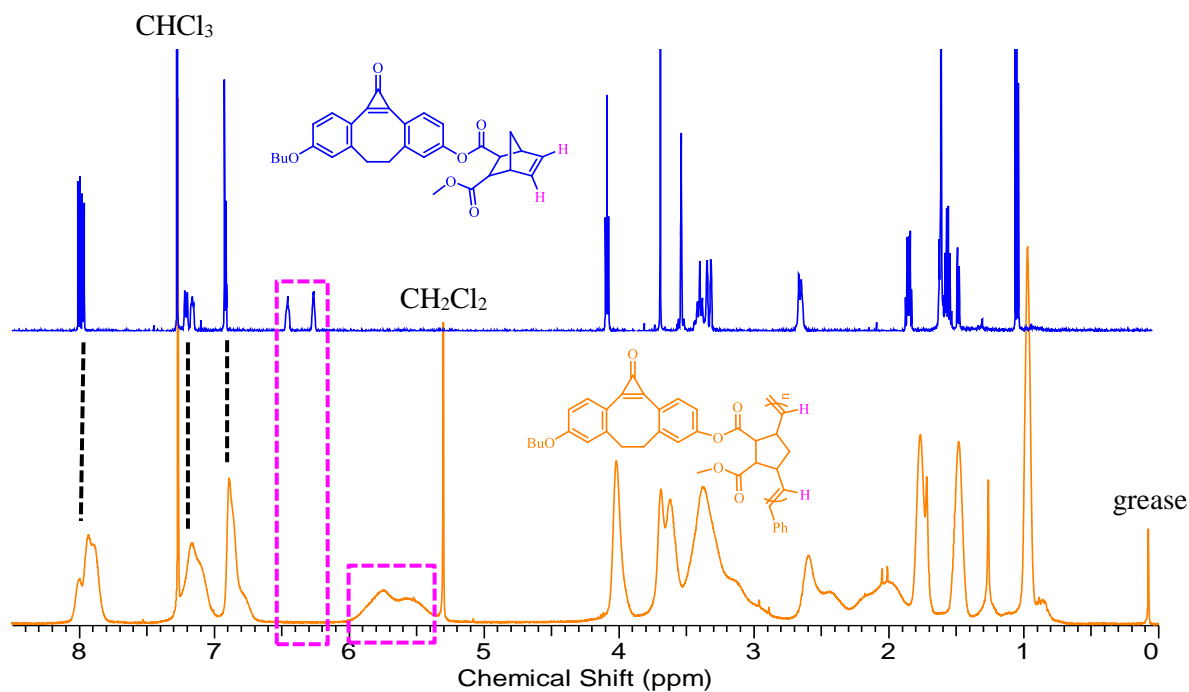


Figure 2.4. ^1H NMR spectra of the photoDIBO-monomer **2.13** and photoDIBO-polymer **2.14**.

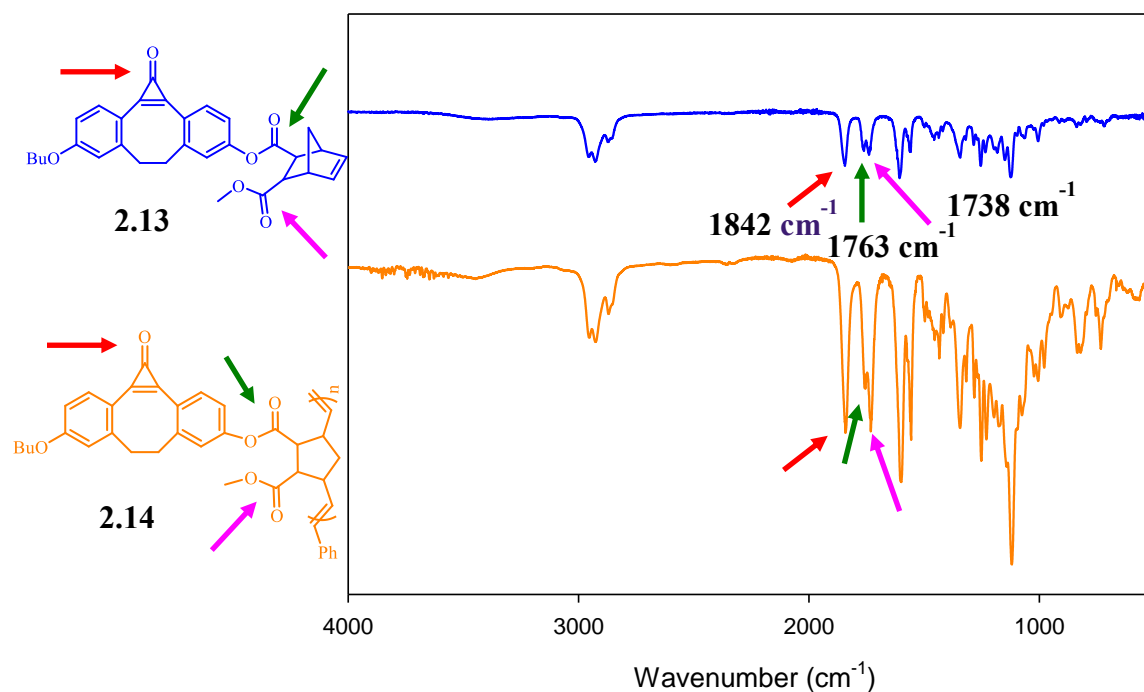


Figure 2.5. IR spectra of the photoDIBO-monomer **2.13** and photoDIBO-polymer **2.14**.

2.2.3 Kinetic study of the photoDIBO-polymer 2.14

The ^1H NMR spectrum of the crude product of the initial polymerization showed that after 1 hour the polymerization was not complete because there was still 86% of the monomer remaining shown in Figure 2.2. The monomer conversions were calculated by comparing the ^1H NMR signals of the alkene protons of the monomer at 6.45-6.44 ppm and 6.25-6.24 ppm to the alkene protons in the backbone of the polymer at 5.63 ppm.

Therefore, a monomer consumption study was conducted to see how long it takes for the polymerization to complete. The consumption study was done for a total of 8 hours, where aliquots of the polymer were taken at 1, 2, 4, 6, 8 h. Chain growth was quenched by addition of excess ethyl vinyl ether and the GPC data for each aliquot is summarized table 2-1 and the GPC traces are shown in Figure 2.6.

Table 2-1. Summary of GPC analysis for aliquots of photoDIBO-polymers **2.14** conducted at room temperature and using 1 mol % of 3-bromopyridine of Grubbs III.

Aliquot #	Time for polymerization (Hours)	M_n (g/mol)	M_w (g/mol)	\mathcal{D}
1	1	30100	52250	1.74
2	2	53550	86650	1.62
3	4	60500	100300	1.70
4	6	59900	121500	2.03
5	8	59700	117400	2.00

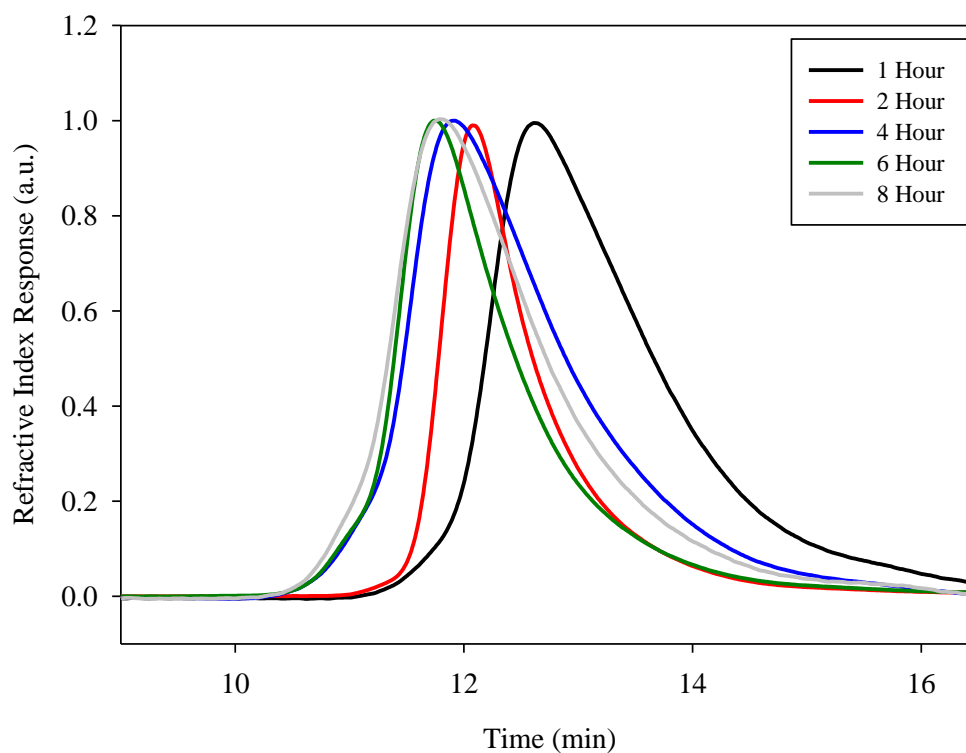


Figure 2.6. GPC traces for aliquots of photoDIBO-polymer **2.14** at various aliquot times from 1-8 h.

The high molecular weights observed confirmed the generation of polymeric species. However, the ^1H NMR spectrum of the polymer aliquot at 8 h showed that 9% of the monomer species remained because there were still peaks at 6.45-6.44 ppm and 6.25-6.24 ppm, which is an indication that the rate of polymerization decreased because most of the monomer was consumed or the polymerization prematurely terminates. The theoretical M_n for the monomer with 100 repeating units is 49,800 g/mol and the reported weights are higher than anticipated but still in good agreement. The high molecular weight was attributed to the structural mismatch with the GPC standard; polystyrene. The structures of polystyrene and the photoDIBO-polymer **2.14** are not similar, potentially leading to the higher molecular weight responses than predicted.

Through ^1H NMR analysis, a semilogarithmic plot was constructed showing a linear relationship between the reaction time and $\ln([M_0]/[M])$ from 1-4 h and a plateau effect at 6-8 h shown in Figure 2.7. Although this is not a traditional “living” polymerization method it is a well-behaved process. The plateau may be expected at the 6-8 h mark because most of the monomer is consumed at the 6 h mark, leading to less accessibility of the monomer and thus the rate of reaction decreases. This semilogarithmic plot, although not technically “living” does show resemblance to literature data¹⁵ for “living” methods because at lower M_n the polymer is well behaved but as the M_n increases there is some side reactivity.

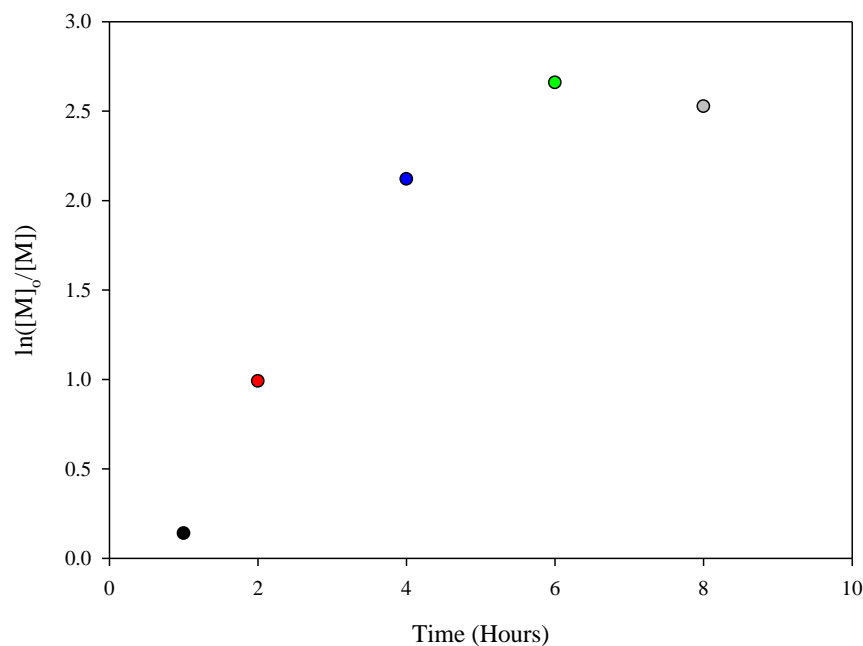


Figure 2.7. Semi-logarithmic plot of initial monomer concentration vs monomer concentration over time.

Also, the molecular weight of the polymers determined by GPC increased linearly with the monomer conversion shown in Figure 2.8A. This plot showed a slight drop of molecular weight at 93% and 92% conversion and the increasing D values of each aliquot which can be an indication of side reactivity. In a second study, a series of polymerization reactions with different molar feed ratios of monomer to catalyst were conducted with all monomer conversion reaching nearly 100%. The catalyst was varied by using 0.8, 1, 1.2, 2, and 4 mol % of the catalyst to monomer leading to 25, 50, 83, 100 and 125 degrees of polymerization, respectively and all other parameters were held constant. The molecular weight of the final polymers increased relatively linearly at lower feed molar ratios, indicating a controlled reactivity (Figure 2.8B). However, at higher ratios deviation from

linear behavior was again observed, confirming that the polymerization was not truly “living”.

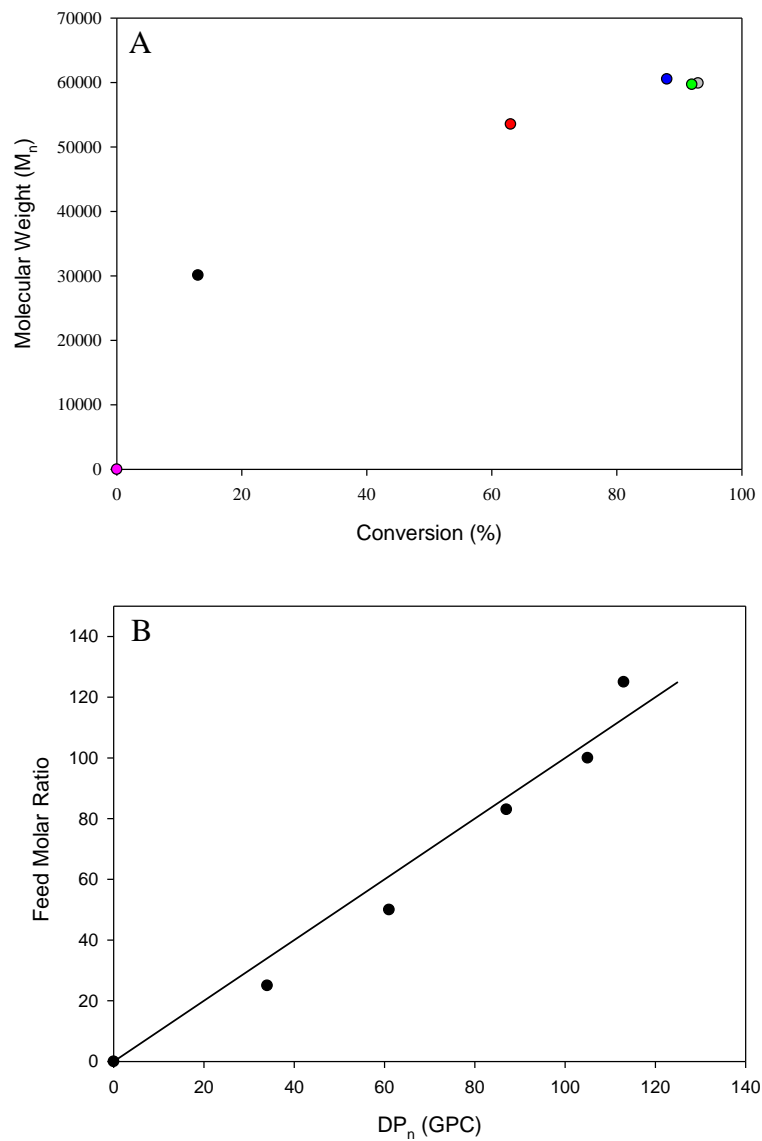
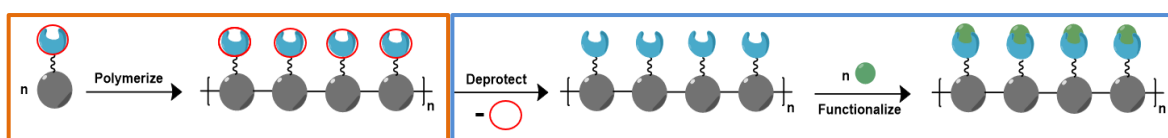


Figure 2.8. Kinetic study of the molecular weight vs conversion percent for polymer **2.14** where the plotted data represents different aliquot intervals (A). Kinetic study of feed molar ratio vs degree of polymerization of polymer **2.14** (B).

2.3 Conclusion

The goal of the work presented in Chapter 2 was to synthesize and characterize a monomer with a unique masking strategy as well as its polymerization. Following the monomer synthesis in relatively good yield, the polymerization of the monomer was a success (highlighted by the orange box in the cartoon Scheme 2.4). Although the polymerization of the photoDIBO-monomer **2.13** was not a “living” method, it was a well-behaved process that afforded reasonable molecular weight control for lower molecular weight examples. The ^1H NMR spectra and GPC traces all indicate that indeed the correct polymer was made, and the IR spectra showed that the cyclopropenone masking group remained intact during the polymerization. The next step is to explore photochemical unmasking of the strained alkyne on each pendant repeating unit and perform SPAAC, introducing functionality to the polymer and this will be discussed in Chapter 3 and is shown in the blue box in Scheme 2.4.



Scheme 2.4. General cartoon scheme showing polymerization with masked monomer in the orange box and post-polymerization modification in the blue box which is discussed in chapter 3.

Materials and Methods

Reagents were used as received and purchased from Sigma-Aldrich and Alfa Aesar. All common solvents and anhydrous drying agents were purchased from Caledon. Solvents were dried using an Innovative Technologies Inc. solvent purification system, collected under vacuum, and stored under a nitrogen atmosphere over 4 Å molecular sieves.

^1H and ^{13}C NMR spectra were recorded on a Mercury 400 MHz spectrometer. ^1H NMR spectra are reported as δ in units of parts per million (ppm) relative to CDCl_3 (δ 7.27, singlet). Multiplicities are reported as follows: s (singlet), d (doublet), t (triplet), q (quartet), quin (quintet), m (multiplet), and bs (broad signal). Coupling constants are reported as J values in Hertz (Hz). The number of protons (n) for a given resonance is indicated as $n\text{H}$ and is based on spectral integration values. ^{13}C NMR spectra are reported as δ in units of parts per million (ppm) relative to CDCl_3 (δ 77.0, t).

Infrared spectra were recorded using a Perking Elmer ATR IR spectrometer by loading sample on to diamond platform. The background was subtracted from each spectrum.

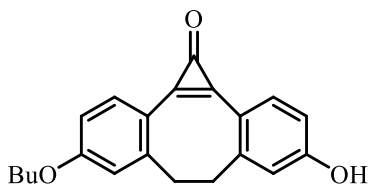
UV-Vis spectra were collected using a Varian UV-Vis spectrophotometer model Cary 300 Bio, by dissolving the sample in spectroscopic grade CH_2Cl_2 to obtain a 10^{-5} M solution. The background was subtracted from each spectrum.

GPC experiments were conducted in chromatography grade DMF at concentrations of 5 mg/mL using a Waters 2695 separations module equipped with a Waters 2414 differential refractometer and two PLgel 5 m mixed-D (300 X 7.5 mm) columns from Polymer

Laboratories connected in series. The calibration was performed using polystyrene standards purchased from Sigma Aldrich.

Thermal degradation studies were performed using a TA Instruments Q50 TGA. The sample was placed in a platinum pan and heated at a rate of 10 °C/min from 25 °C to 1000 °C under a flow of nitrogen (100 mL min⁻¹). Glass transition temperatures were determined using Differential Scanning Calorimetry (DSC) on a TA Instruments DSC Q2000. The polymer samples were placed in an aluminum Tzero pan and heated from 40 °C to 200 °C at 10 °C min⁻¹ under a flow of nitrogen (50 mL min⁻¹) and cooled down to 0 °C at 10 °C min⁻¹, before the sample underwent two more heating/cooling cycles. T_g taken from second cycle.

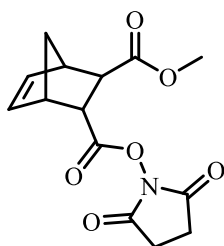
Synthesis of photo-DIBO-OH 2.9



This molecule was synthesized per procedure reported by Locklin and co-workers.¹⁰ The product was a pale yellow solid (0.99 g, 47% yield)

Photo-DIBO-OH: δ 10.42 (s, 1H), 7.77-7.75 (d, J = 8.0 Hz, 1H), 7.70-7.68 (d, J = 8.0 Hz, 1H), 7.08 (s, 1H), 7.01 - 6.98 (m, 1H), 6.90-6.89 (d, J = 4.0 Hz, 1H), 6.84-6.82 (dd, J = 8.0 & 4.0 Hz, 1H), 4.06-4.09 (t, 2H), 3.44-3.34 (m, 2H), 2.70- 2.43 (m, 2H), 1.75-1.70 (m, 2H), 1.48-1.41 (m, 2H), 0.96-0.93 (t, 3H).

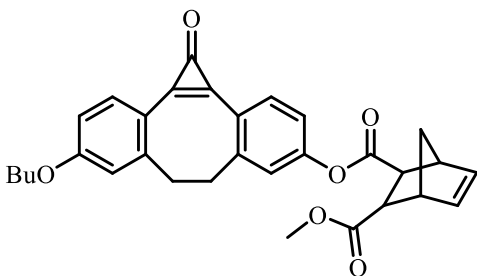
Synthesis of NHS-activated-norbornene dicarboxylate **2.12**



Compound (**2.10**) (1.00 g, 5.10 mmol), 4-dimethylaminopyridine (0.12 g, 1.02 mmol), N,N'-dicyclohexylcarbodiimide (1.26 g, 6.12 mmol), succinimide (0.70 g, 6.12 mmol) were dissolved in dry THF (40 mL) under argon. The reaction mixture was stirred at r.t. over night and monitored by TLC. The THF was evaporated, replaced with CH₂Cl₂, solids were removed by gravity filtration and the filtrate was concentrated *in vacuo*. The crude product was purified by column chromatography (5% MeOH/ CH₂Cl₂) to give compound **2.12** as a white solid (1.30 g, 87% yield).

NHS-activated norbornene dicarboxylate: ¹H NMR (CDCl₃, 400 MHz): δ 6.48 (dd, J = 5.6 & 3.1 Hz, 1H), 6.20 (dd, J = 5.6 & 2.9 Hz, 1H), 3.65 (dd, J = 10.2 & 3.5 Hz, 1H), 3.61 (s, 3H), 3.42-3.39 (m, 1H), 3.37 (dd, J = 10.2 & 3.3 Hz, 1H), 3.25-3.24 (m, 1H), 2.81 (s, 4H), 1.58 (dt, J = 8.9 Hz, 1H), 1.43-1.41 (m, 1H). ¹³C NMR (CDCl₃, 74 MHz): δ 172.0, 169.2, 168.2, 137.3, 133.5, 52.0, 49.4, 49.0, 48.1, 45.8, 44.9, 25.8. IR (ATR, cm⁻¹): 2982, 2949, 1786, 1730, 1434, 1371, 1216, 1071, 1041, 752, 649. ESI-HRMS: calculated for C₁₂H₁₅NO₆⁺ [M]⁺: 293.0899, found 293.0903. UV-Vis in CH₂Cl₂ (λ_{max} = 229 nm).

Synthesis of photo-DIBO-monomer **2.13**

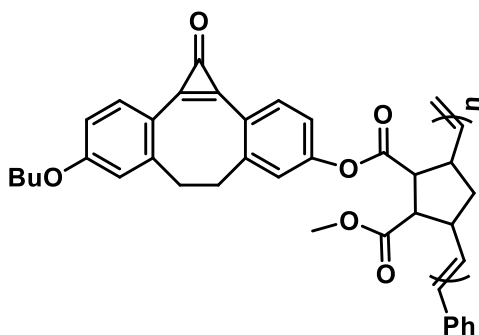


Compound (**2.9**) (0.430 g, 1.34 mmol) and K₂CO₃ (0.223 g, 1.61 mmol) were dissolved in MeCN (50 mL). Compound (**2.12**) (0.472 g, 1.61 mmol) was dissolved in CH₃CN (15 mL) and added to reaction mixture. The reaction mixture was stirred at r.t. over night, monitored by TLC and upon completion concentrated *in vacuo*. The crude product was purified by column chromatography (15% EtOAc/CH₂Cl₂) to give compound (**2.13**) as an off white solid (0.487 g, 73% yield).

Photo-DIBO-monomer: ¹H NMR (CDCl₃, 400 MHz): δ 8.01-7.96 (dd, J = 8 & 12 Hz, 2H), 7.21-7.14 (m, 2H), 6.92-6.91 (m, 2H), 6.46-6.43 (m, 1H), 6.26-6.25 (m, 1H), 4.06 (t, 2H), 3.67 (s, 3H), 3.53-3.49 (m, 2H), 3.37 (t, 3H), 3.36 (d, J = 12 Hz, 2H), 2.63-2.61 (m, 2H),

1.84-1.79 (m, 2H), 1.59-1.49 (m, 3H), 1.45-1.44 (m, 1H), 1.01 (t, 3H). ^{13}C NMR (CDCl_3 , 74 MHz): δ 172.5, 170.6, 162.3, 153.7, 153.1, 147.9, 147.0, 144.9, 141.2, 136.0, 135.5, 134.7, 134.4, 122.9, 120.9, 120.2, 116.1, 115.8, 112.3, 67.9, 51.7, 48.6, 48.2, 47.9, 46.8, 46.1, 37.2, 36.6, 30.9, 19.0, 13.7. IR (ATR, cm^{-1}): 2954, 2933, 2875, 1847, 1763, 1734, 1610, 1556, 1343, 1254, 1112. ESI-HRMS: calculated for $\text{C}_{31}\text{H}_{30}\text{O}_6^+$ $[\text{M}]^+$: 498.2042, found 498.2032. UV-Vis in CH_2Cl_2 ($\lambda_{\text{max}} = 323$ nm).

Synthesis of photoDIBO-polymer **2.14**



Under a nitrogen atmosphere, compound **2.13** (0.250 g, 0.50 mmol) was dissolved in dry CH_2Cl_2 (24.5 mL) in a schlenk flask. Grubbs III catalyst (4.4 mg, 1% mol) was also dissolved in dry and degassed CH_2Cl_2 (24.5 mL) in a separate schlenk flask. The catalyst solution was added to the monomer solution and stirred for 8 h at 25 °C. The catalyst was quenched with ethyl vinyl ether (25 equiv.) and stirred for 30 min. The catalyst was removed by column chromatography using neutral alumina (CH_2Cl_2) to give the crude polymer. The crude polymer was dissolved in CH_2Cl_2 (10 mL) and precipitated out in pentane (50 mL) at 0 °C to afford the photoDIBO-polymer **2.14** as an off white solid. Yield = 0.190 g, 76%.

Photo-DIBO-polymer: ^1H NMR (CDCl_3 , 400 MHz): δ 7.95 (bs), 7.15 (bs), 6.85 (bs), 5.27 (bm), 4.00 (bs), 3.66 (bs), 3.25 (bs), 2.50 (bs), 1.97 (bs), 1.75 (bs), 1.48 (bs), 0.97 (bs). ^{13}C NMR (CDCl_3 , 74 MHz): δ 170.4, 162.2, 153.5, 152.5, 146.8, 135.8, 134.4, 122.9, 122.7, 116.0, 115.6, 112.1, 67.7, 51.6, 48.0, 37.0 36.4, 30.8, 18.8, 13.5. IR (ATR, cm^{-1}): 2953, 2924, 2870, 1847, 1729, 1600, 1556, 1348, 1255, 1122. UV-Vis in CH_2Cl_2 ($\lambda_{\text{max}} = 322$ nm). $M_n = 41,640$ g/mol, $M_w = 87,190,800$ g/mol, $D = 2.09$.

2.4 References

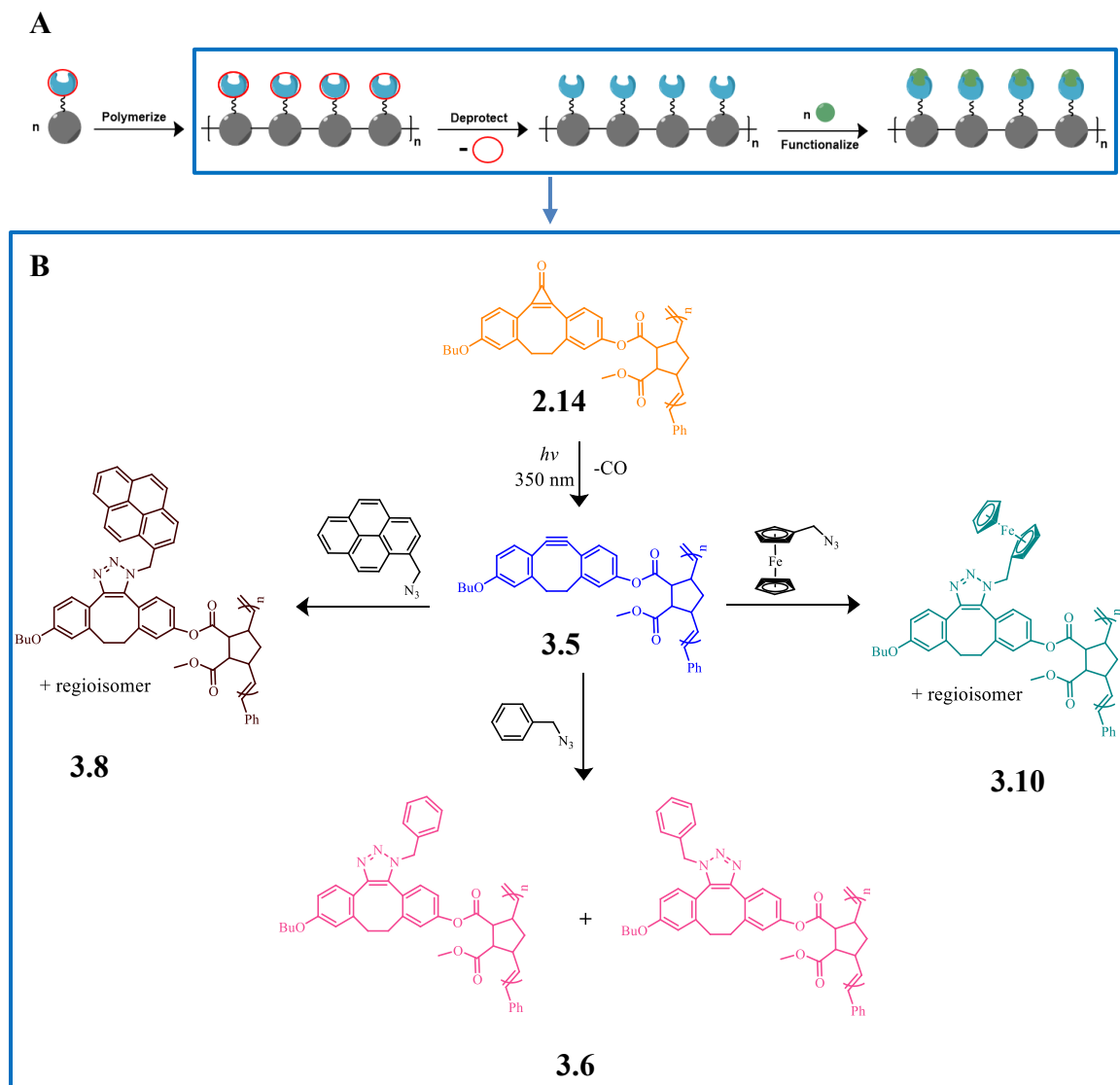
1. Du, X.; Li, L.; Li, J.; Yang, C.; Frenkel, N.; Welle, A.; Heissler, S.; Nefedov, A.; Grunze, M.; Levkin, P. A., *Adv. Mater.* **2014**, *26*, 8029-8033.
2. Cameron, D. J. A.; Shaver, M. P., *Chem. Soc. Rev* **2011**, *40*, 1761-1776.
3. Javier, A. E.; Patel, S. N.; Hallinan, J. D. T.; Srinivasan, V.; Balsara, N. P., *Angew. Chem. Int. Ed.* **2011**, *50*, 9848-9851.
4. Chiefari, J.; Chong, Y. K.; Ercole, F.; Krstina, J.; Jeffery, J.; Le, T. P. T.; Mayadunne, R. T. A.; Meijs, G. F.; Moad, C. L.; Moad, G.; Rizzardo, E.; Thang, S. H., *Macromolecules* **1998**, *31*, 5559-5562.
5. Hadjichristidis, N.; Iatrou, H.; Pispas, S.; Pitsikalis, M., *J. Polym. Sci., Part A: Polym. Chem.* **2000**, *38*, 3211-3234.
6. Higashimura, T.; Aoshima, S.; Sawamoto, M., *Macromol. Chem. Phys.* **1988**, *13-14*, 457-471.
7. Wang, X.; Song, Y.; Qu, J.; Luo, Y., *Organometallics* **2017**, *36*, 1042-1048.
8. Gleede, T.; Reisman, L.; Rieger, E.; Mbarushimana, P. C.; Rupar, P. A.; Wurm, F. R., *Polym. Chem.* **2019**, *1*, 3257-3283.
9. Bielawski, C. W.; Grubbs, R. H., *Angew. Chem. Int. Ed.* **2000**, *39*, 2903-2906.
10. Arnold, R. M.; McNitt, C. D.; Popik, V. V.; Locklin, J., *Chem. Commun.* **2014**, *50*, 5307-5309.
11. Wang, Y.; Rapakousiou, A.; Latouche, C.; Daran, J.-C.; Singh, A.; Ledoux-Rak, I.; Ruiz, J.; Saillard, J.-Y.; Astruc, D., *Chem. Commun.* **2013**, *49*, 5862.
12. Luo, W.; Gobbo, P.; McNitt, C. D.; Sutton, D. A.; Popik, V. V.; Workentin, M. S., *Chem. Eur. J.* **2017**, *23*, 1052-1059.
13. Bielawski, C. W.; Grubbs, R. H., *Prog. Polym. Sci.* **2007**, *32*, 1-29.
14. Yang, X. J.; Ren, X. L.; Li, Y. S., *Chin. J. Polym. Sci.* **2017**, *35*, 36-45.
15. Hawker, C. J.; Bosman, A. W. T.; Harth, E., *Chem. Rev.* **2001**, *101*, 3661-3688.

3 Polymer Post-Polymerization Functionalization

3.1 Introduction

In recent decades, post-polymerization modification (PPM) has garnered a lot of interest because in principle, with proper design considerations, a bulk polymer can be synthesized and modified as physically and chemically desired. Click chemistry, coined by Sharpless and co-workers,¹ provides an accessible way to perform PPM.² As previously mentioned, some click reactions include the thiol-ene addition,³ Diels-Alder cycloaddition,⁴ copper assisted alkyne-azide cycloaddition,⁵ and SPAAC.⁶ In this chapter, SPAAC will be the main focus for PPM because it fulfills the click chemistry criteria by producing compounds in high yields, occurring under mild conditions, producing chemo-selective products and as an added benefit does not require the use of a catalyst or initiator.⁷ Although the reactivity of the strained alkyne is desired, it is susceptible to side reactivity such as nucleophilic attack,⁸ making the development of orthogonal reaction chemistry a difficult challenge. To overcome this problem, the strained alkyne masking/unmasking via a cyclopropanone strategy developed by Popik and co-workers will be employed.⁹ The cyclopropanone was used to mask the strained alkyne during the polymerization process, but can be unmasked by UV irradiation. The advantages for the unmasking strategy are that only CO gas is evolved, no purification is required and, because it is photochemically initiated, there is the possibility for spatial and temporal control.⁹ The polymerization method outlined in Chapter 2 showed that the target polymer was made, and the masking group remained intact during the polymerization. Chapter 3 will focus on the unmasking of the strained alkyne for both the monomer and polymer and subsequent SPAAC with benzyl azide as a model reaction, azidomethyl pyrene to highlight the introduction of a

redox-active group and azidomethyl ferrocene to highlight the introduction of an emissive group, as shown in Scheme 3.1. The modified monomers were characterized by ^1H NMR, ^{13}C NMR, IR, UV-Vis spectroscopy, and MS. The modified polymers were characterized by ^1H NMR, ^{13}C NMR, IR, UV-Vis spectroscopy, GPC, TGA and DSC.



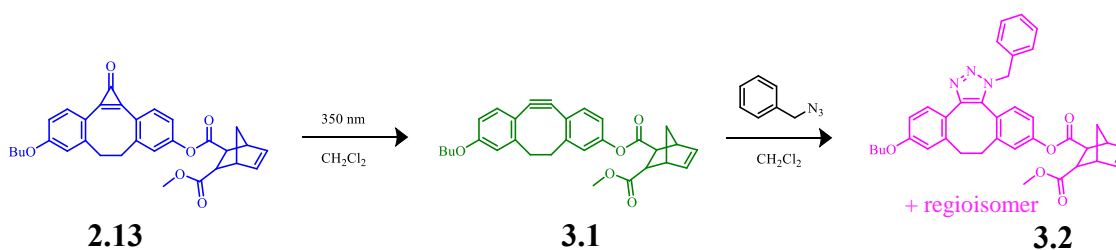
Scheme 3.1. General strategy showing polymerization with masked monomer and post-polymerization modification (**A**). General scheme for the different click partners with DIBO-polymer **3.5** to highlight PPM introduction of different functionalities (**B**).

3.2 Photo-unmasking and SPAAC reaction involving the photoDIBO-monomer **2.13** and photoDIBO-polymer **2.14**

Before proceeding to the photo-unmasking of the photoDIBO-polymer **2.14** and introduction of SPAAC PPM functionalities to the DIBO-polymer **3.5**, the photo-unmasking and SPAAC was investigated on the photoDIBO-monomer **2.13** and DIBO-monomer **3.1** as a control.

3.2.1 Photo-unmasking and SPAAC with benzyl azide as a model reaction

After the photo-DIBO-monomer **2.13** was synthesized, it was unmasked with UV irradiation at 350 nm to give the DIBO-monomer **3.1** followed by SPAAC with benzyl azide (Scheme 3.2). The unmasking was tracked by UV-Vis Spectroscopy with an initial UV-Vis spectrum taken before irradiation (0 min) where the concentration of the monomer **2.13** was 80 μM in CH_2Cl_2 . Then, a solution of the photo-DIBO-monomer **2.13** was placed in a photochemical Luzchem reactor fitted with 350 nm lamps and irradiated for 2 min. The UV-vis spectra of the solution after irradiation showed the disappearance of the 323-341 nm bands corresponding to the cyclopropanone masked monomer **2.13** and appearance of 303-318 nm bands corresponding to the unmasked strained alkyne monomer **3.1** via loss of the C=O highlighted by the green UV-Vis spectrum. The UV-Vis spectrum showed that there was no presence of starting material remaining (Figure 3.1). The photo-unmasking strategy is consistent with literature results developed by Popik and coworkers⁹ and the masking/unmasking strategy, previously reported by the Workentin group on AuNPs.¹⁰



Scheme 3.2. Photo-unmasking of the photoDIBO-monomer **2.13** (blue) and SPAAC reaction between DIBO-monomer **3.1** (green) and BzN₃ yielding benzyltriazole-monomer **3.2** (purple).

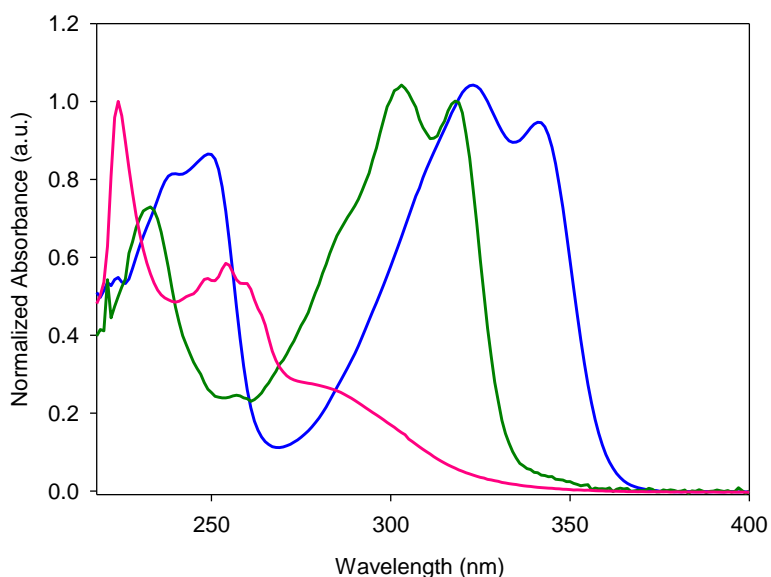


Figure 3.1. UV-Vis Spectra for the photoDIBO-monomer **2.13** (blue), DIBO-monomer **3.1** (green) and benzyltriazole-monomer **3.2** (purple) to highlight unmasking and SPAAC.

In addition to UV-Vis spectroscopy, ¹H NMR spectroscopy was also used to check that the unmasking reaction was a success. The phenyl protons on the photoDIBO-monomer **2.13** show up at 6.92-6.91 ppm as a multiplet, 7.21-7.15 ppm as a multiplet and 7.99 ppm as a doublet of doublet shown in the ¹H NMR spectrum of Figure 3.2A. After the irradiation, the new phenyl protons appear as five separate multiplet peaks; 6.79-6.76 ppm, 6.99-6.89 ppm, 6.99-6.97 ppm, 7.09-7.07 ppm and 7.24-7.22 ppm shown in Figure 3.2B

corresponding to the DIBO phenyl protons. ^{13}C NMR spectroscopy showed the loss of peaks 162.3 ppm and 141.2 ppm which correspond to the C=O and C=C of the cyclopropenone, respectively.

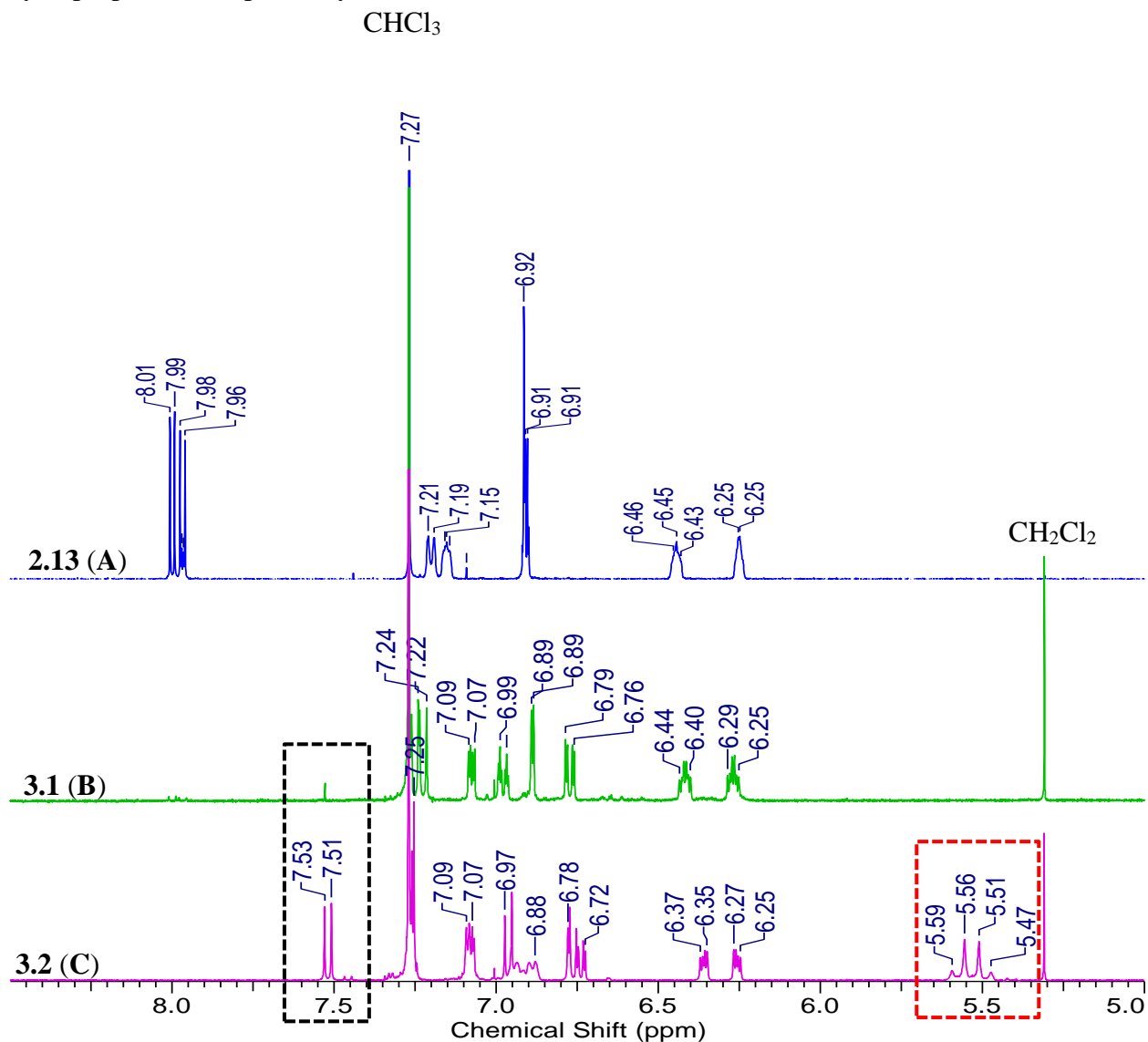


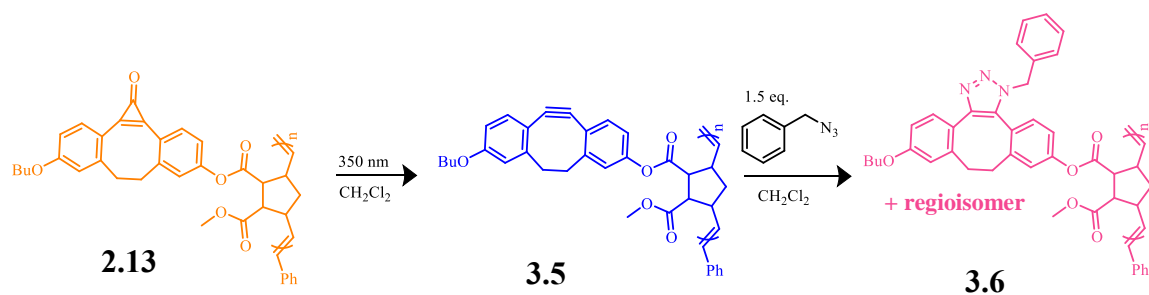
Figure 3.2. ^1H NMR spectra for the photoDIBO-monomer **2.13** (A), DIBO-monomer **3.1** (B) and benzyltriazole-monomer **3.2** (C) to highlight unmasking and SPAAC. The black box represents the addition of phenyl peaks from the benzyl azide and DIBO-monomer **3.5**. The red box indicates the benzylic CH_2 peaks from the benzyltriazole-monomer **3.2**.

Finally, IR spectroscopy shows the loss of the C=O at 1842 cm^{-1} and appearance of the C \equiv C stretch at 2169 cm^{-1} in compound **3.1**, which also indicates the loss of the cyclopropenone masking group and appearance of the strained alkyne. The unmasking of **2.13** was a model reaction to investigate the efficiency of this to give the strained alkyne, which was shown to be clean, fast and high yielding.

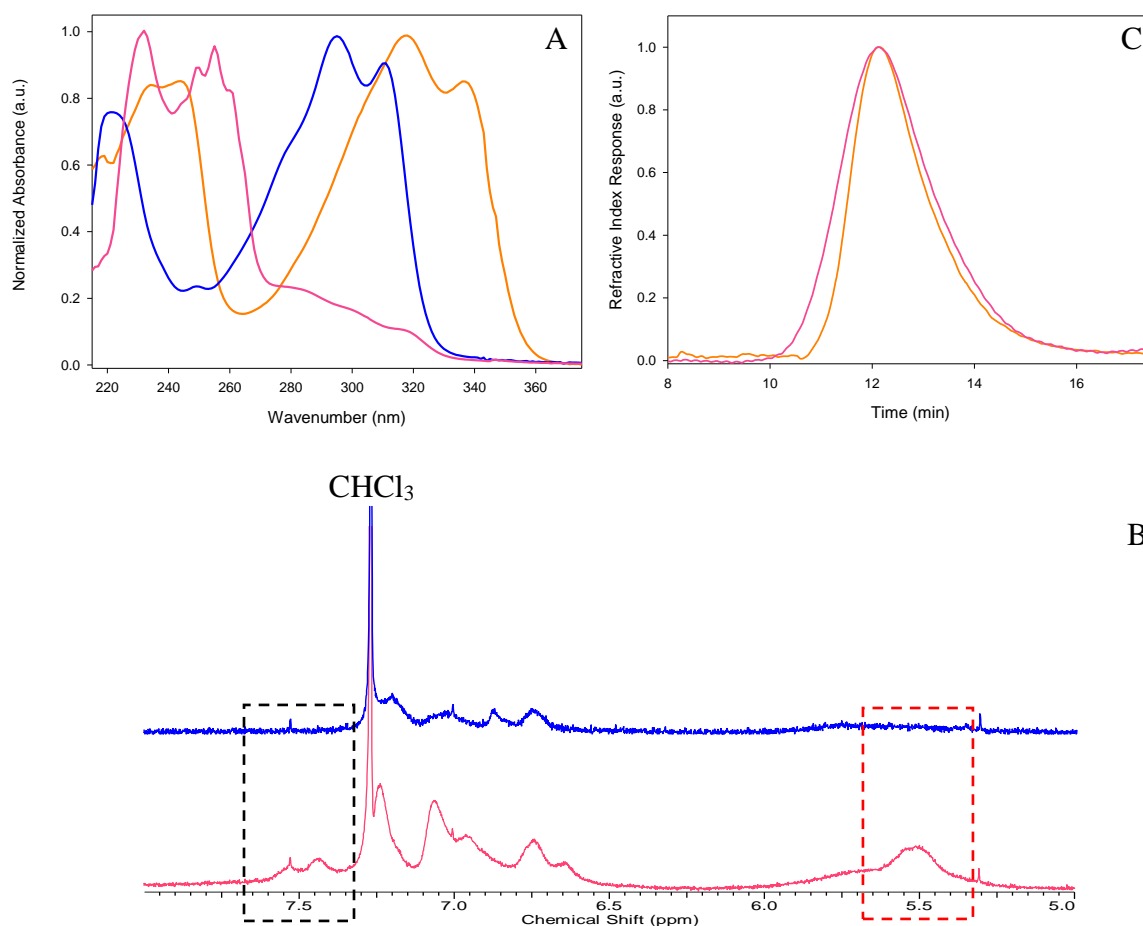
The SPAAC reactivity of the DIBO-monomer **3.1** was investigated using benzyl azide (BzN₃) as a model molecule because of its low cost, commercial availability and high reactivity in solution.¹¹ The reaction was monitored using UV-Vis and ¹H NMR spectroscopy. An initial UV-Vis spectrum was taken at 0 min for the DIBO-monomer **3.1** (80 μM) in CH₂Cl₂. Then 1.5 eq. of BzN₃ was added to the DIBO-monomer **3.1** solution and stirred for 30 min (Scheme 3.2). The UV-Vis spectrum of the clicked product showed the disappearance of 311 nm bands highlighted by the purple UV-Vis spectrum in Figure 3.1 indicating that that the DIBO-monomer **3.1** had been completely consumed. This was further confirmed by ¹H NMR spectroscopy (Figure 3.2C), the spectrum included additional multiplets in the aromatic region corresponding to phenyl protons shown in the dashed black box, and a doublet at 5.54 ppm corresponding to the benzylic protons adjacent to the triazole ring shown in the dashed red box. These results together confirm that the SPAAC reaction proceeded effectively to afford the benzyltriazole-clicked-monomer **3.2**. It is worth noting that that regioisomers were formed with this click reaction as expected. The presence of regioisomers was confirmed by the benzylic CH₂ peaks of the benzyl azide being split into a multiplet instead of being a doublet at 5.54 ppm on the ¹H NMR spectrum.

After the successful model reaction of benzyl azide with the monomer **2.13**, polymer **2.14** was unmasked with 350 nm light in the Luzchem reactor and then reacted

with 1.5 eq. benzyl azide as shown in Scheme 3.3. After the addition of benzyl azide, the reaction was checked after 30 min but there was still presence of the 311 nm bands indicating that the strained alkyne was not completely consumed, so the reaction was left over night (12 h), which was enough time for the reaction because there was the complete disappearance of the 311 nm bands (Figure 3.3A). This indicated that there was no unreacted strained alkyne remaining from polymer **3.6** in the reaction mixture. This matched what was observed previously in the model reaction of the monomer in Figure 3.1. Since 1.5 eq of benzyl azide was added to the reaction, polymer **3.6** was purified by precipitation at 0 °C into rapidly stirred pentane and isolated via centrifugation. The success of the benzyl azide click reaction was also confirmed by ¹H NMR spectroscopy (Figure 3.3B). There were additional broad multiplets in the aromatic region corresponding to phenyl protons from the addition of the benzyl group (shown in the black box), and a broad doublet at 5.54 ppm corresponding to the benzylic protons (shown in the red box) adjacent to the triazole ring. GPC data also showed an increase in the molecular weight (M_n) from 41,640 g/mol for polymer **2.14** to $M_n = 44,780$ g/mol for polymer **3.6** signifying that the click reaction had occurred because of the expected increase in molecular weight (Figure 3.3C). Thermogravimetric analysis (TGA) and differential scanning calorimetry (DSC) were also conducted on the benzyltriazole-clicked-polymer **3.6**. The TGA data (Figure A.3.17) showed that there were 2 steps involved in the decomposition of polymer **3.6** and the initial step of decomposition was 195 °C. DSC (Figure A.3.18) did not reveal a glass transition temperature (T_g) within the thermal stability of the polymer.

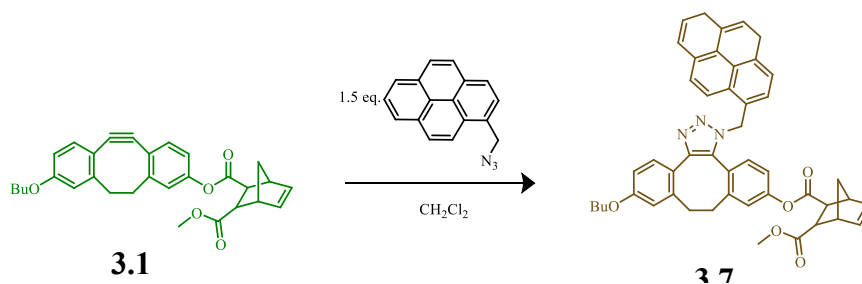


Scheme 3.3. Photo-unmasking of the photoDIBO-polymer **2.14** (orange) and SPAAC reaction between DIBO-polymer **3.5** (blue) and BzN₃ yielding benzyltriazole-DIBO-polymer **3.6** (light purple).



3.2.2 SPAAC with azidomethyl pyrene and fluorescence study

The photo-unmasking of the monomer **2.13** and polymer **2.14** and subsequent SPAAC with benzyl azide proceeded cleanly and efficiently served as successful model reactions, to explore the methodology for PPM and introduce functionality. The photoDIBO-monomer **2.13** and photoDIBO-polymer **2.14** were photo-unmasked and clicked with azidomethyl pyrene to bring emissive functionality to the polymer **2.14**. The exact same conditions were used from the model benzyl azide reaction. Again, the masking was tracked by UV-vis spectroscopy where the concentration of the monomer **2.13** was 80 μM in CH_2Cl_2 . After a successful unmasking of the monomer **2.14**, 1.5 eq. azidomethyl pyrene was added to the DIBO-monomer **3.5** solution, shown in Scheme 3.4. The UV-Vis spectrum of the clicked product showed the disappearance of the 303-318 nm bands highlighted by the brown spectrum in Figure 3.4A indicating that the DIBO-monomer **3.1** had been completely consumed. The new pyrene-clicked-monomer **3.7** had absorptions at $\lambda_{\text{max}} = 244, 270$ and 335 nm which are characteristic of pyrene.¹² This was further confirmed by ^1H NMR spectroscopy (Figure 3.4B). The ^1H NMR spectrum displayed additional peaks in the aromatic region corresponding to the pyrene protons highlighted in the black box at 8.19-7.51 ppm and the bridge $-\text{CH}_2-$ protons in the red box at 5.85 ppm in Figure 3.4B. These results, along with MS confirm that the SPAAC reaction proceeded cleanly to afford the pyrene-clicked-monomer **3.7**. Regioisomers were also formed, as confirmed by the olefin peaks highlighted in the red box in Figure 3.4B being split into a multiplet at 6.37-6.23 ppm in the ^1H NMR spectrum.



Scheme 3.4. SPAAC reaction between DIBO-monomer **3.1** (green) and azidomethyl pyrene yielding the pyrene-clicked-monomer **3.7** (light brown).

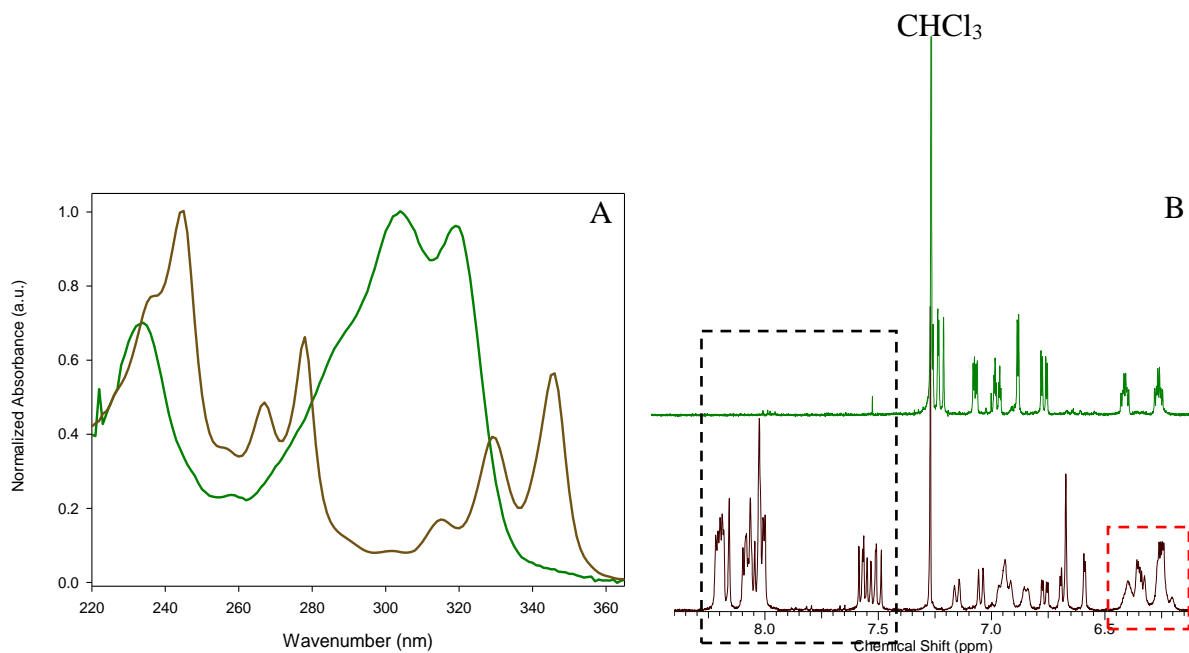
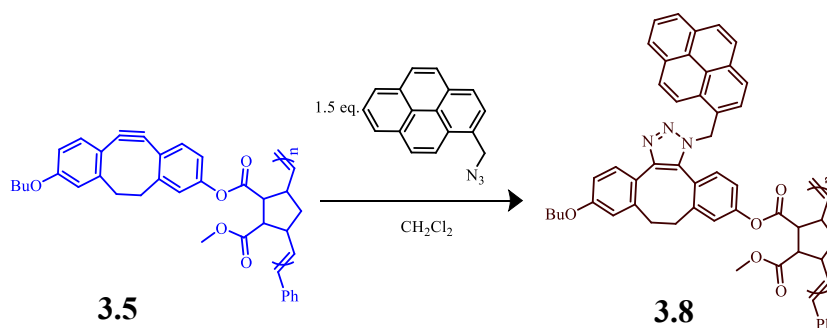


Figure 3.4. UV-Vis spectra (A) and ^1H NMR spectra (B) for the DIBO-monomer **3.1** (green) and pyrene-clicked-monomer **3.7** (light brown) to highlight SPAAC. The black and red boxes are discussed in the text.

The photoDIBO-polymer **2.14** was also unmasked and clicked with 1.5 eq azidomethyl pyrene under the same conditions as the monomer **3.1**. The UV-Vis spectra, shown in Scheme 3.5, were virtually identical as the pyrene-clicked-monomer **3.7** photo-unmasking and click reaction where the 311 nm bands of the DIBO-polymer **3.5** disappeared and the appearance of the characteristic absorption bands of pyrene for the new pyrene-clicked-

polymer **3.8** shown in Figure 3.6A. The resulting polymer **3.8** was purified by precipitation into rapidly stirred pentane at 0 °C and centrifugation to remove the excess azidomethyl pyrene. The click reaction between the azidomethyl pyrene and polymer **3.5** was also confirmed by ¹H NMR spectroscopy with additional broad aromatic peaks in the 8.21-7.40 ppm region highlighted by the black box in Figure 3.6B. There was some discrepancy in the GPC data because the M_n showed a slight decrease in molecular weight (M_n) from photoDIBO-polymer **2.14** $M_n = 41,640$ g/mol to pyrene-clicked-polymer **3.8** $M_n = 41,300$ g/mol in Figure 3.6C. This is unusual but it could be due to polymer-solvent interactions.¹³ The polymer may not be very soluble in DMF causing itself to coil and appearing as lower molecular weight polymer. Fortunately, the UV-Vis and ¹H NMR spectroscopy did confirm that click reaction was a success. A fluorescence study was performed on the pyrene-clicked-monomer **3.7** and pyrene-clicked-polymer **3.8**, which will be discussed in a later section. Thermogravimetric analysis (TGA) and differential scanning calorimetry (DSC) were also conducted on the pyrene-clicked-polymer **3.8**. The TGA data (Figure A.3.29) showed that there were 3 steps involved in the decomposition of the polymer **3.8** and the initial step of decomposition was 265 °C. DSC (Figure A.3.30) did not show a T_g within the thermal stability window of polymer **3.8**.



Scheme 3.5. SPAAC reaction between DIBO-polymer **3.5** (blue) and azidomethyl pyrene yielding the pyrene-clicked-polymer **3.8** (dark brown).

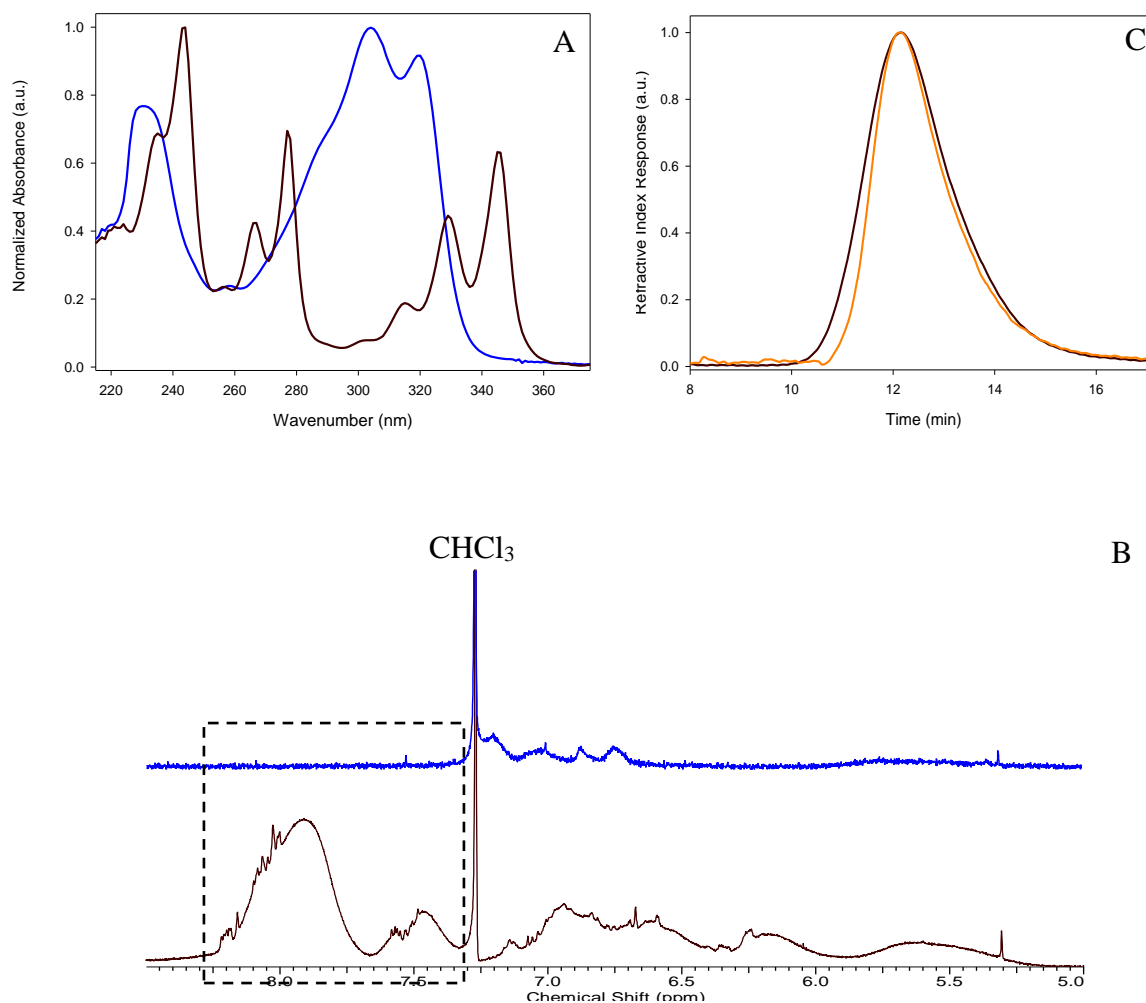


Figure 3.5. UV-Vis spectra (A) of the DIBO-polymer **3.5** (blue) and pyrene-clicked-polymer **3.8** (light brown) to highlight the click reaction with azidomethyl pyrene. ^1H NMR spectra (B) for the DIBO-polymer **3.5** (blue) and pyrene-clicked-polymer **3.8** (light brown). GPC traces (C) of the photoDIBO-polymer **2.14** (orange) and pyrene-clicked-polymer **3.7** (light brown).

The fluorescence properties of the pyrene-clicked-monomer **3.7** and the pyrene-clicked-polymer **3.8** were also studied. The normalized absorption profile (solid line) and the emission spectra (dotted line) are shown in Figure 3.7A and 3.7B for the monomer **3.7** and polymer **3.8**, respectively. The pyrene monomer **3.7** shows an absorption profile with a $\lambda_{\text{max}} = 244$ nm and emission peaks 373, 384 and 394 nm at an excitation wavelength of 345 nm, as expected for the pyrene emission.¹² The pyrene polymer **3.8** showed a virtually identical absorption profile relative to the monomer **3.7**. In addition to the monomer pyrene emission, a broad peak can be seen centered at 479 nm in the emission spectrum, which is distinctive of pyrene excimer formation.¹⁴ The emission spectrum of polymer **3.8** is not unexpected because the pendant repeating units are in close proximity meaning that once every repeating unit is functionalized, excimer formation is very favorable.

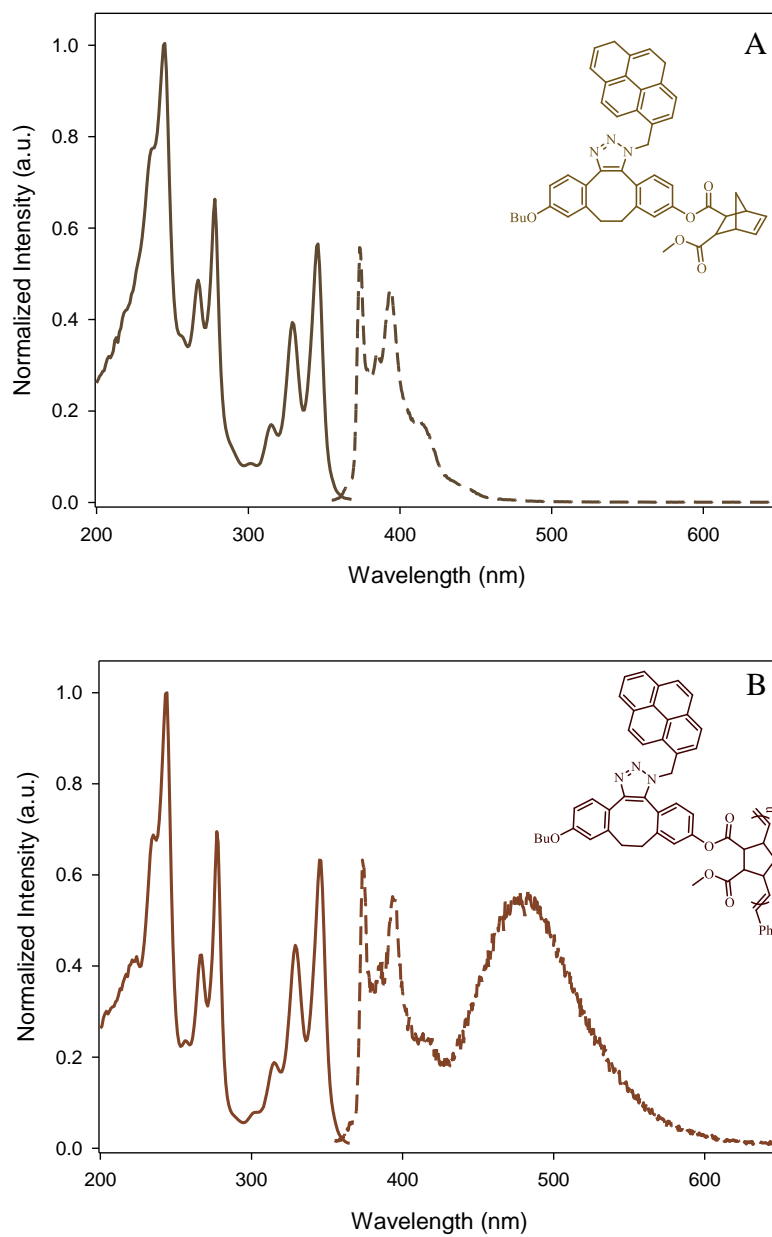
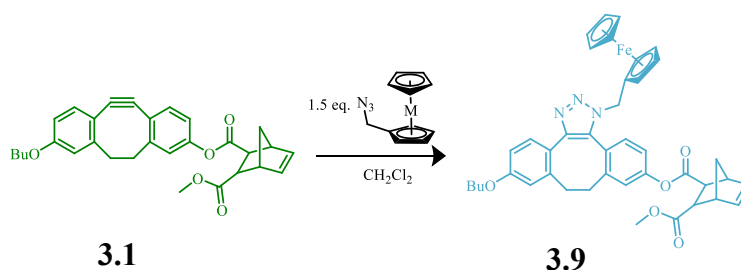


Figure 3.6. UV-Vis absorption spectra (solid line) and emission spectra (dashed line) of the pyrene-clicked-monomer **3.7** (A) and pyrene-clicked-polymer **3.8** (B), recorded in degassed CH_2Cl_2 at a concentration of 10^{-6} M.

3.2.3 SPAAC with azidomethyl ferrocene and Cyclic Voltammetry study

The DIBO-monomer **3.1** and DIBO-polymer **3.5** was also clicked with azidomethyl ferrocene to bring redox active functionality. The exact same conditions were used from the model benzyl azide click reaction and azidomethyl pyrene click reactions. Once the unmasking of the photo-DIBO-monomer (80 μ M in CH_2Cl_2) **2.13** was complete and verified by UV-Vis spectroscopy, 1.5 eq. azidomethyl ferrocene was added to the DIBO-monomer **3.1** shown in Scheme 3.6. The UV-Vis spectrum of the ferrocene-clicked product **3.9** showed the disappearance of the 303-318 nm bands highlighted by the light blue colored spectrum in Figure 3.7A indicating that the strained alkyne **3.1** had been completely consumed and the new ferrocene-clicked-monomer **3.9** had a relatively featureless absorption spectrum.¹⁵ This was further confirmed by ^1H NMR spectroscopy (Figure 3.7B). The ^1H NMR spectrum of the ferrocene-clicked-monomer **3.9** showed that the phenyl protons (black box) split differently than the phenyl protons of the DIBO-monomer **3.1**, although both show complex multiple splitting, the range of the phenyl protons of the ferrocene monomer **3.9** range from 7.48-6.63 ppm versus the DIBO-monomer **3.1** where the phenyl proton range is narrow from 7.26-6.77 ppm due to the presence of a different proton environment. The $-\text{CH}_2-$ bridge protons adjacent to the ferrocene highlighted in the red box show up as a broad singlet at 5.26 ppm and finally the metallocene protons from the ferrocene show up at 4.29-4.09 ppm which is consistent with literature data.¹⁶ The UV-vis data, the ^1H NMR data along with MS all confirm that the SPAAC reaction with azidomethyl ferrocene was a clean and efficient reaction affording the ferrocene-click-monomer **3.9**. Regioisomers were also formed, which was confirmed by ^1H NMR spectroscopy. The olefin proton peaks highlighted in the blue box at 6.47-6.25

ppm in Figure 3.7B undergo a more complex multiplet splitting than the olefin peaks in the DIBO-monomer **3.1** ^1H NMR spectrum.



Scheme 3.6. SPAAC reaction between DIBO-monomer **3.1** (green) and azidomethyl ferrocene yielding the ferrocene-clicked-monomer **3.9** (light blue).

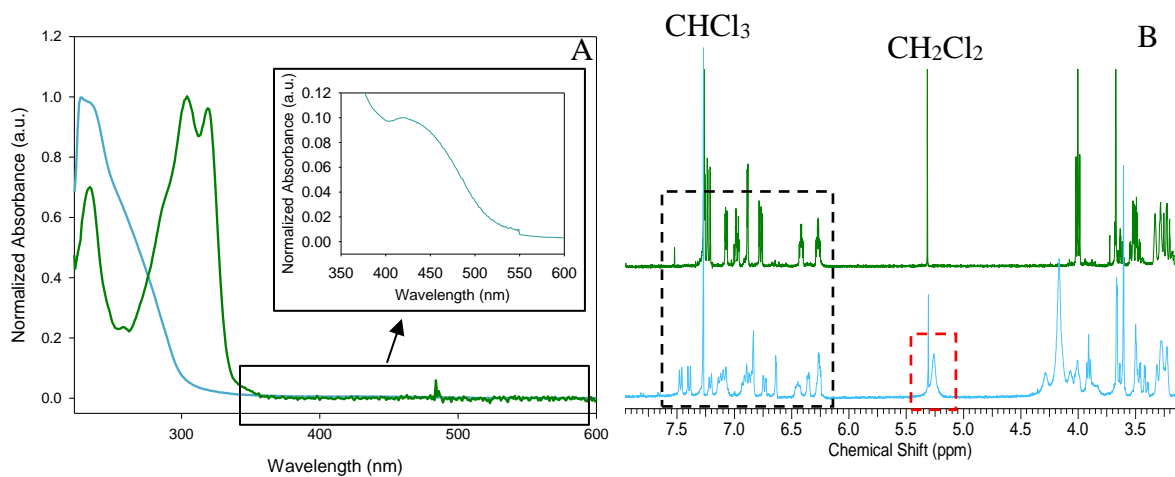
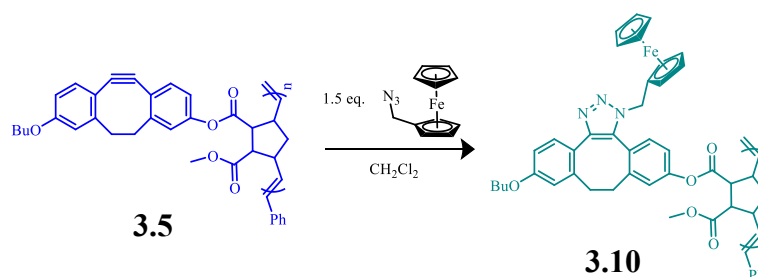


Figure 3.7. UV-Vis spectra (A) and ^1H NMR spectra (B) for the DIBO-monomer **3.1** (green) and the ferrocene-clicked-monomer **3.9** (light blue) to highlight SPAAC. The inset is a zoom in of the ferrocene-clicked-monomer **3.9** (light blue) at a higher concentration of $7.00\text{E-}4$ M representing the $d \rightarrow d$ transition of Ferrocene.

The photo-DIBO-polymer **2.14** was also unmasked and clicked with 1.5 eq. azidomethyl ferrocene shown in Scheme 3.7 under the same conditions as the ferrocene-clicked-monomer **3.9**. The UV-Vis spectrum of the ferrocene-clicked-polymer **3.10** was virtually identical to the ferrocene-clicked-monomer's **3.9** UV-Vis spectrum shown in Figure 3.8A.

The resulting polymer **3.10** was purified by precipitation into rapidly stirred pentane at 0 °C and centrifugation to remove the excess azidomethyl ferrocene. The click ferrocene reaction was also confirmed by ¹H NMR spectroscopy. The splitting pattern for the phenyl protons from the ferrocene-clicked-polymer **3.10** show broad peaks from 7.49-6.64 ppm whereas the splitting pattern for the DIBO-monomer **3.5** show broad splitting in the 6.75-5.24 ppm region, the bridge -CH₂- ferrocene protons show up as broad singlet at 5.25 ppm denoted by the black box and the metallocene protons¹⁶ show up as a broad multiplet at 4.25-4.02 ppm highlighted in the red box (Figure 3.8B). The GPC data also showed an increase molecular weight (M_n) for the ferrocene-clicked polymer **3.10** M_n = 45,020 g/mol, whereas the photoDIBO-polymer **2.14** M_n = 41,640 g/mol (Figure 3.8C). Thermogravimetric analysis (TGA) and differential scanning calorimetry (DSC) were also conducted on the ferrocene-clicked-polymer **3.10**. The TGA data (Figure A.3.42) showed that there were 3 steps involved in the decomposition of polymer **3.10** and the initial step of decomposition was 316 °C. DSC (Figure A.3.43) did not show a T_g within the stability window of polymer **3.10**.



Scheme 3.7 SPAAC reaction between the DIBO-polymer **3.5** (blue) and azidomethyl ferrocene yielding ferrocene-clicked-polymer **3.10** (turquoise).

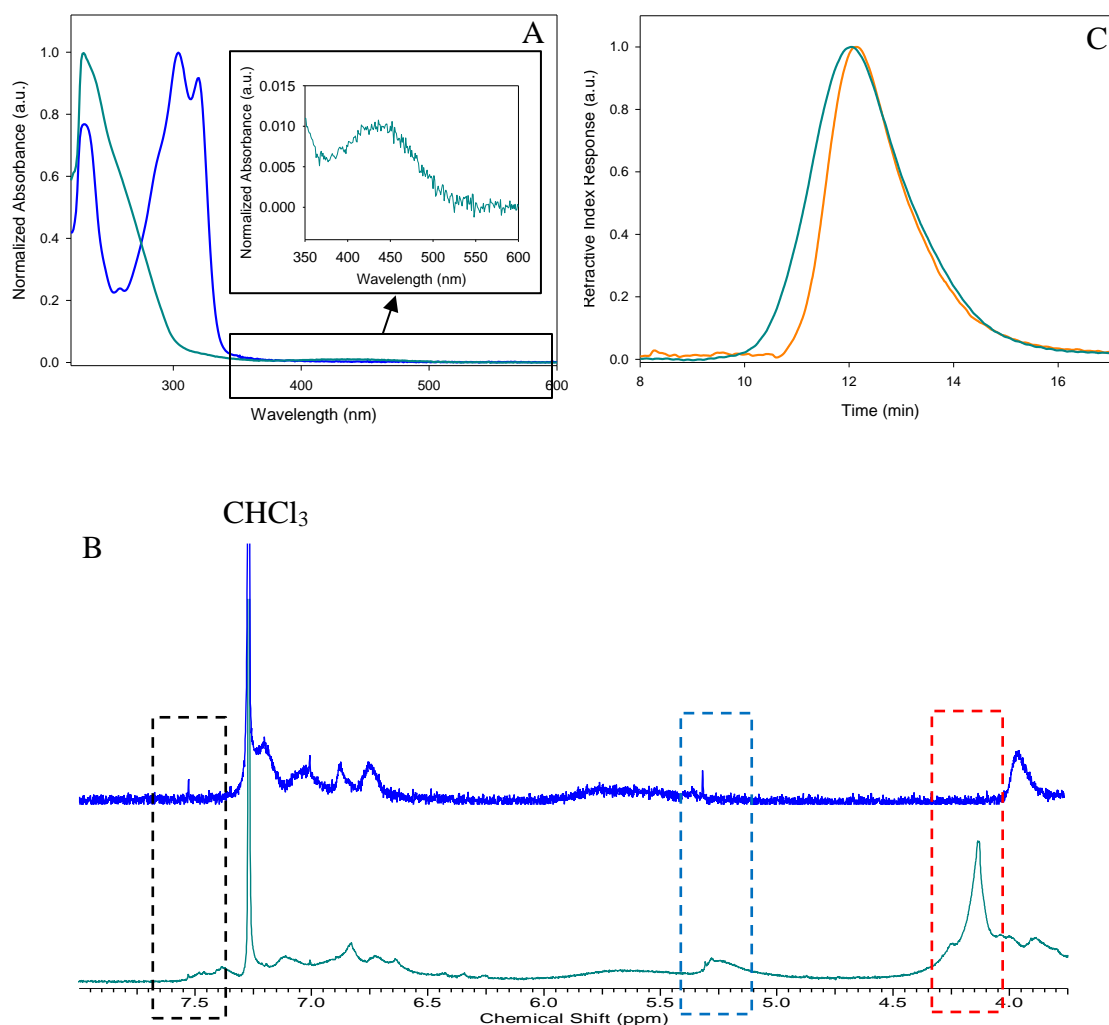


Figure 3.8. UV-Vis spectra (A) of the DIBO-polymer **3.5** (blue), ferrocene-clicked-polymer **3.10** (turquoise) to highlight deprotection and SPAAC. The inset is a zoom in of the ferrocene-clicked-polymer **3.10** (light blue) representing the d → d transition of Ferrocene. ^1H NMR spectra (B) of the DIBO-polymer **3.5** (blue) and ferrocene-clicked-polymer **3.10** (turquoise). GPC traces (C) of the photoDIBO-polymer **2.13** (orange) and ferrocene-clicked-polymer **3.10** (turquoise).

Cyclic voltammetry studies of the model ferrocene-clicked-monomer **3.9** and ferrocene-clicked-polymer **3.10** were also performed. The CVs were measured with decamethyl ferrocene as an internal standard because monomer **3.9** and polymer **3.10** already had ferrocene incorporated into it. The data was further compared to decamethyl ferrocene and ferrocene under identical conditions. The ΔE_p value was 0.068 V, which are close to the value 0.059 V that satisfies the Nernst equation for the oxidation. The ferrocene-clicked-monomer **3.9** was reversibly oxidized to the corresponding ferrocenium-clicked-monomer (Figure 3.9) at $E^{\circ}_{ox} = 0.06$ V (light blue CV) relative to the ferrocene/ferrocenium redox couple as a reversible wave which is consistent with literature data.¹⁶ The ferrocene-clicked-polymer complex **3.10** was reversibly oxidized to its polycation form (Figure 3.9) at $E^{\circ}_{ox} = 0.02$ V (turquoise spectrum). However, the ferrocene polymer **3.10** does not show the same electrochemical behavior as the ferrocene monomer **3.9**. The ferrocene-polymer **3.10** behaves like a surface wave¹⁷ rather than a reversible wave as the ferrocene monomer **3.9** does, which could be due to the ferrocene polymer **3.10** being adsorbed onto the electrode surface or precipitation of the polycationic form at the electrode interface, limiting diffusion.

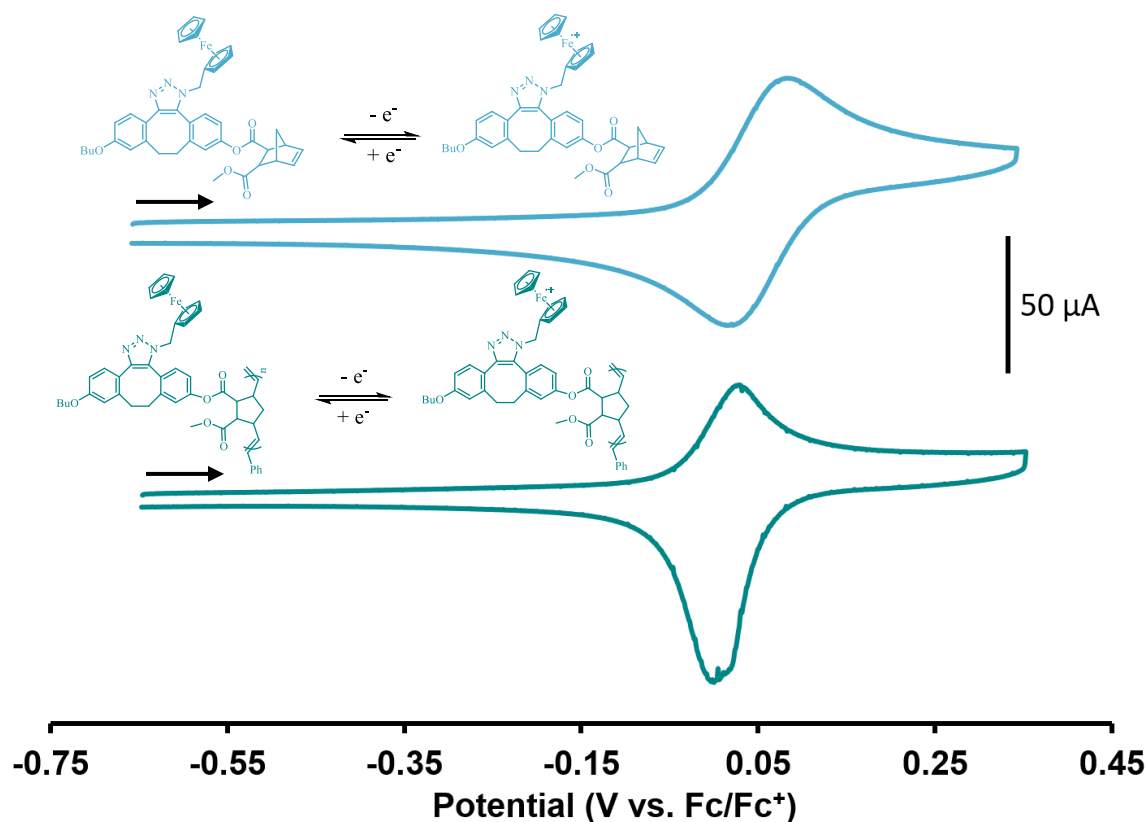


Figure 3.9 CVs of compounds **3.9** and **3.10** recorded in dry, degassed CH_2Cl_2 containing ~ 1 mM analyte and 0.1 M $[\text{nBu}_4\text{N}][\text{PF}_6]$ as a supporting electrolyte at a scan rate of 250 mV/s. The arrows indicate the scan direction.

3.3 Conclusion

The goal of the work presented in Chapter 3 was to expand the scope of post-polymerization functionalization of a ROMP, strained alkyne polymer. The photoDIBO-monomer **2.13** and polymer **2.14** were cleanly and efficiently unmasked and clicked with benzyl azide in good yield as a model reaction, to explore the methodology for PPM and introduce different types of functionality. The success of the model reactions was

confirmed by ^1H NMR spectroscopy, IR spectroscopy, UV-Vis spectroscopy and GPC. Subsequently the monomer **2.13** and polymer **2.14** were also unmasked and clicked with azidomethyl pyrene to show emissive properties and with azidomethyl ferrocene to show redox properties. The pyrene-clicked-monomer **3.7** and pyrene-clicked-polymer **3.8** formation were also confirmed by ^1H NMR spectroscopy, IR spectroscopy, UV-Vis spectroscopy and GPC. The fluorescence study showed excimer formation for polymer **3.8** which was expected due to the close proximity of the repeating units. The ferrocene-clicked-monomer **3.9** and ferrocene-clicked-polymer **3.10** formation were also confirmed by ^1H NMR spectroscopy, IR spectroscopy, UV-Vis spectroscopy and GPC. The cyclic voltammetry study showed that the monomer **3.9** behaved as a reversible wave¹⁸ and the polymer behaved as a surface wave relative to ferrocene. In Chapter 3, it was demonstrated that the PPM of the monomer **2.13** and polymer **2.14** is a clean and efficient process.

3.4 Experimental

Reagents were used as received and purchased from Sigma-Aldrich and Alfa Aesar. All common solvents and anhydrous drying agents were purchased from Caledon. Solvents were dried using an Innovative Technologies Inc. solvent purification system, collected under vacuum, and stored under a nitrogen atmosphere over 4 Å molecular sieves.

^1H and ^{13}C NMR spectra were recorded on a Mercury 400 MHz spectrometer. ^1H NMR spectra are reported as δ in units of parts per million (ppm) relative to CDCl_3 (δ 7.27, singlet). Multiplicities are reported as follows: s (singlet), d (doublet), t (triplet), q (quartet), quin (quintet), m (multiplet), and bs (broad signal). Coupling constants are reported as J values in Hertz (Hz). The number of protons (n) for a given resonance is indicated as $n\text{H}$

and is based on spectral integration values. ^{13}C NMR spectra are reported as δ in units of parts per million (ppm) relative to CDCl_3 (δ 77.0, t).

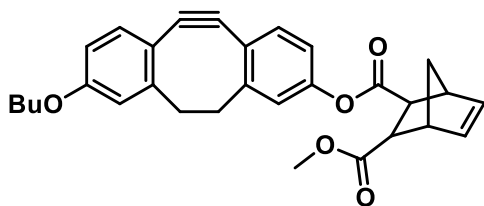
Infrared spectra were recorded using a Perking Elmer ATR IR spectrometer by loading a sample on to diamond platform. The background was subtracted from each spectrum.

UV-Vis spectra were collected using a Varian UV-Vis spectrophotometer model Cary 300 Bio by dissolving the sample in spectroscopic grade CH_2Cl_2 to obtain a 10^{-6} M solution. The background was subtracted from each spectrum.

GPC experiments were conducted in chromatography grade DMF at concentrations of 5 mg mL^{-1} using a Waters 2695 separations module equipped with a Waters 2414 differential refractometer and two PLgel 5 m mixed-D (300 x 7.5 mm) columns from Polymer Laboratories connected in series. The calibration was performed using polystyrene standards purchased from Sigma Aldrich.

Thermal degradation studies were performed using a TA Instruments Q50 TGA. The sample was placed in a platinum pan and heated at a rate of $10\text{ }^\circ\text{C}/\text{min}$ from $25\text{ }^\circ\text{C}$ to $1000\text{ }^\circ\text{C}$ under a flow of nitrogen ($100\text{ mL}/\text{min}$). Glass transition temperatures were determined using Differential Scanning Calorimetry (DSC) on a TA Instruments DSC Q2000. The polymer samples were placed in an aluminum Tzero pan and heated from $40\text{ }^\circ\text{C}$ to $200\text{ }^\circ\text{C}$ at $10\text{ }^\circ\text{C}/\text{min}$ under a flow of nitrogen ($50\text{ mL}/\text{min}$) and cooled down to $0\text{ }^\circ\text{C}$ at $10\text{ }^\circ\text{C}/\text{min}$, before the sample underwent two more heating/cooling cycles. T_g taken from first cycle.

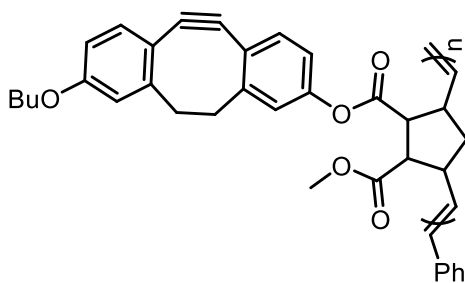
Synthesis of DIBO-monomer 3.1



Compound (**2.13**) (9.80 mg, 0.02 mmol) was dissolved in glass distilled CH_2Cl_2 (250 mL) and purged with argon for 15 min. The solution was irradiated in the photochemical Luzchem rayonet reactor using 350 nm UV light. Compound (**3.1**) was isolated as a pale-yellow oil (9.30 mg, 99% yield) with no further purification required.

DIBO-monomer: ^1H NMR (CDCl_3 , 400 MHz): δ 7.24 (dd, $J = 10.2$ & 8.3 Hz, 2H), 7.08 (dd, $J = 5$ & 2.3 Hz, 1H), 6.98 (dt, $J = 8.3$ Hz, 1H), 6.89 (d, $J = 2.5$ Hz, 1H), 6.78 (dd, $J = 8.5$ & 2.7 Hz, 1H), 6.44-6.40 (m, 1H), 6.29-6.25 (m, 1H), 3.99 (t, 3H), 3.71-3.60 (m, 3H), 3.54-3.44 (m, 2H), 3.31-3.12 (m, 4H), 2.44-2.41 (m, 2H), 1.82-1.75 (m, 2H), 1.58-1.42 (m, 5H), 1.26 (s, 2H), 0.99 (t, 3H). ^{13}C NMR (CDCl_3 , 74 MHz): δ 172.7, 171.0, 158.9, 155.2, 154.3, 149.8, 135.4, 134.8, 126.9, 126.3, 122.9, 121.8, 119.5, 116.7, 115.4, 111.9, 111.8, 109.5, 77.2, 67.8, 51.8, 48.7, 48.2, 46.8, 46.3, 36.5, 36.4, 31.3, 19.2, 13.8. IR (ATR, cm^{-1}): 2959, 2923, 2865, 1758, 1734, 1556, 1487, 1176, 1146. ESI-HRMS: calculated for $\text{C}_{30}\text{H}_{30}\text{O}_5^+$ $[\text{M}]^+$: 470.2093, found 470.2082. UV-Vis in CH_2Cl_2 ($\lambda_{\text{max}} = 304$ nm).

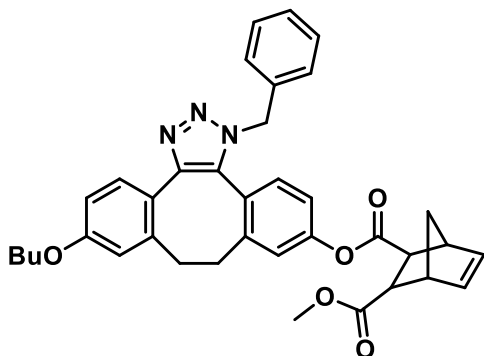
Synthesis of DIBO-polymer 3.5



Compound (**2.14**) (0.01 g, 0.02 mmol) was dissolved in glass distilled CH_2Cl_2 (250 mL) and purged with argon for 15 min. The solution was irradiated in the photochemical rayonet reactor using 350 nm UV light. Compound (**3.5**) was isolated as a pale-yellow oil (9.30 mg, 98%) with no further purification was required.

DIBO-polymer: ^1H NMR (CDCl_3 , 400 MHz): δ 7.20 (bs), 7.01 (bs), 6.87 (bs), 6.75 (bs), 5.71 (bs), 3.94 (bs), 3.64 (bs), 3.24 (bs), 2.37 (bs), 2.03 (bs), 1.75 (bs), 1.47 (bs), 1.26 (bs), 0.92 (bs). IR (ATR, cm^{-1}): 2954, 2924, 2870, 2253, 2164, 1734, 1561, 1482, 1216, 1137, 894, 726. UV-Vis in CH_2Cl_2 ($\lambda_{\text{max}} = 303$ nm)

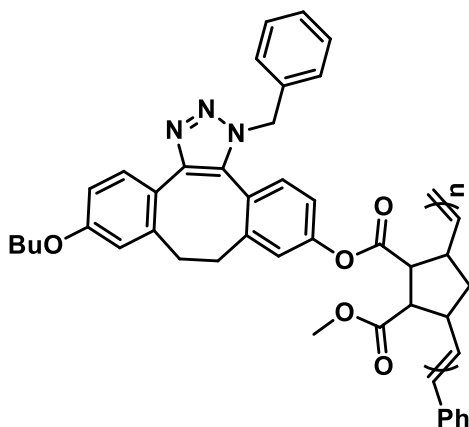
Synthesis of benzyltriazole-clicked-monomer 3.2



Compound (3.1) (0.01 g, 0.02 mmol) was dissolved in glass distilled CH_2Cl_2 (2 mL). Benzyl azide (0.005 ml, 0.04 mmol) was added to the reaction mixture. The reaction mixture was stirred for 30 min. The crude product was purified by column chromatography (5% EtOAc/ CH_2Cl_2) to give compound (3.2) as a regioisomer as a yellow oil (0.01 g, 97% yield).

Benzyltriazole-clicked--monomer: ^1H NMR (CDCl_3 , 400 MHz): δ 7.52 (d, $J = 8$ Hz, 1H), 7.25-7.24 (m, 2H), 7.09-7.08 (m, 3H), 6.97-6.88 (m, 2H), 6.78-6.72 (m, 2H), 6.37-6.35 (m, 1H), 6.27-6.25 (m, 1H), 5.59-5.47 (m, 2H), 3.98-3.94 (m, 2H), 3.61 (s, 3H), 3.49-3.40 (m, 2H), 3.27-2.64 (m, 4H), 2.32-2.18 (m, 1H), 2.08-2.05 (m, 1H), 1.81-1.74 (m, 2H), 1.54-1.25 (m, 5H), 1.00-0.07 (m, 3H). ^{13}C NMR (CDCl_3 , 74 MHz): δ 172.9, 171.1, 160.5, 159.1, 150.6, 143.3, 139.2, 138.1, 136.8, 135.7, 133.2, 130.2, 129.2, 127.7, 126.3, 123.6, 118.3, 115.9, 112.7, 72.8, 70.8, 68.0, 60.7, 52.1, 48.5, 46.9, 36.8, 34.9, 31.9, 29.7, 25.6, 21.3, 20.0, 19.5, 14.4, 11.7, 1.3. IR (ATR, cm^{-1}): 2934, 2865, 1739, 1610, 1516, 1343, 1245, 1201, 1146. ESI-HRMS: calculated for $\text{C}_{37}\text{H}_{37}\text{N}_3\text{O}_5^+$ $[\text{M}]^+$: 603.2733, found 603.2738. UV-Vis in CH_2Cl_2 ($\lambda_{\text{max}} = 229$ nm).

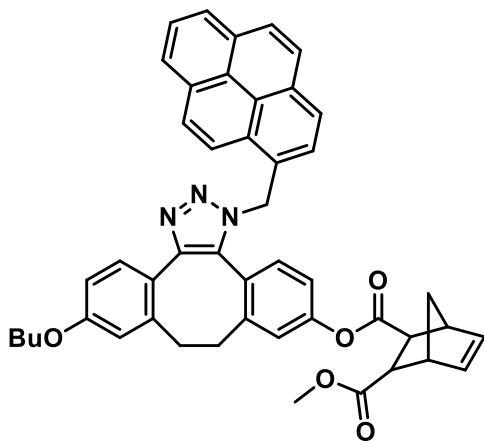
Synthesis of benzyltriazole-clicked-polymer 3.6



Compound (2.14) (0.03 g, 0.07 mmol) and benzyl azide (0.01 g, 0.08 mmol) and was dissolved in CH_2Cl_2 (250 mL) and purged with argon for 15 min. The solution was irradiated in the photochemical rayonet reactor using 350 nm UV light. The reaction mixture was concentrated to 2 mL and monitored by UV-Vis. The crude polymer was dissolved in CH_2Cl_2 (10 mL) and precipitated into rapidly stirred pentane (50 mL) at 0°C to afford the benzyltriazole-polymer as a yellow solid. Yield = 0.04 g, 98%.

Benzyltriazole-clicked-polymer: $^1\text{H NMR}$ (CDCl_3 , 400 MHz): δ 7.53 (bs), 7.44 (bs), 7.24 (bs), 7.06-6.97 (bm), 6.74-6.63 (bm), 5.75-5.67 (bm), 5.51 (bs), 3.90 (bs), 3.63-3.24 (bm), 3.01-2.64 (bm), 1.96 (bs), 1.65 (bs), 1.38-1.27 (bm), 0.94-8.87 (bm). $^{13}\text{C NMR}$ (CDCl_3 , 74 MHz): δ 128.4, 127.1, 64.1, 61.1, 51.4, 51.2, 36.0, 31.3, 28.2, 26.0, 22.4, 18.9, 13.5. IR (ATR, cm^{-1}): 3368, 2924, 2855, 1734, 1605, 1457, 1206, 1132. UV-Vis in CH_2Cl_2 ($\lambda_{\text{max}} = 229 \text{ nm}$). $M_n = 44,780 \text{ g/mol}$, $M_w = 100,900 \text{ g/mol}$, $D = 2.43$.

Synthesis of Pyrene-clicked-monomer 3.7

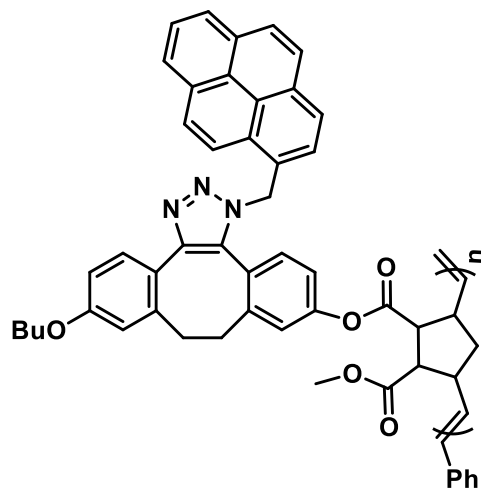


yield).

Compound (**3.1**) (0.01 g, 0.02 mmol) was dissolved in glass distilled CH_2Cl_2 (2 mL). Pyrene azide (5 mL, 0.04 mmol) was added to the reaction mixture. The reaction mixture was stirred for 30 min. The crude product was purified by column chromatography (100% CH_2Cl_2 followed by 100% EtOAc) to give compound (**3.7**) as a regioisomer as an orange solid (0.01 g, 97%

Pyrene-clicked--monomer: $^1\text{H NMR}$ (CDCl_3 , 400 MHz): δ 8.21-8.16 (m, 3H), 8.10-8.00 (m, 5H), 7.59-7.49 (m, 2H), 7.16-7.04 (m, 1H), 6.97-6.92 (m, 1H), 6.86-6.75 (m, 1H), 6.70-6.67 (m, 1H), 6.59 (s, 1H), 6.36-6.34 (m, 1H), 6.26-6.24 (m, 1H), 3.91 (t, 8Hz, 2H), 3.60 (s, 3H), 3.48-3.38 (m, 2H), 3.28-3.22 (m, 2H), 3.15-3.03 (m, 1H), 2.91-2.75 (m, 1H), 2.65-2.58 (m, 1H), 1.77-1.70 (m, 2H), 1.56-1.38 (m, 5H), 1.31-1.30 (m, 1H), 0.99-0.93 (m, 3H). $^{13}\text{C NMR}$ (CDCl_3 , 74 MHz): δ 172.6, 170.7, 160.1, 158.8, 151.6, 150.3, 146.9, 146.2, 142.8, 139.2, 139.0, 135.1, 134.8, 134.4, 133.5, 132.7, 132.6, 131.3, 131.1, 130.5, 130.2, 130.0, 128.4, 128.2, 128.1, 127.7, 127.5, 127.3, 126.4, 126.1, 125.5, 125.4, 124.7, 124.6, 124.5, 123.8, 123.2, 122.0, 119.2, 118.0, 116.3, 115.7, 112.8, 112.4, 67.7, 67.5, 60.4, 53.4, 51.7, 50.4, 48.7, 48.2, 46.7, 46.6, 46.3, 36.1, 36.0, 32.7, 31.2, 19.2, 14.2, 13.8. IR (ATR, cm^{-1}): 3043, 2954, 2924, 2865, 1753, 1739, 1605, 1511, 1339, 1260, 1196, 1146, 845, 701. ESI-HRMS: calculated for $\text{C}_{47}\text{H}_{41}\text{N}_3\text{O}_5^+$ $[\text{M}]^+$: 727.3046, found 728.3112. UV-Vis in CH_2Cl_2 ($\lambda_{\text{max}} = 245 \text{ nm}$).

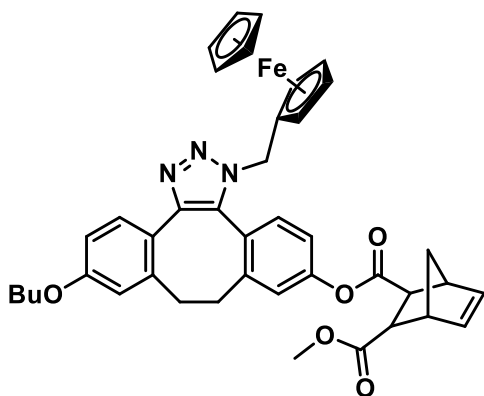
Synthesis of pyrene-clicked-polymer 3.8



Compound (**2.14**) (0.03 g, 0.09 mmol) and azidomethylpyrene (0.025 g, 0.087 mmol) were dissolved in CH₂Cl₂ (250 ml) and purged with Ar for 15 min. The solution was irradiated in the photochemical rayonet reactor using 350 nm UV light. The reaction mixture was concentrated to 2 mL and monitored by UV-Vis. The crude polymer was dissolved in CH₂Cl₂ (10 mL) and precipitated into rapidly stirred pentane (50 mL) at 0 °C to afford the ferrocene-azide-polymer **3.8** as a yellow solid. Yield = 0.05 g, 98%.

Pyrene-clicked-polymer: ¹H NMR (CDCl₃, 400 MHz): 8.21-7.72 (bm), 7.60-7.40 (bm), 7.17-7.11 (bm), 7.02-6.81 (bm), 6.69-6.46 (bm), 6.35-6.05 (bm), 5.77-5.34 (bs), 3.91-3.78 (bm), 3.60-3.44 (bm), 3.27-3.09 (bm), 2.89-2.73 (bm), 2.59-2.37 (bm), 1.75-1.52 (bm), 1.38-1.27 (bm), 0.91-0.86 (bm). IR (ATR, cm⁻¹): 3043, 2959, 2870, 2361, 2257, 1734, 1605, 1205, 1132, 904, 845, 726. UV-Vis in CH₂Cl₂ (λ_{max} = 243 nm). M_n = 33, 710 g/mol, M_w = 84, 860 g/mol, Đ = 2.52.

Synthesis of Ferrocene-azide-clicked-monomer **3.9**

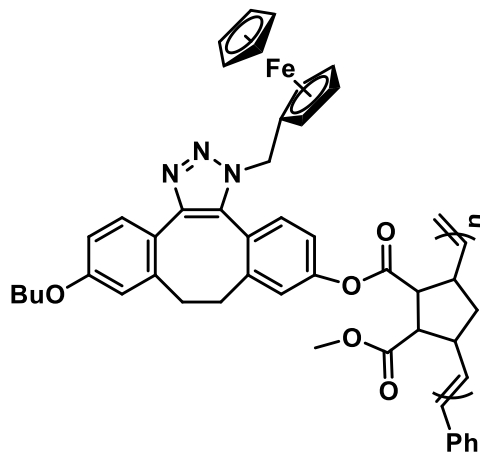


Compound (**3.1**) (0.01 g, 0.02 mmol) was dissolved in glass distilled CH_2Cl_2 (2 mL). Ferrocene azide (0.005 L, 0.04 mmol) was added to the reaction mixture. The reaction mixture was stirred for 30 min. The crude product was purified by column chromatography (100% CH_2Cl_2 followed by 100% EtOAc) to give compound

(**3.9**) as a regioisomer as an orange solid (0.01 g, 98% yield).

Ferrocene-azide-clicked--monomer: ^1H NMR (CDCl_3 , 400 MHz): δ 7.48-7.38 (m, 1H), 7.22-7.07 (m, 2H), 6.93-6.83 (m, 2H), 6.75-6.63 (m, 1H), 6.47-6.34 (m, 1H), 6.27-6.25 (m, 2H), 5.26 (s, 2H), 4.29-4.00 (m, 7H), 3.93-3.83 (m, 2H), 3.67-3.60 (m, 2H), 3.50-3.39 (m, 2H), 3.31-3.23 (m, 3H), 3.00-2.72 (m, 3H), 1.82-1.69 (m, 3H), 1.62-1.38 (m, 4H), 1.31-1.29 (m, 2H), 1.03-0.93 (m, 3H). ^{13}C NMR (CDCl_3 , 74 MHz): δ 173.0, 171.4, 171.2, 160.4, 159.0, 151.8, 150.5, 146.9, 146.2, 143.5, 143.3, 139.3, 139.2, 135.9, 135.7, 135.1, 135.0, 134.8, 133.6, 133.1, 132.7, 130.5, 130.4, 127.9, 124.5, 123.6, 123.2, 123.1, 122.5, 120.1, 120.0, 119.5, 118.7, 116.7, 115.9, 113.0, 112.6, 69.2, 68.8, 68.0, 67.8, 60.6, 53.7, 52.1, 52.0, 49.0, 48.5, 47.1, 46.9, 46.5, 36.7, 36.6, 33.2, 31.9, 31.6, 30.0, 29.6, 29.3, 25.5, 22.9, 21.3, 19.5, 14.5, 14.1. IR (ATR, cm^{-1}): 3071, 2949, 2934, 2865, 1739, 1610, 1511, 1343, 1250, 1201, 1151, 1003, 820, 736. ESI-HRMS: calculated for $\text{C}_{41}\text{H}_{41}\text{FeN}_3\text{O}_5^+$ $[\text{M}]^+$: 711.2396, found 711.2381. UV-Vis in CH_2Cl_2 ($\lambda_{\text{max}} = 229$ nm).

Synthesis of ferrocene-clicked-polymer **3.10**



Compound **2.14** (0.04 g, 0.09 mmol) and azidomethylferrocene (0.03 g, 0.11 mmol) was dissolved in CH_2Cl_2 (250 mL) and purged with argon for 15 min. The solution was irradiated in the photochemical rayonet reactor using 350 nm UV light. The reaction mixture was concentrated to 2 mL and monitored by UV-Vis. The crude polymer was dissolved in CH_2Cl_2 (10 mL) and precipitated into rapidly

stirred pentane (50 mL) at 0 °C to afford the ferrocene-azide-polymer **3.10** as a yellow solid. Yield = 0.06 g, 97%.

Ferrocene-clicked-polymer: $^1\text{H NMR}$ (CDCl_3 , 400 MHz): 7.49-7.39 (bm), 7.15-7.08 (bs), 6.85 (bs), 6.73 (bs), 6.64 (bs), 5.79-5.45 (bs), 5.31-5.22 (bs), 4.25-4.02 (bm), 3.90-3.80 (bm), 3.70-3.43 (bm), 3.29-3.20 (bm), 2.99-2.71 (bm), 1.79-1.45 (bm), 0.98-0.82 (bm). IR (ATR, cm^{-1}): 3437, 3092, 2959, 2924, 2865, 2242, 1739, 1605, 1511, 1206, 1137, 983, 914, 820, 721. UV-Vis in CH_2Cl_2 ($\lambda_{\text{max}} = 229 \text{ nm}$). $M_n = 50,890 \text{ g/mol}$, $M_w = 110,600 \text{ g/mol}$, $D = 2.17$.

3.5 References

1. Kolb, H. C.; Finn, M. G.; Sharpless, K. B., *Angew. Chem. Int. Ed.* **2001**, *40*, 2004-2021.
2. Gauthier, M. A.; Gibson, M. I.; Klok, H.-A., *Angew. Chem. Int. Ed.* **2009**, *48*, 48-58.
3. Hoyle, C. E.; Bowman, C. N., *Angew. Chem. Int. Ed.* **2010**, *49*, 1540-1573.
4. Liu, Y. L.; Chuo, T. W., *Polym. Chem.* **2013**, *4*, 2194-225.
5. Meldal, M.; Tornøe, C. W., *Chem. Rev.* **2008**, *108*, 2952-3015.

6. Sutton, D. A.; Yu, S.-H.; Steet, R.; Popik, V. V., *Chem. Commun.* **2016**, 52, 553-556.
7. Manova, R. K.; Beek, V. T. A.; Zuilhof, H., *Angew. Chem. Int. Ed.* **2011**, 50, 5428-5430.
8. Arnold, R. M.; McNitt, C. D.; Popik, V. V.; Locklin, J., *Chem. Commun.* **2014**, 50, 5307-5309.
9. Poloukhine, A.; Popik, V. V., *J. Phys. Chem. A* **2006**, 110, 1749-1757.
10. Luo, W.; Gobbo, P.; McNitt, C. D.; Sutton, D. A.; Popik, V. V.; Workentin, M. S., *Chem. Eur. J.* **2017**, 23, 1052-1059.
11. Partyka, D. V.; Gao, L.; Teets, T. S.; Updegraff, J. B.; Deligonul, N.; Gray, T. G., *Organometallics* **2009**, 28, 6171-6182.
12. D'Abramo, M.; Aschi, M.; Amadei, A., *Chem. Phys. Lett.* **2015**, 639, 17-22.
13. Pavlopoulou, E.; Kim, C. S.; Lee, S. S.; Chen, Z.; Facchetti, A.; Toney, M. F.; Loo, Y.-L., *Chem. Mater.* **2014**, 26, 5020-5027.
14. Yip, J.; Duhamel, J.; Qiu, X. P.; Winnik, F. o. M., *Macromolecules* **2011**, 44, 5363-5372.
15. Salzner, U., *J. Chem. Theory Comput.* **2013**, 9, 4064-4073.
16. Peigneguy, F.; Allain, M.; Cougnon, C.; Frère, P.; Siegler, B.; Bressy, C.; Gohier, F., *New. J. Chem* **2019**, 43, 976-971.
17. Piro, B.; Haccoun, J.; Pham, M. C.; Tran, L. D.; A.Rubin; Perrot, H.; Gabrielli, C., *J. Electroanal. Chem.* **2005**, 577, 155-165.
18. Elgrishi, N.; Rountree, K. J.; McCarthy, B. D.; Rountree, E. S.; Eisenhart, T. T.; Dempsey, J. L., *J. Chem. Educ.* **2018**, 95, 197.

Chapter 4

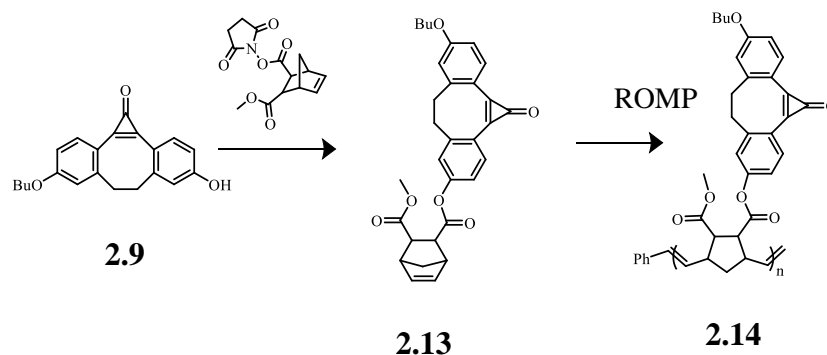
4 Conclusions and Future Work

4.1 Conclusions

Post-polymerization modification represents a powerful tool to generate a library of polymers with various chemical properties from a common, modifiable polymer backbone. Having accessibility to a well-designed modifiable polymer can lead to the generation of emissive materials, redox-active materials and applications in photopatterning with spatial and temporal control purposes. The modification is made possible by click chemistry. In this thesis, a strained alkyne was utilized as the functional group of choice because it satisfies the click chemistry criteria and undergoes a strain-promoted alkyne-azide cycloaddition without the assistance of a transition metal catalyst. The strained alkyne is highly reactive and although desirable, required a masking-unmasking strategy to be employed, and thus a cyclopropanone masking group was used to prevent side reactivity. The advantage of the cyclopropanone masking group was that it can be unmasked via UV irradiation, only CO gas is lost, and no further purification is required which can be quite advantageous for polymers because their unpredictable physical and chemical nature, can complicate their purification.

In chapter 2, I described the synthesis and characterization of the first dibenzocyclooctyne monomer masked via a cyclopropanone monomer (photoDIBO-monomer) **2.13**. The monomer **2.13** was synthesized by performing a nucleophilic acyl substitution between *n*-hydroxysuccinimide activated norbornene derivative **2.11** in CH₂Cl₂ overnight. The success of the acyl substitution was confirmed by ¹H NMR spectroscopy where the phenyl protons show up as multiplets from 7.46 ppm and the olefin protons show up as multiplets

at 6.43-6.25 which is characteristic of alkene norbornene protons. The IR spectrum showed preservation of the cyclopropenone group with the C=O stretch at 1842 cm^{-1} and UV-Vis spectroscopy showed the characteristic photoDIBO bands at 323-341 nm. The subsequent ring-opening metathesis polymerization of the photoDIBO-monomer **2.13** (Scheme 4.1) was also a success as confirmed by GPC and ^1H NMR spectroscopy. The polymer **2.14** was purified by a simple process, first, removal of the Grubbs III catalyst using a neutral alumina plug, then precipitation into rapidly stirred $0\text{ }^\circ\text{C}$ pentane and isolation by centrifugation. The GPC data showed that there was indeed a high molecular species generated with an $M_n = 41,640\text{ g/mol}$. The ^1H NMR spectrum helped confirm that the correct polymer was formed with broad multiplets at 8.01-6.91 ppm indicative of the phenyl DIBO protons and the disappearance of the photoDIBO-monomer **2.13** olefin multiplet peaks at 6.43-6.25 ppm and reappearance of the olefin protons at 5.91-5.35 ppm as broad multiplets for the polymer **2.14**. IR spectroscopy showed the diagnostic 1842 cm^{-1} stretch of the C=O, which confirmed that the cyclopropenone group remained intact during the polymerization in the presence of the GIII catalyst. Finally, the polymerization kinetics study revealed that, although, the polymerization is not considered “living”, it is a well-behaved process at lower molecular weights.



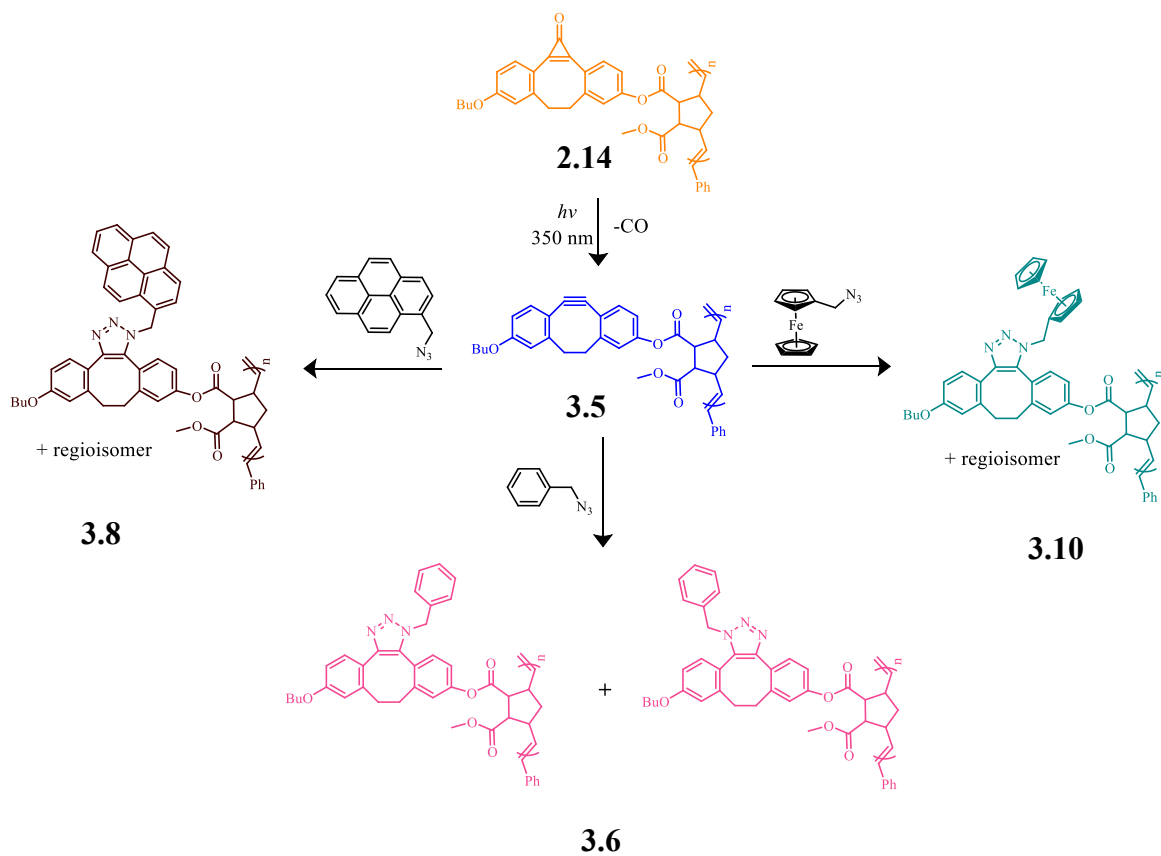
Scheme 4.1. General scheme of monomer **2.13** synthesis and ROMP.

Chapter 3 focused on the post-polymerization modification of the photoDIBO-monomer **2.13** and the photoDIBO-polymer **2.14** (Scheme 4.2). The post synthetic modification was first explored with benzyl azide as a model reaction. The unmasking of the monomer **2.13** proved to be quick, clean and efficient. The unmasking was tracked by UV-Vis spectroscopy which showed disappearance of the characteristic photoDIBO bands at 332 nm and appearance of 311 nm corresponding to the unmasked strained alkyne. The ^1H NMR spectrum was also used to track the unmasking, the photoDIBO-monomer **2.13** showed a distinct splitting pattern of the phenyl protons at 8.01-6.76 ppm and upon irradiation and loss of the C=O the DIBO-monomer **3.1** showed a different splitting pattern with multiplets ranging from 7.24-6.76 ppm. The SPAAC reaction with benzyl azide and the DIBO-monomer **3.1** was also accomplished and tracked by UV-Vis and ^1H NMR spectroscopy. The UV-Vis spectrum showed disappearance of the characteristic DIBO bands at 311 nm indicating the strained alkyne had been completely consumed and the ^1H NMR spectrum showed the appearance of additional aromatic multiplet peaks at 7.53-7.51 ppm and the benzylic $-\text{CH}_2-$ proton peaks at 5.53 ppm. The success of the monomer **2.13**

unmasking and SPAAC with benzyl azide served as a great model reaction for the photoDIBO-polymer **2.14**. Again, the unmasking was tracked by UV-Vis spectroscopy, ^1H NMR spectroscopy and GPC to track the molecular weight increase of the clicked polymer. The UV-Vis spectra for the unmasking and SPAAC of the photoDIBO-polymer **2.14** with benzyl azide was virtually identical to that of the photoDIBO-monomer **2.13**. Also, the ^1H NMR spectra of the unmasking and SPAAC of the photoDIBO-polymer **2.14** with benzyl azide was very similar to the photoDIBO-monomer **2.13** albeit the peaks were broad. Finally, the GPC confirmed an increase of M_n from 41,640 g/mol for the photoDIBO-polymer **2.14** to $M_n = 44,780$ g/mol for the benzyltriazole-clicked-polymer **3.6**. The monomer **2.13** and polymer **2.14** were also clicked with azidomethyl pyrene and azidomethyl ferrocene. The success of these click reactions were confirmed with UV-Vis and ^1H NMR spectroscopy for the monomer and the same for the polymer but with the addition of GPC. The fluorescence study of the pyrene-clicked-polymer **3.8** showed that there was excimer formation which is expected because of the close proximity of the pyrene repeating units. The cyclic voltammetry study showed that the ferrocene-clicked-polymer **3.10** was indeed a reversible process. The peaks shape observed for the oxidation of the polymer indicated a loss of diffusion control at the electrode interface.

Overall, this work, examines a way to synthesize a novel method for the synthesis of a strained alkyne as a pendant group polymer with a clean and efficient unmasking strategy, with simple purification steps allowing the highly reactive strained alkyne to remain dormant until required. Once the polymer is ready for modification, it utilizes the fast mechanism of SPAAC with commercially available azide click partners and because of the high atom economy of the polymer, every repeating unit is functionalized. This work not

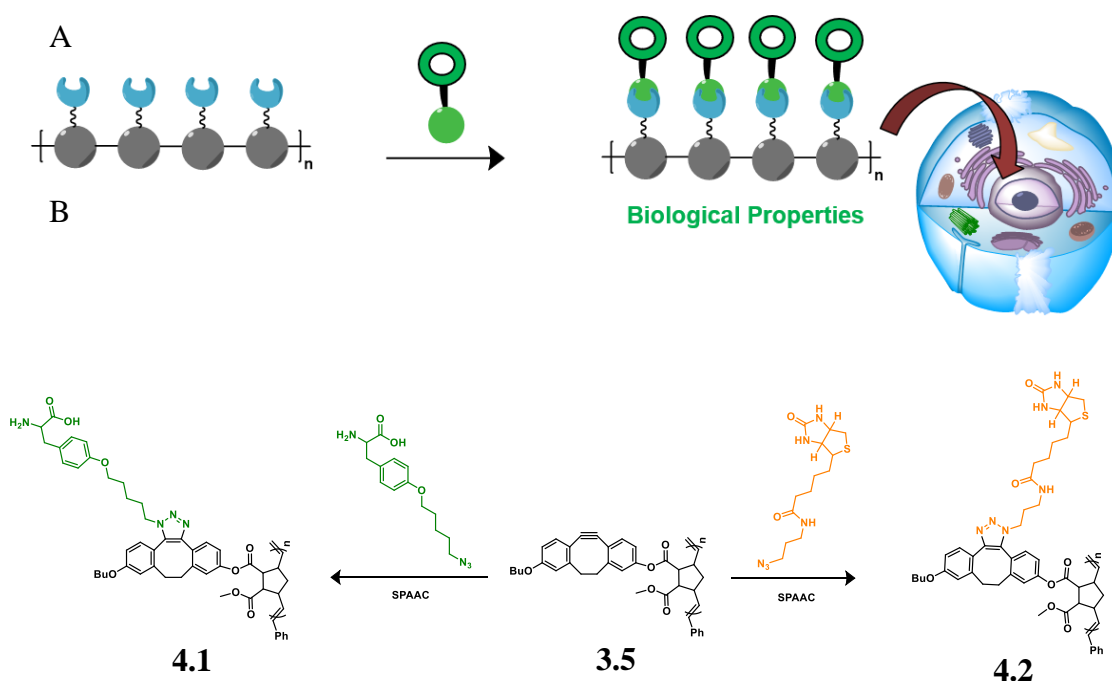
only represents a way to generate a library of polymers but also a way to expand the scope of strained-alkynes in materials chemistry with applications that require spatial and temporal control of polymers.



Scheme 4.2. General scheme for the different click partners with DIBO-polymer 3.5 to highlight PPM introduction of different functionalities.

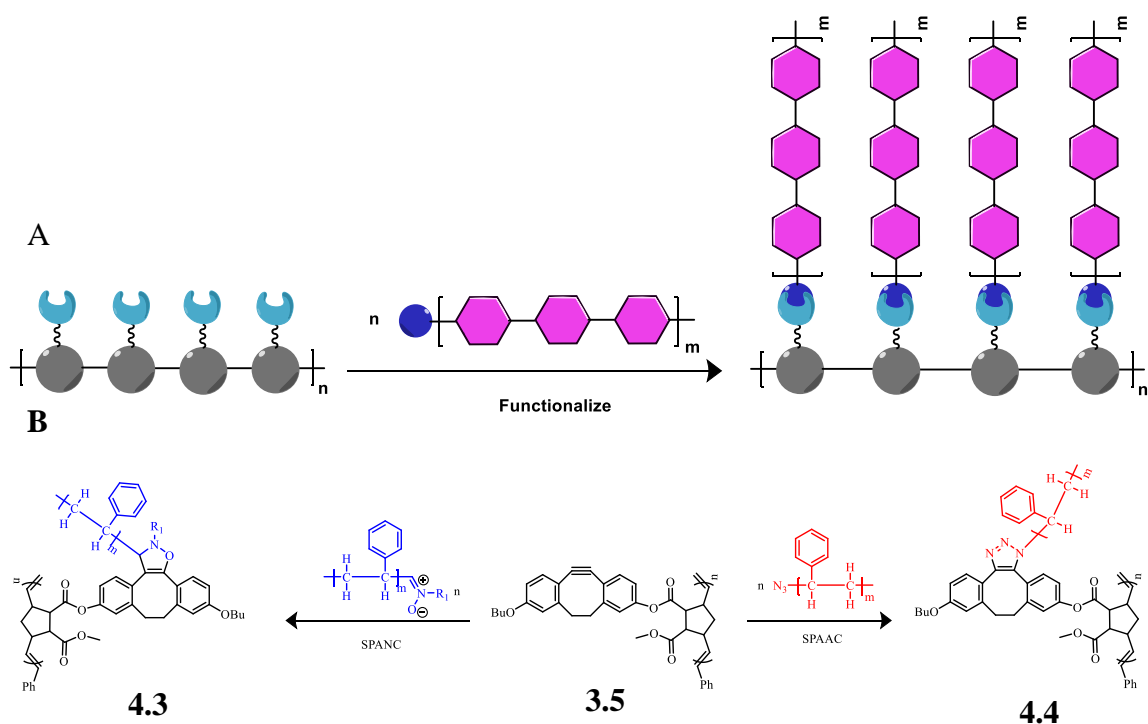
4.2 Future Work

Future work may include optimizing the polymerization to gain more control of the molecular weight distributions and providing lower \mathcal{D} values. Also, bringing biological functionality to the polymer by employing a phenylalanine azide derivative to produce polymer **4.1** for protein modification or a biotin-azide to produce polymer **4.2** for immunotherapy (Scheme 4.3). These polymers may find applications in drug delivery by fine tuning the molecular weight and molecular weight distribution to be incorporated into cells.



Scheme 4.3. General scheme for a biological polymer. The grey polymer represents polymer **3.5** and the green partner represents a biological azide to perform SPAAC (**A**). Scheme for polymer **3.5** undergoing SPAAC to generate biological polymers and a phenylalanine azide derivative **4.1** and biotin azide **4.2** (**B**).

Also, synthesizing graft co-polymers where polymer 3.5 (gray polymer) will be used as the functional polymer to graft end-functionalized polymers (Scheme 4.4A). The end functionalized polymers in this case will have an azide functional group or a nitron functional group so the polymers can undergo SPAAC and SPANC, respectively (Scheme 4.4B). This would have a major impact in graft co-polymer field because traditional methods have select repeating units with functional properties whereas this would allow every repeating unit to be functionalized. This will help expand the scope of ‘grafting to’ polymers in materials chemistry with applications such as membranes for the separation of gasses or liquids,¹ hydrogels,² and drug delivery.³



Scheme 4.4. General scheme for a ‘grafting to’ polymer. The grey polymer represents polymer 3.5 and the pink polymer represents an azide or nitron end functionalized polystyrene chain to perform SPAAC or SPANC, respectively (A). Scheme for polymer 3.5 undergoing SPAAC and SPANC to generate graft polymers with polystyrene (B).

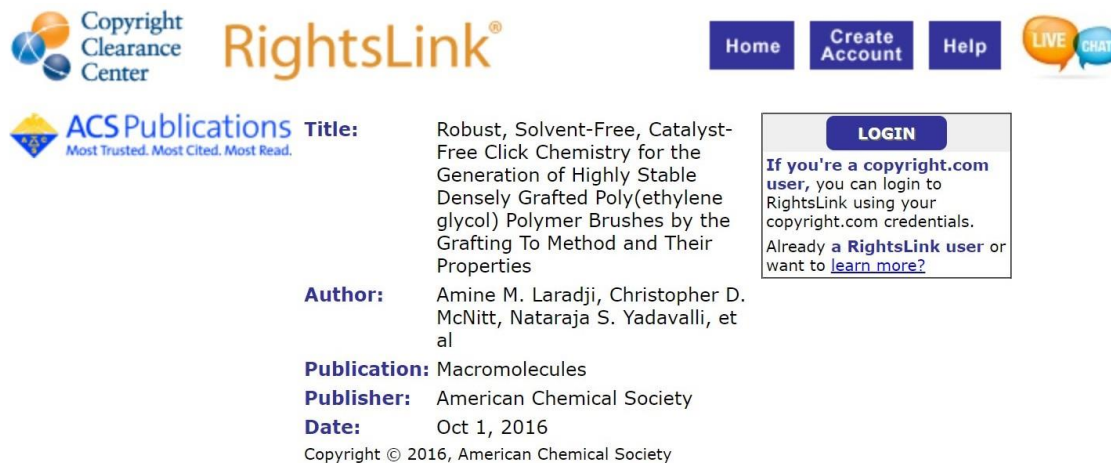
4.3 References

1. Marsh, D.; Bartucci, R.; Sportelli, L., Lipid membranes with grafted polymers: physicochemical aspects. Elsevier B.V: Amsterdam, 2003; Vol. 1615, pp 33-59.
2. Essawy, H. A.; Ghazy, M. B. M.; El-Hai, F. A.; Mohamed, M. F., *Int. J. Biol. Macromol.* **2016**, *89*, 144-151.
3. Sakhare, M. S.; Rajput, H. H., *Asian J. Pharm.* **2017**, *10*, 59.

Appendices

Appendix A1 – Permission to Reuse Copyright Material

Permission to reproduce figure 1.6



The screenshot shows the Copyright Clearance Center RightsLink interface. At the top, there are navigation buttons for Home, Create Account, Help, and a Live Chat icon. The main content area displays the ACS Publications logo and the following information:

Title: Robust, Solvent-Free, Catalyst-Free Click Chemistry for the Generation of Highly Stable Densely Grafted Poly(ethylene glycol) Polymer Brushes by the Grafting To Method and Their Properties

Author: Amine M. Laradji, Christopher D. McNitt, Nataraja S. Yadavalli, et al

Publication: Macromolecules

Publisher: American Chemical Society

Date: Oct 1, 2016

Copyright © 2016, American Chemical Society

A login box on the right side of the page contains the following text:

LOGIN
 If you're a **copyright.com** user, you can login to RightsLink using your copyright.com credentials. Already a **RightsLink** user or want to [learn more?](#)

PERMISSION/LICENSE IS GRANTED FOR YOUR ORDER AT NO CHARGE

This type of permission/license, instead of the standard Terms & Conditions, is sent to you because no fee is being charged for your order. Please note the following:

- Permission is granted for your request in both print and electronic formats, and translations.
- If figures and/or tables were requested, they may be adapted or used in part.
- Please print this page for your records and send a copy of it to your publisher/graduate school.
- Appropriate credit for the requested material should be given as follows: "Reprinted (adapted) with permission from (COMPLETE REFERENCE CITATION). Copyright (YEAR) American Chemical Society." Insert appropriate information in place of the capitalized words.
- One-time permission is granted only for the use specified in your request. No additional uses are granted (such as derivative works or other editions). For any other uses, please submit a new request.

Permission to reproduce figure 1.7.




Title: Rapid Synthesis of Functionalized High-Generation Polyester Dendrimers via Strain-Promoted Alkyne–Azide Cycloaddition

Author: Stuart A. McNelles, Alex Adronov

Publication: Macromolecules

Publisher: American Chemical Society

Date: Oct 1, 2017

Copyright © 2017, American Chemical Society

Home **Create Account** **Help** **LIVE CHAT**

LOGIN

If you're a **copyright.com** user, you can login to RightsLink using your copyright.com credentials. Already a **RightsLink** user or want to [learn more?](#)

PERMISSION/LICENSE IS GRANTED FOR YOUR ORDER AT NO CHARGE

This type of permission/license, instead of the standard Terms & Conditions, is sent to you because no fee is being charged for your order. Please note the following:

- Permission is granted for your request in both print and electronic formats, and translations.
- If figures and/or tables were requested, they may be adapted or used in part.
- Please print this page for your records and send a copy of it to your publisher/graduate school.
- Appropriate credit for the requested material should be given as follows: "Reprinted (adapted) with permission from (COMPLETE REFERENCE CITATION). Copyright (YEAR) American Chemical Society." Insert appropriate information in place of the capitalized words.
- One-time permission is granted only for the use specified in your request. No additional uses are granted (such as derivative works or other editions). For any other uses, please submit a new request.

If credit is given to another source for the material you requested, permission must be obtained from that source.

Appendix A2 – Supporting Information for Chapter 2

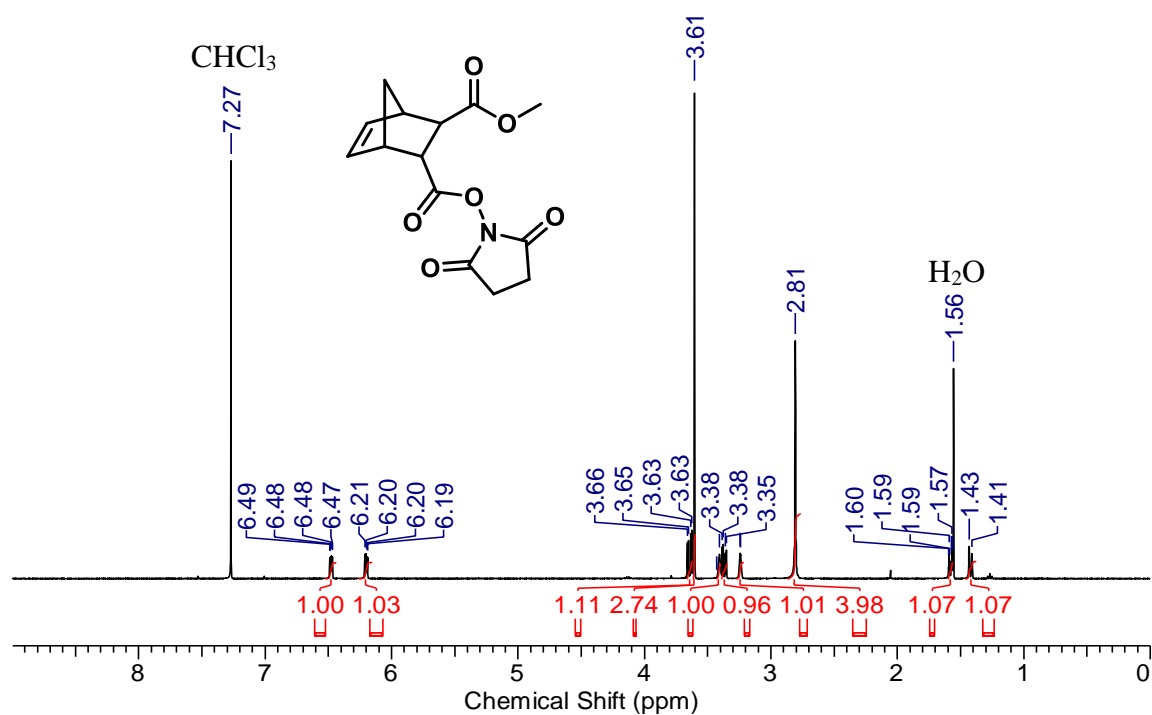


Figure A2.1. ^1H NMR spectrum of compound **2.12**.

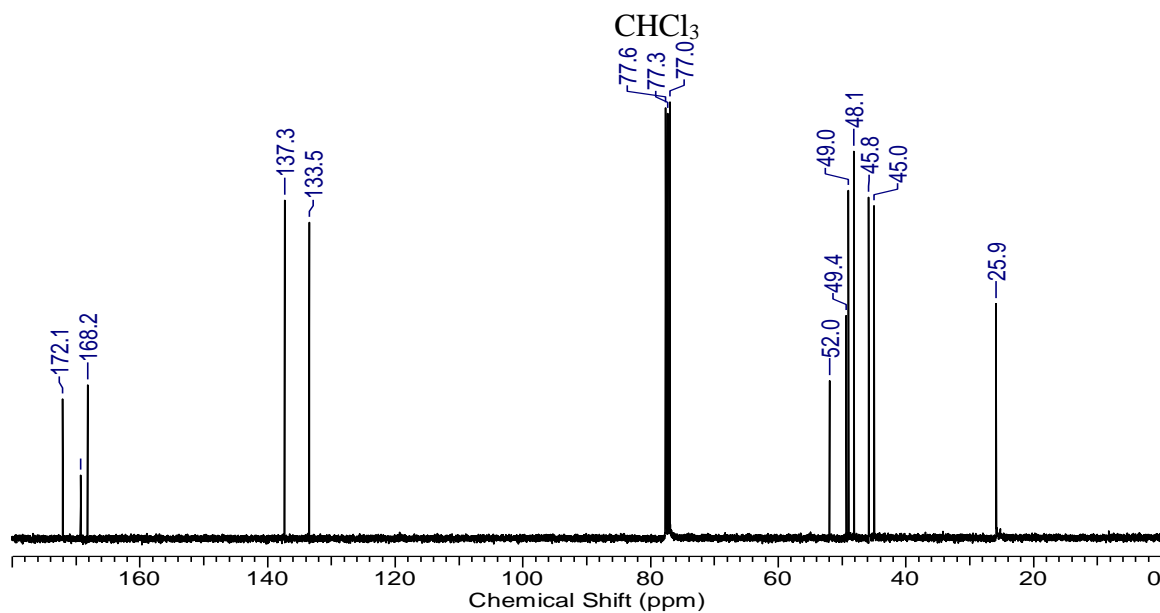


Figure A2.2. $^{13}\text{C}\{^1\text{H}\}$ NMR spectrum of compound **2.12**.

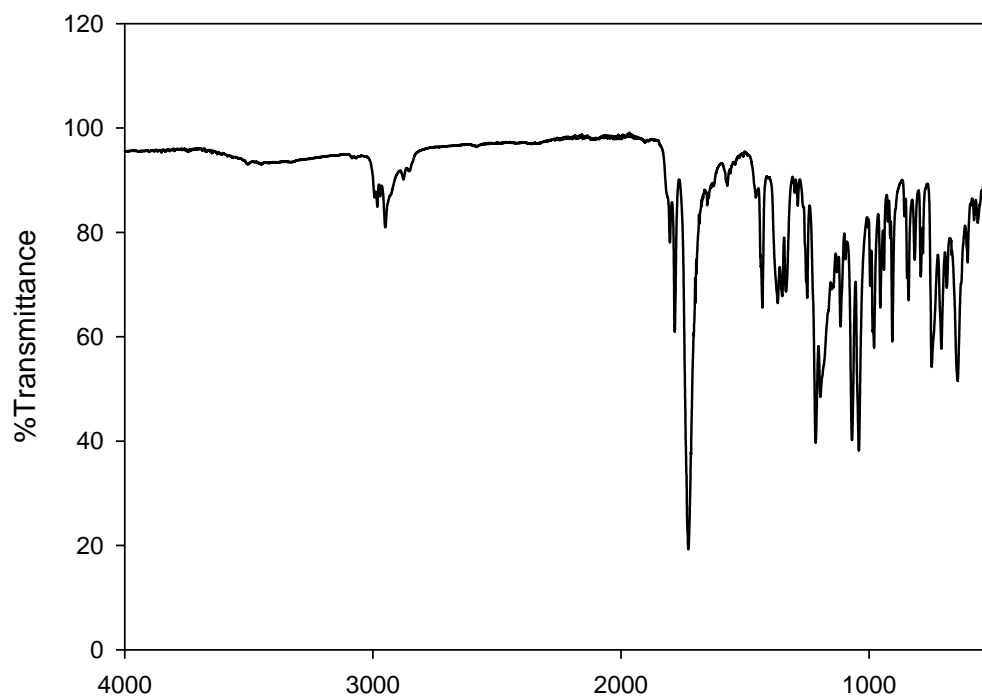


Figure A2.3. IR spectrum of compound **2.12**.

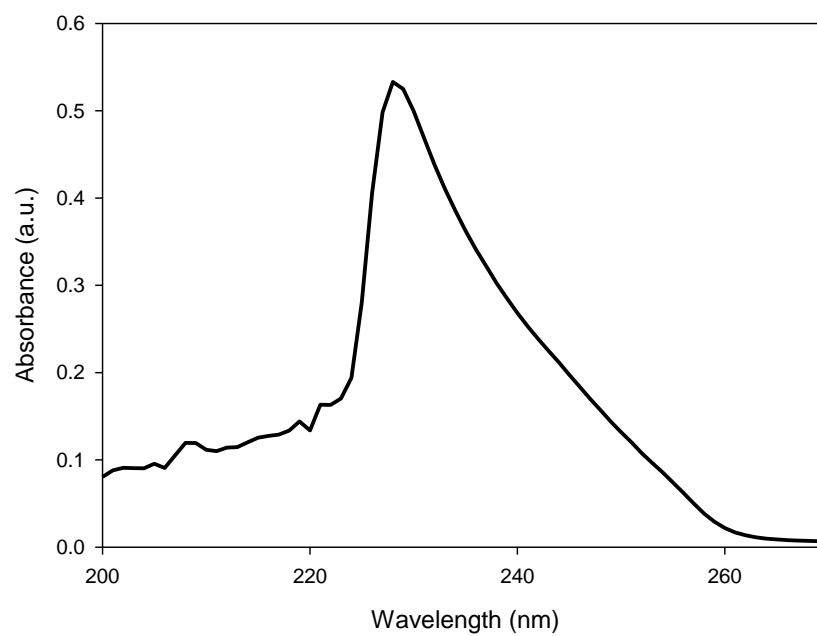


Figure A2.4. UV-Vis spectrum of compound **2.12** in CH₂Cl₂.

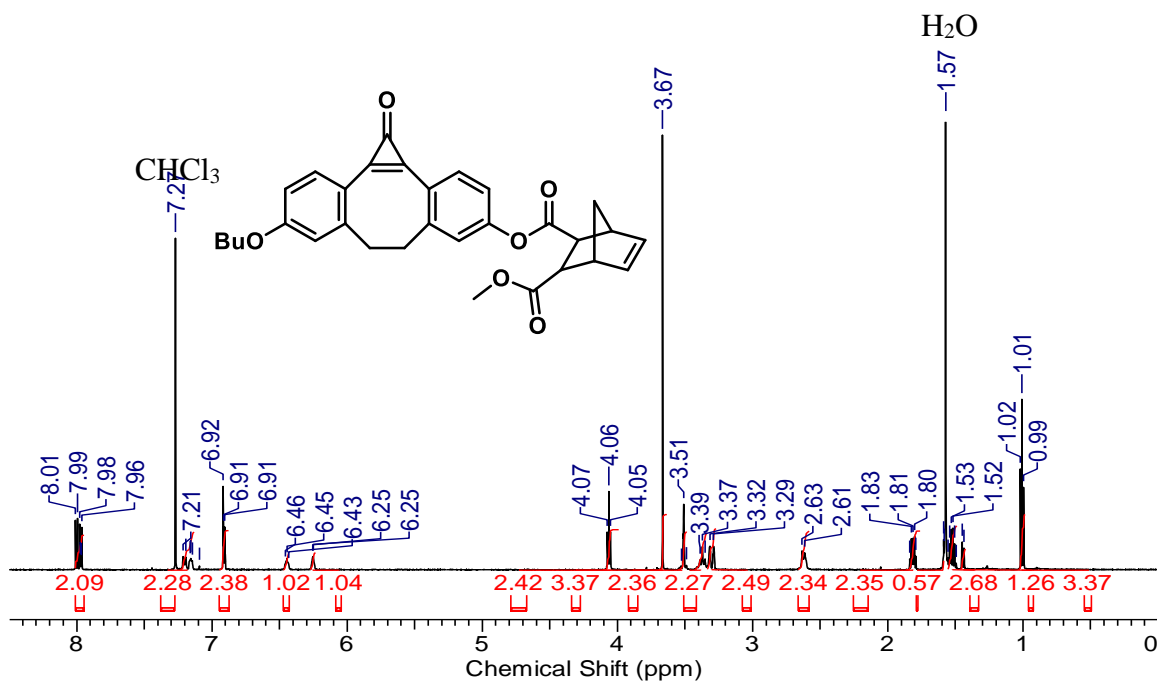


Figure A2.5. ^1H NMR spectrum of compound 2.13.

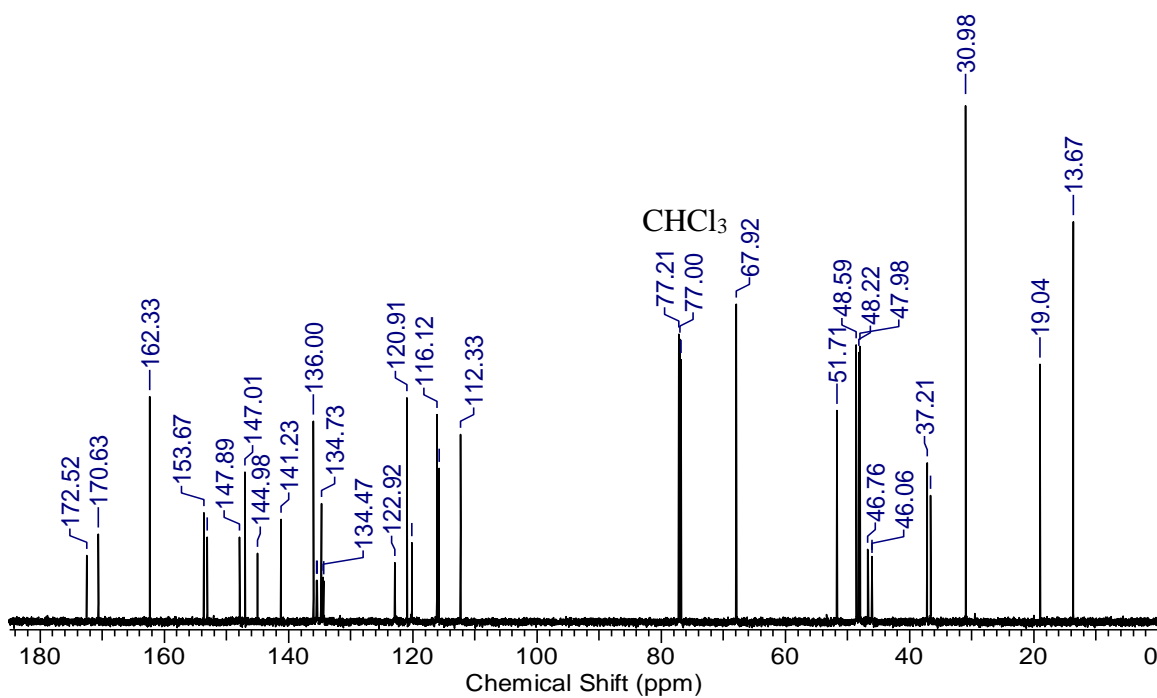


Figure A2.6. $^{13}\text{C}\{^1\text{H}\}$ NMR spectrum of compound 2.13.

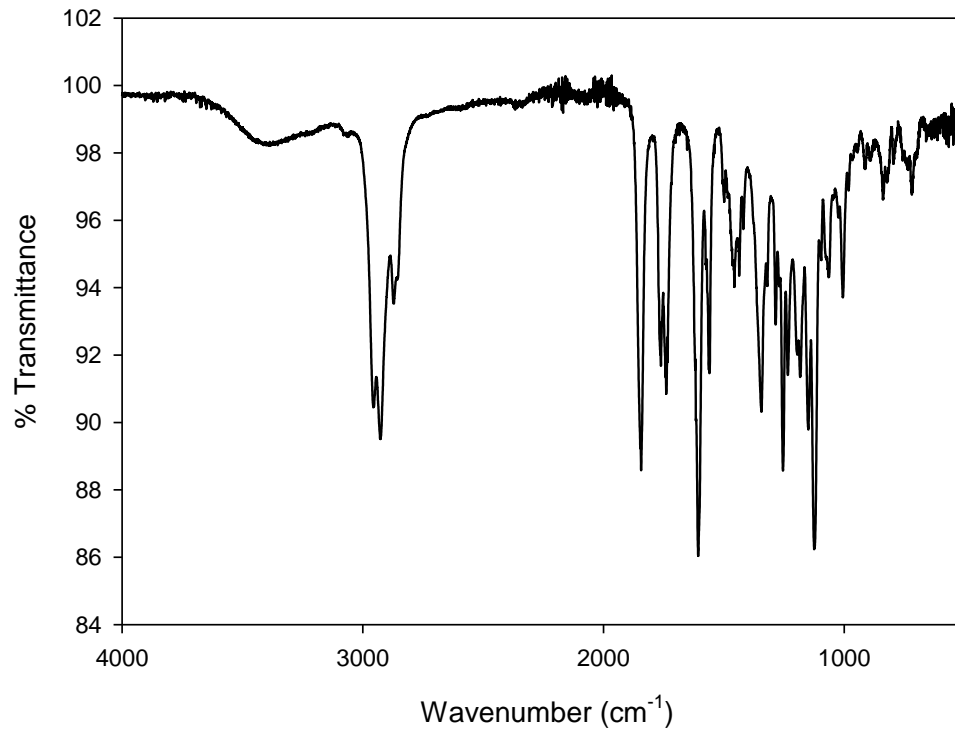


Figure A2.7. IR spectrum of compound **2.13**.

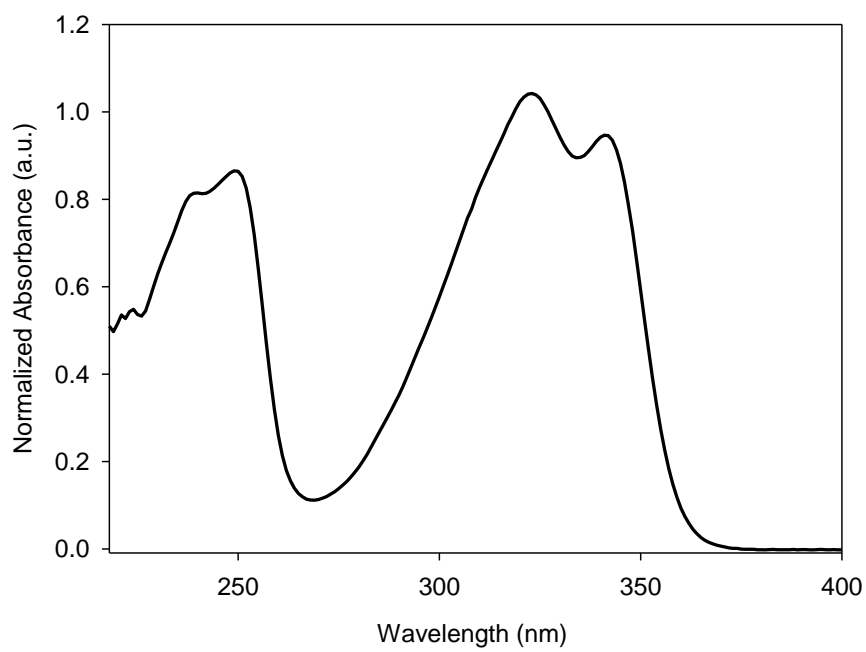


Figure A2.8. UV-Vis spectrum of compound **2.13** in CH₂Cl₂.

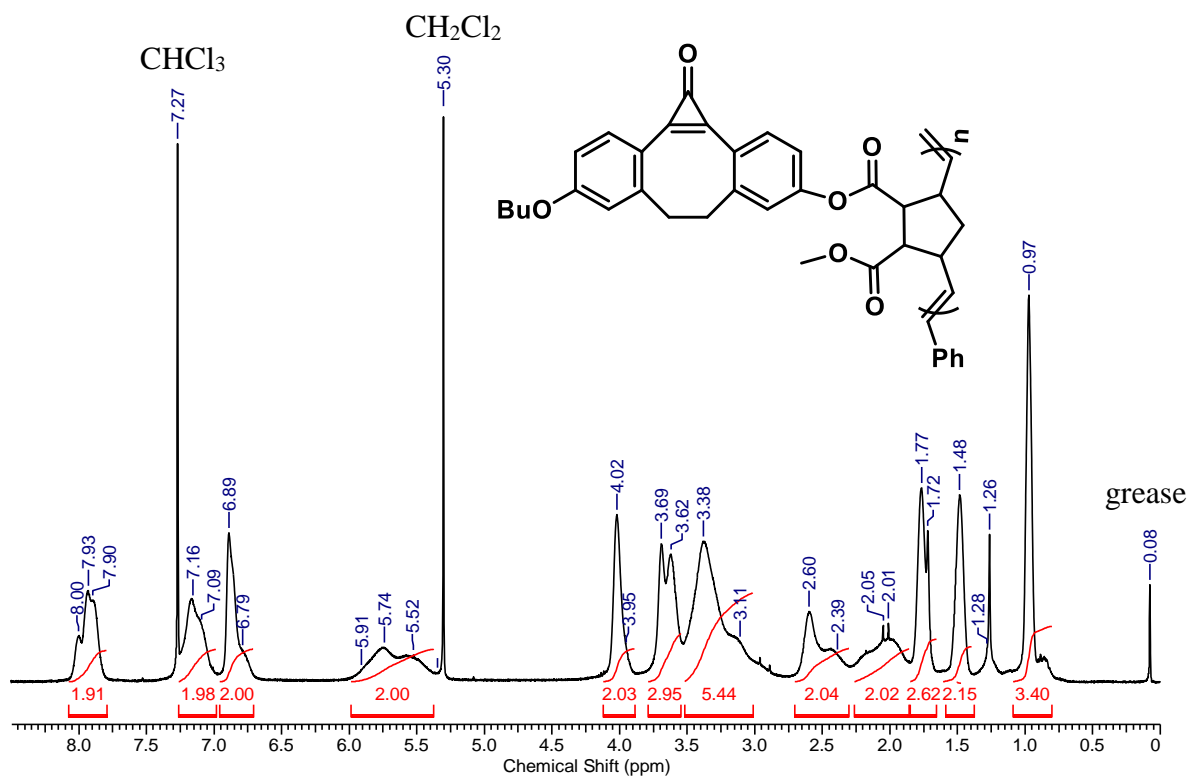


Figure A2.9. ^1H NMR spectrum of compound 2.14.

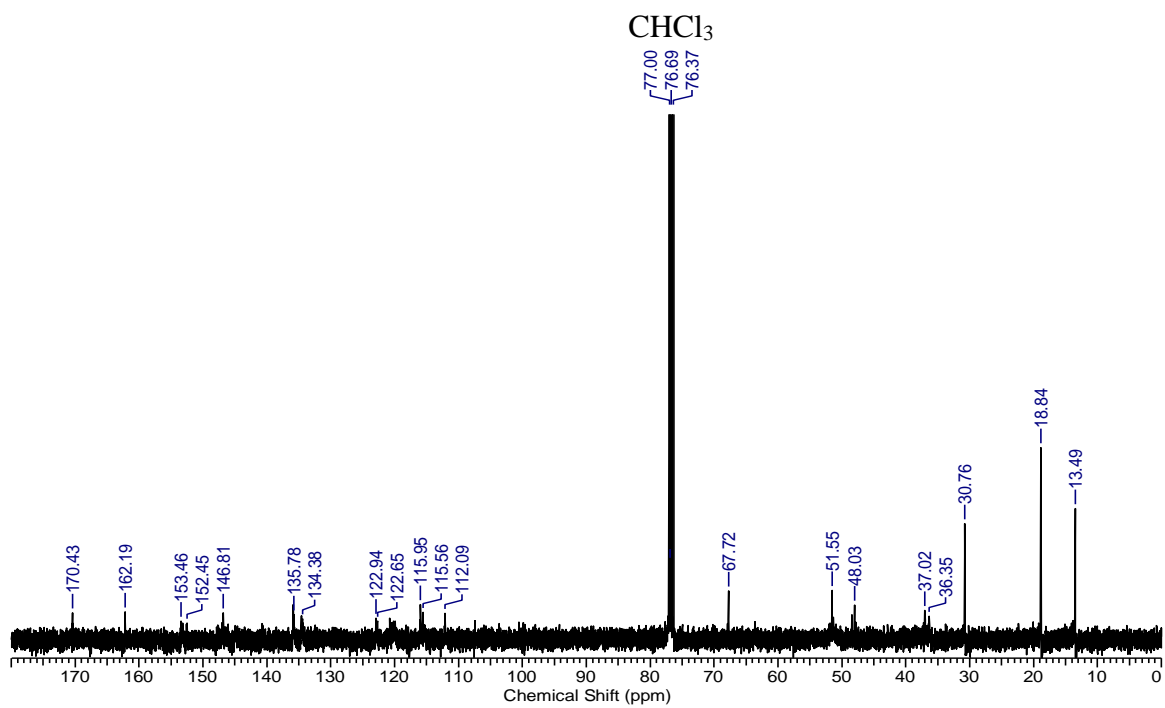


Figure A2.10. $^{13}\text{C}\{^1\text{H}\}$ NMR spectrum of compound 2.14.

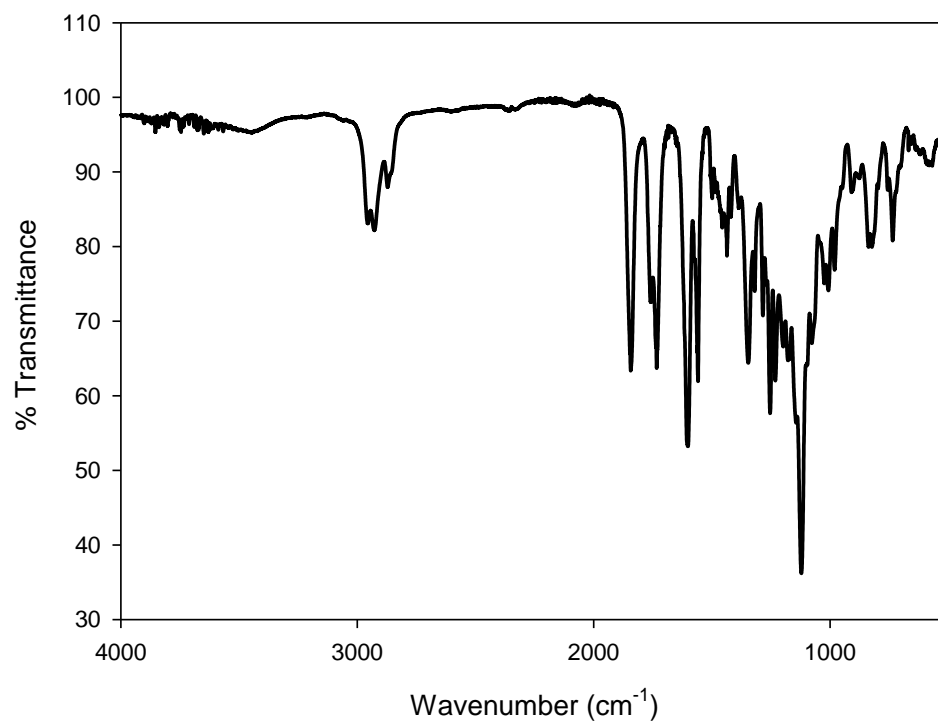


Figure A2.11. IR spectrum of compound **2.14**.

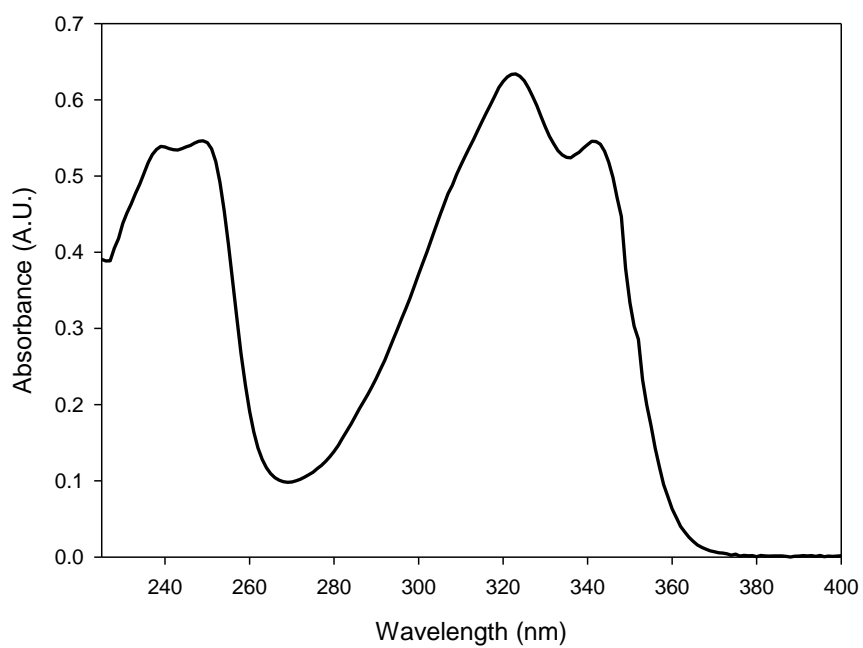


Figure A2.12. UV-Vis spectrum of compound **2.14** in CH₂Cl₂.

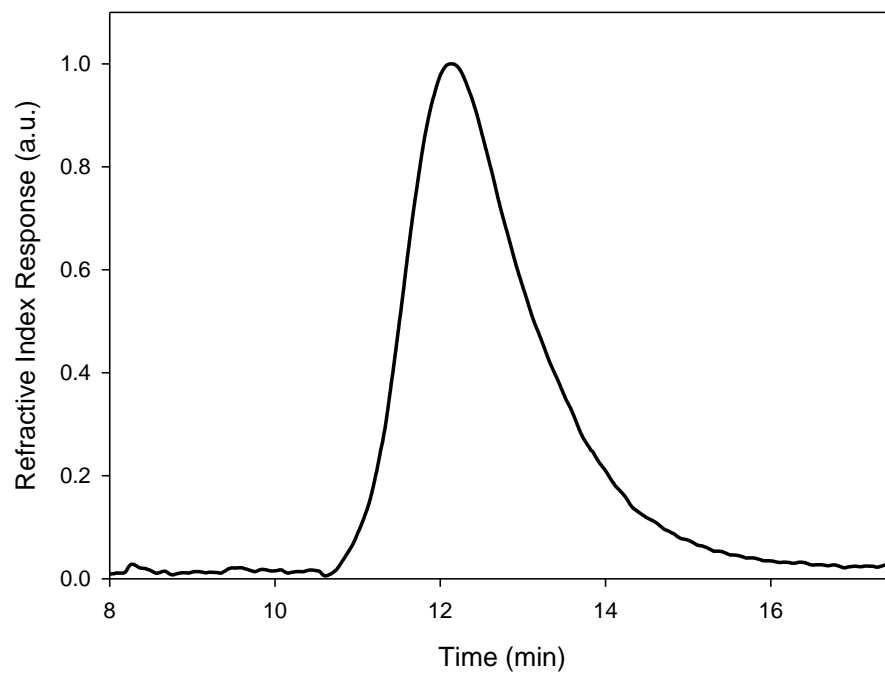
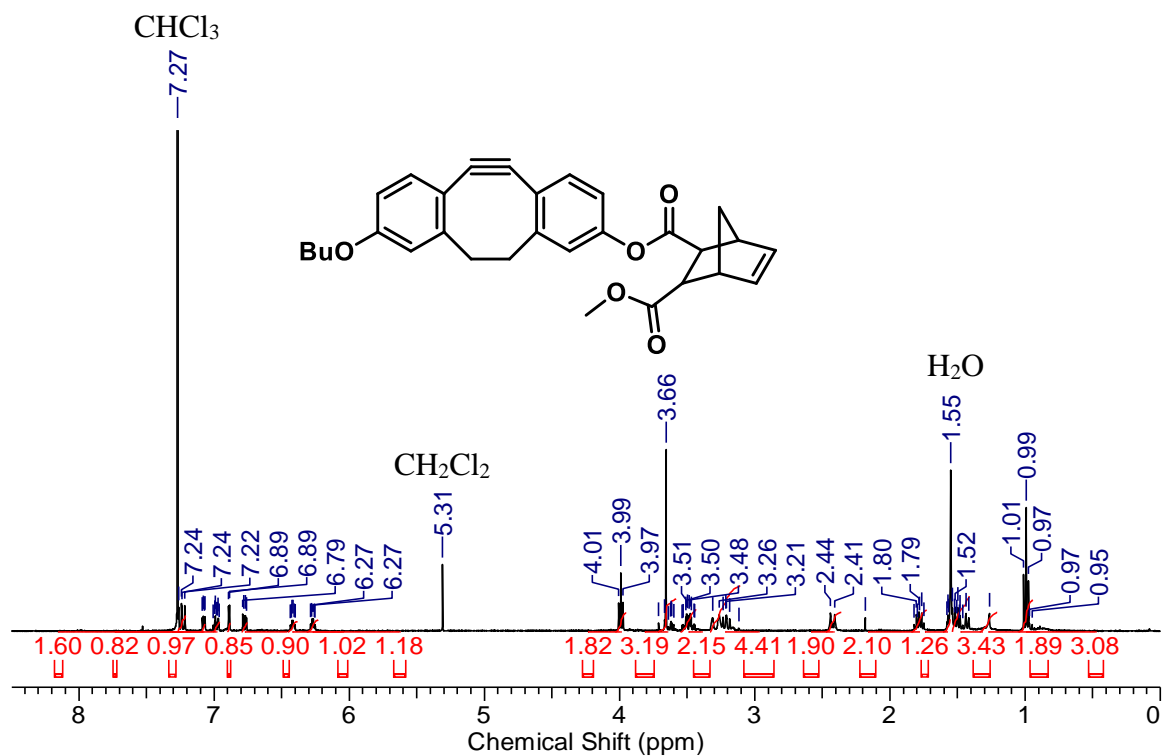
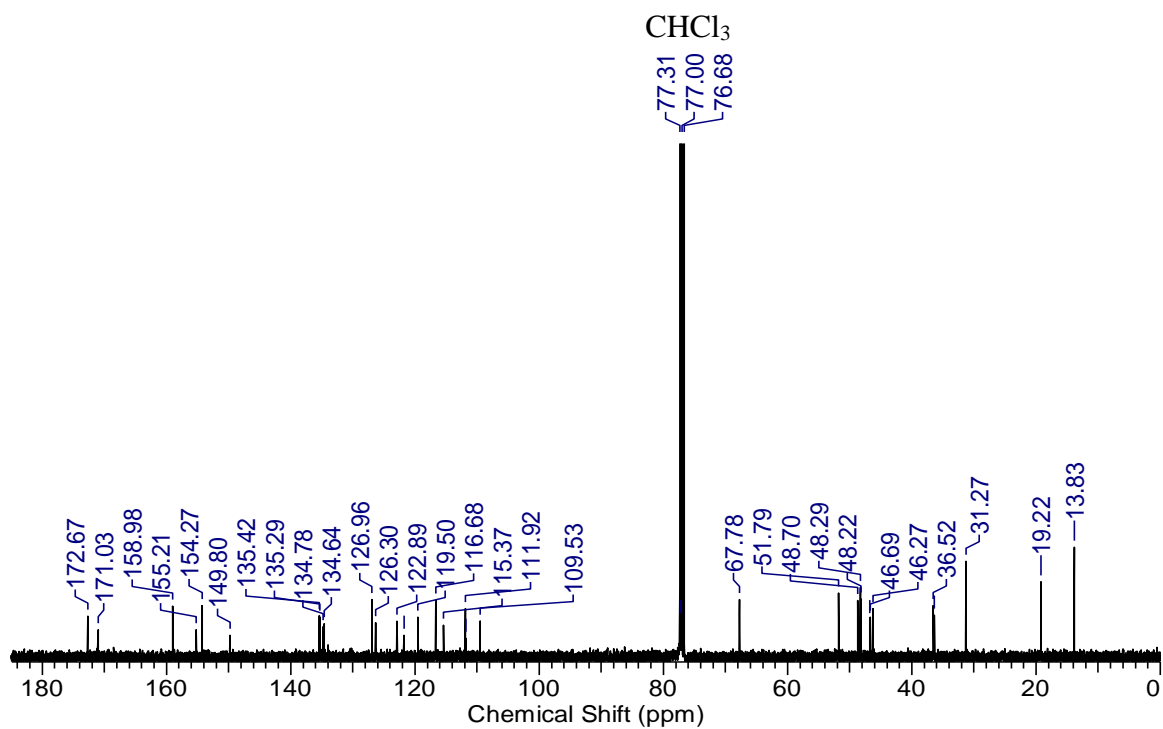


Figure A2.13. GPC of compound **2.14** in DMF.

Appendix A3 – Supporting Information for Chapter 3

Figure A3.1. ^1H NMR spectrum of compound 3.1.Figure A3.2. $^{13}\text{C}\{^1\text{H}\}$ NMR spectrum of compound 3.1.

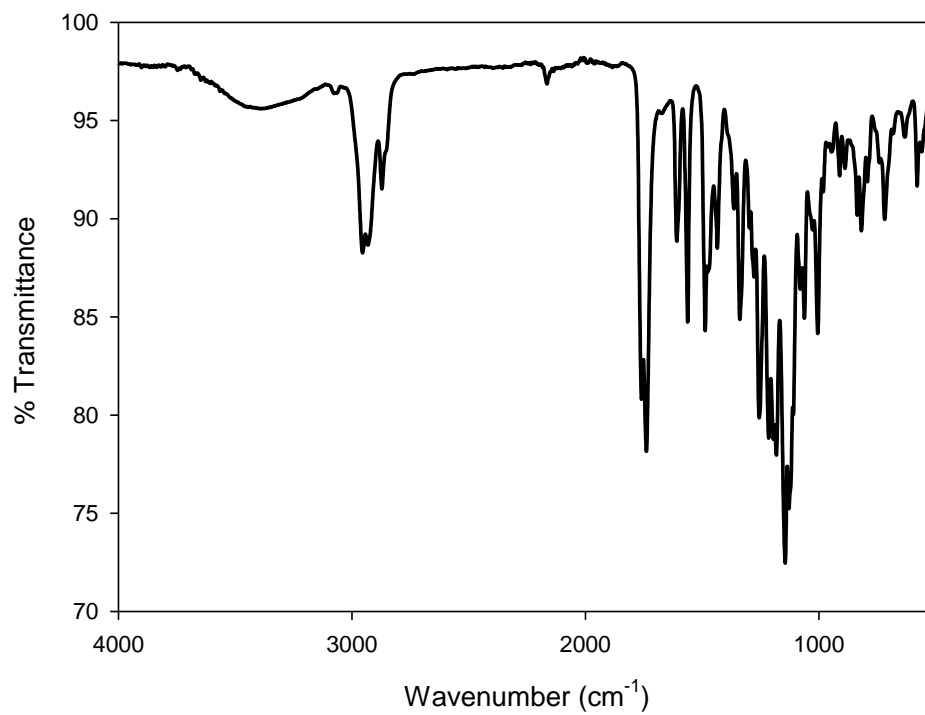


Figure A3.3. IR spectrum of compound **3.1**.

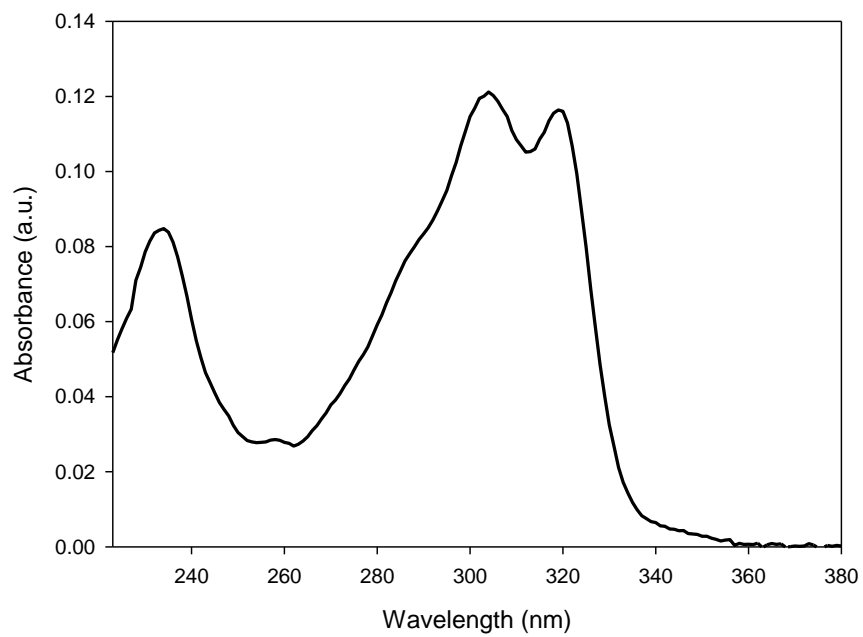


Figure A3.4. UV-Vis spectrum of compound **3.1** in CH₂Cl₂.

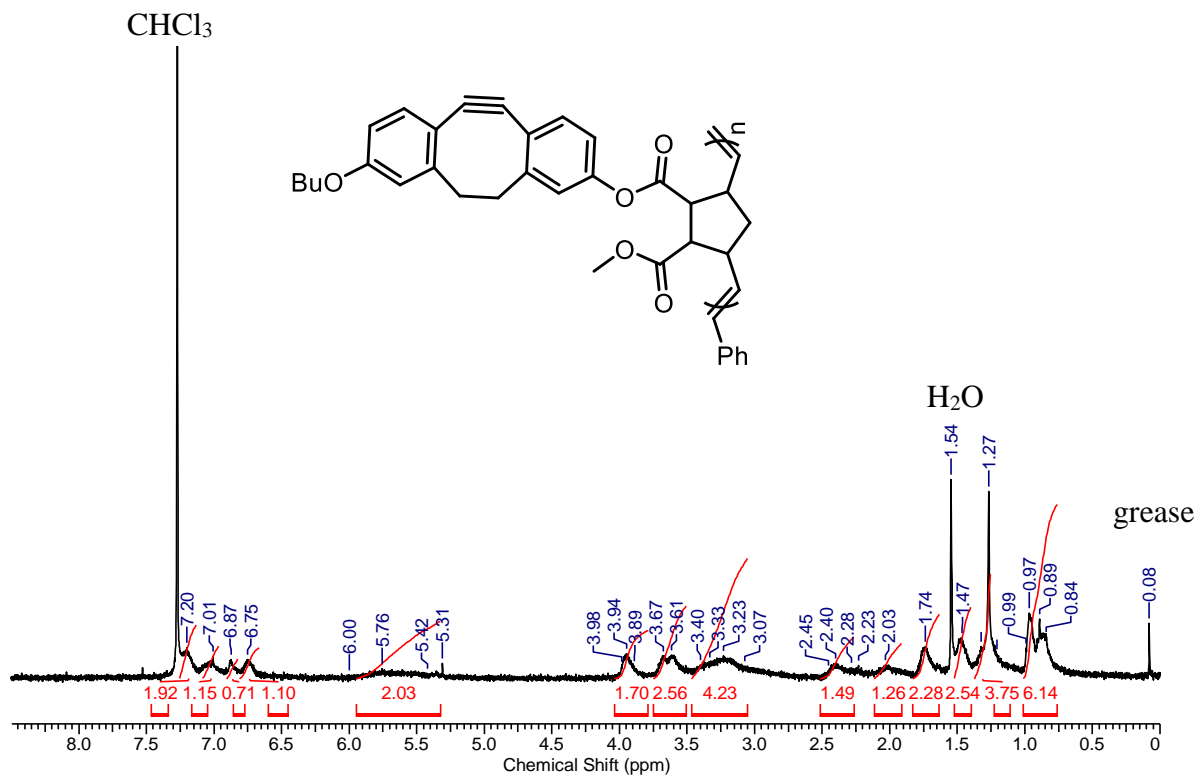


Figure A3.5. ^1H NMR spectrum of compound 3.5.

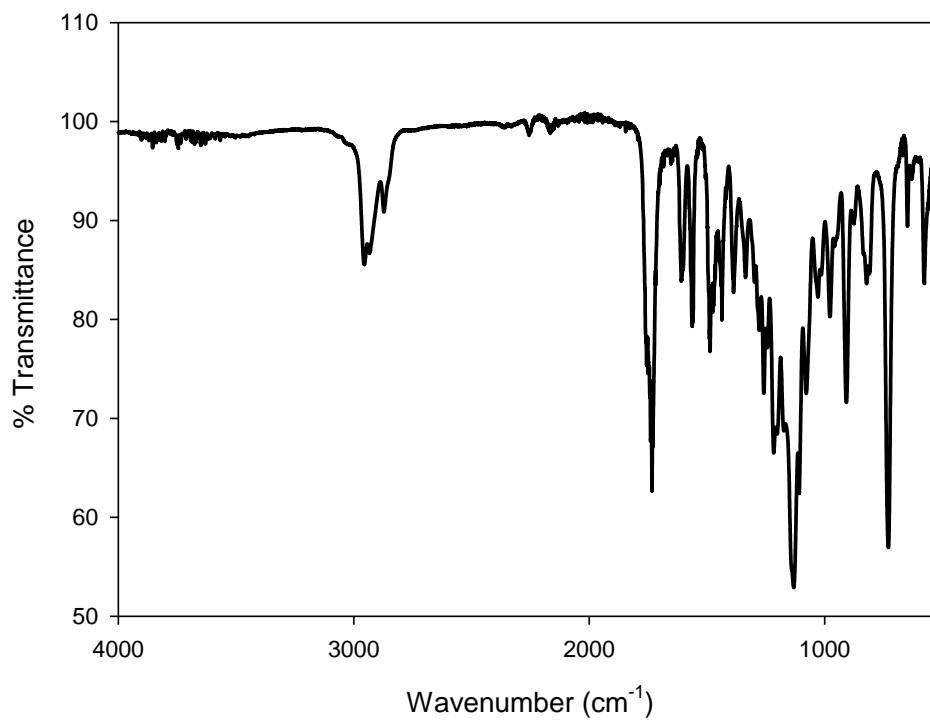


Figure A3.6. IR spectrum of compound 3.5.

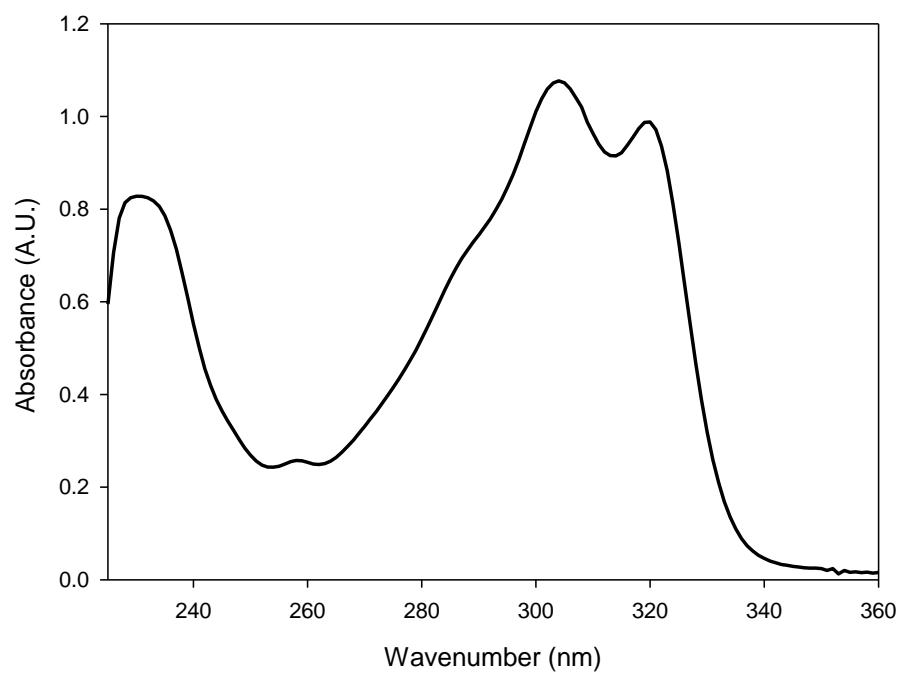


Figure A3.7. UV-Vis spectrum of compound **3.5** in CH₂Cl₂.

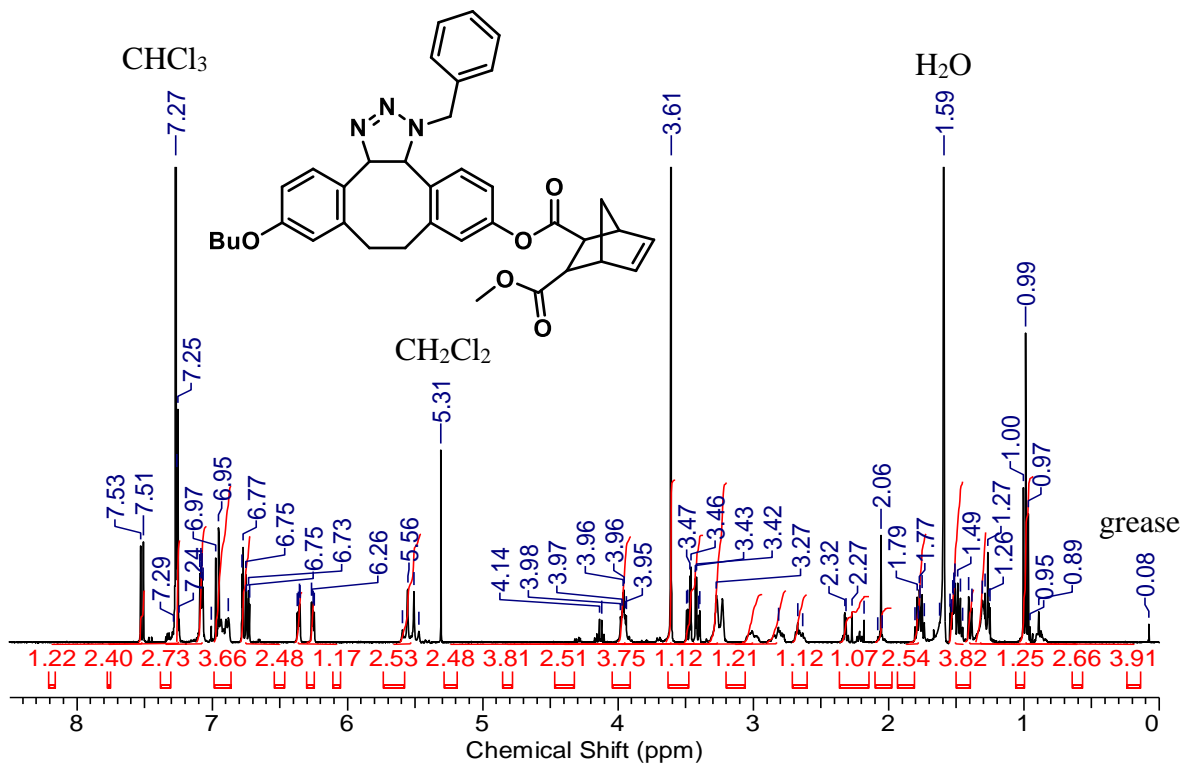


Figure A3.8. ^1H NMR spectrum of compound 3.2.

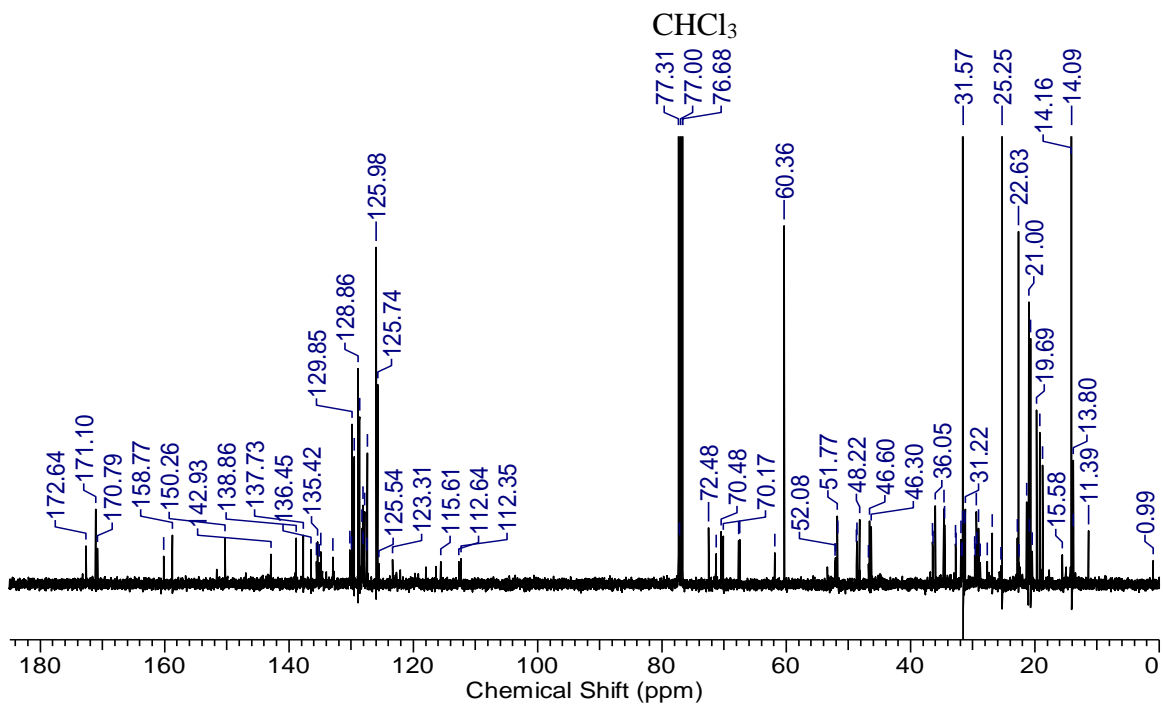


Figure A3.9. $^{13}\text{C}\{^1\text{H}\}$ NMR spectrum of compound 3.2.

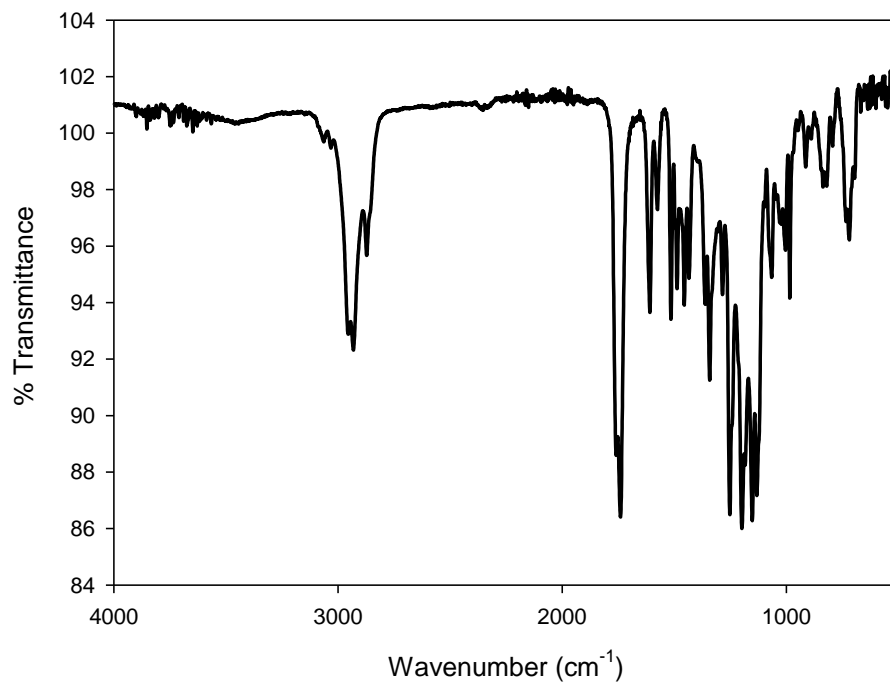


Figure A3.10. IR spectrum of compound **3.2**.

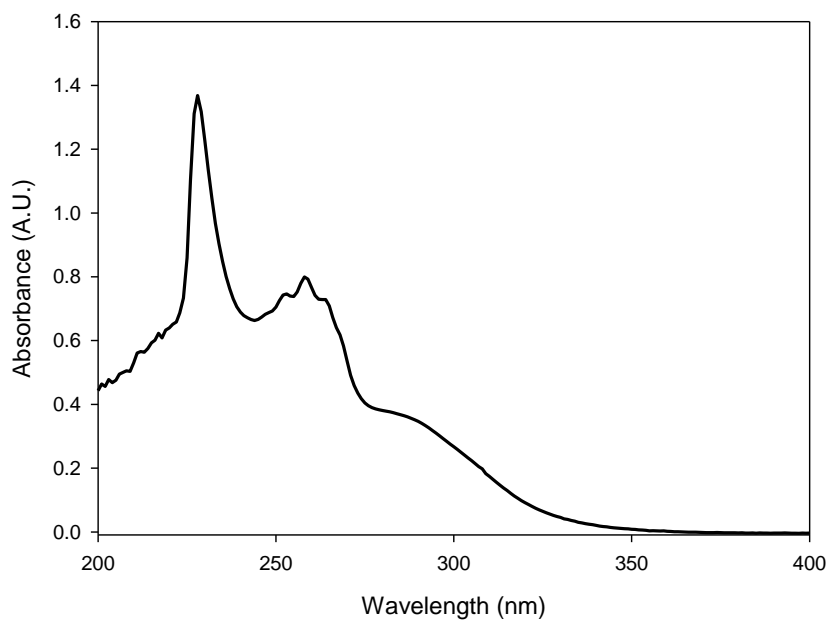


Figure A3.11. UV-Vis spectrum of compound **3.2** in CH₂Cl₂.

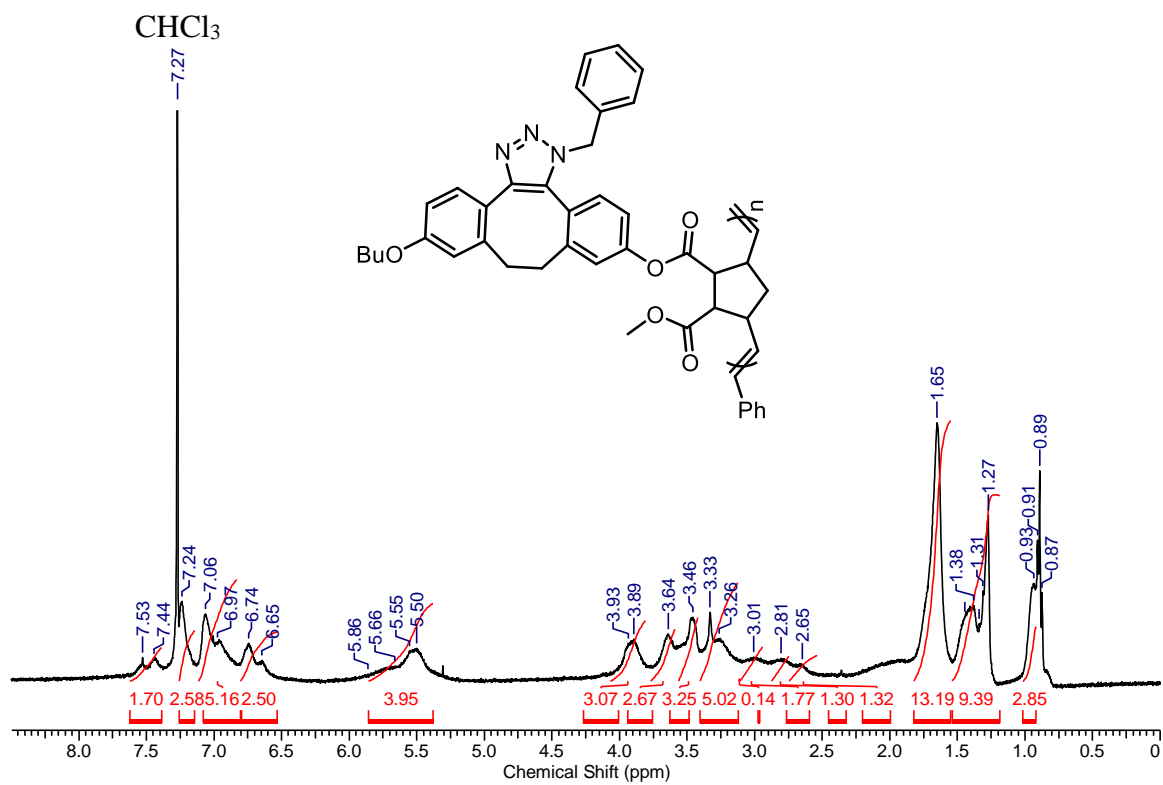


Figure A3.12. ¹H NMR spectrum of compound 3.6.

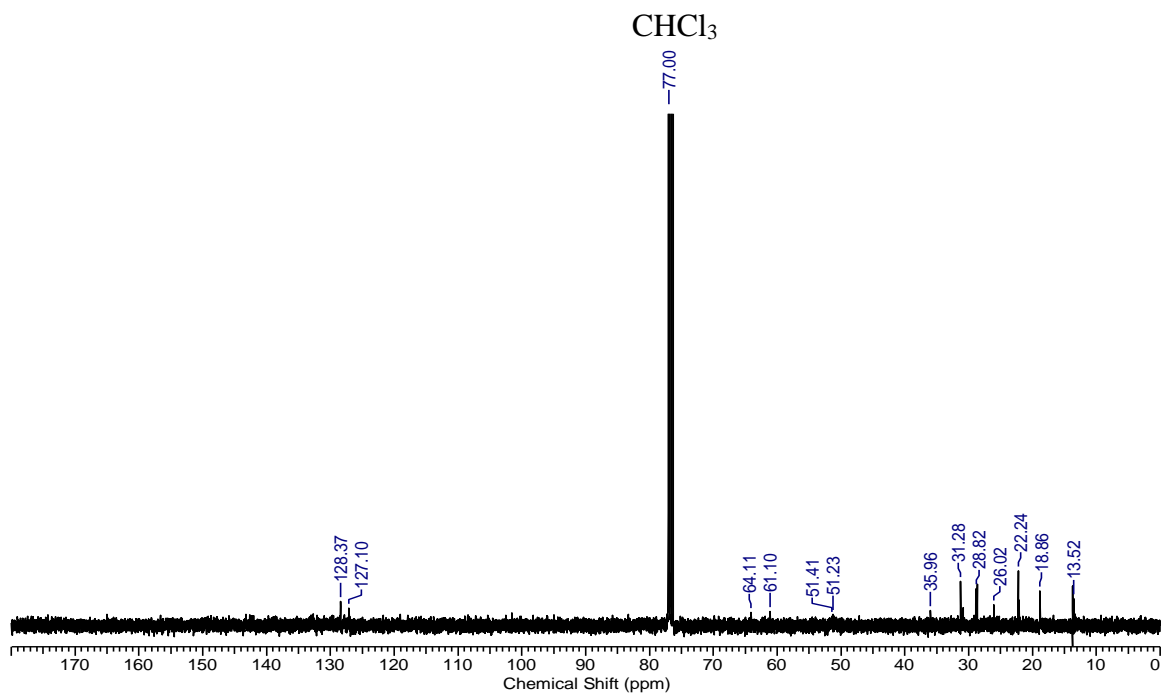


Figure A3.13. ¹³C {¹H} NMR spectrum of compound 3.6.

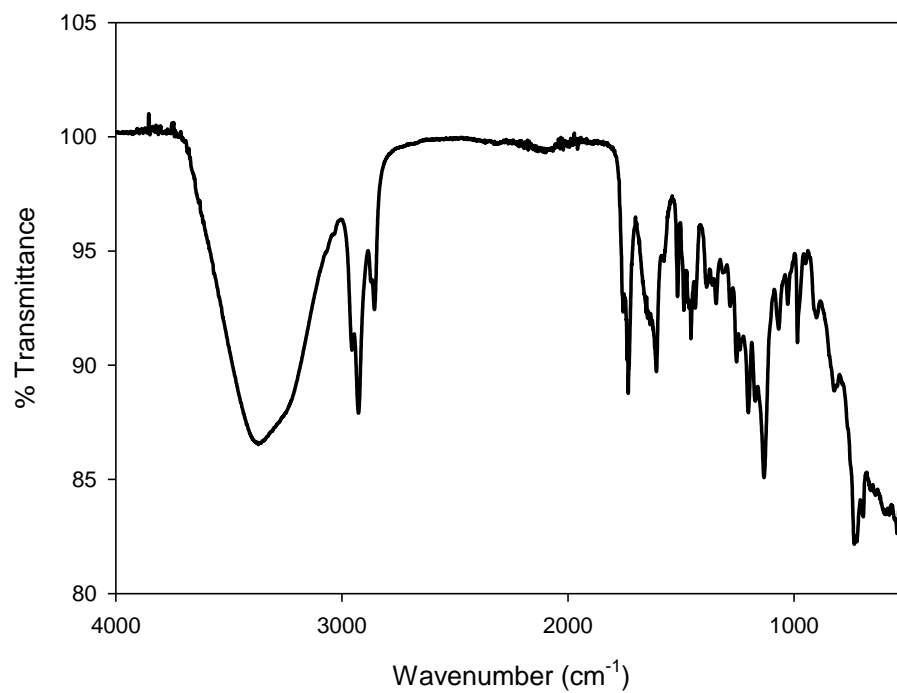


Figure A3.14. IR spectrum of compound **3.6**.

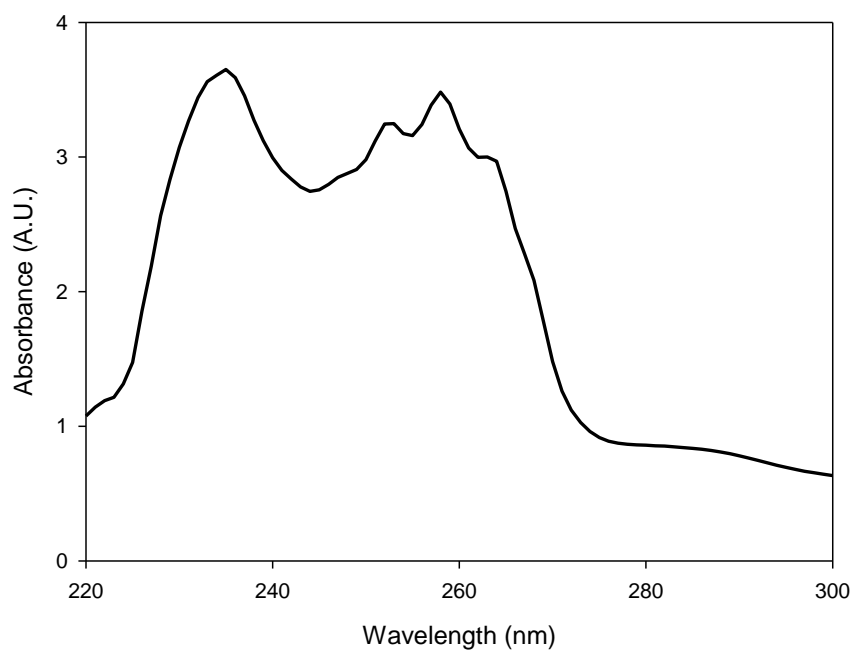


Figure A3.15. UV-Vis spectrum of compound **3.6** in CH₂Cl₂.

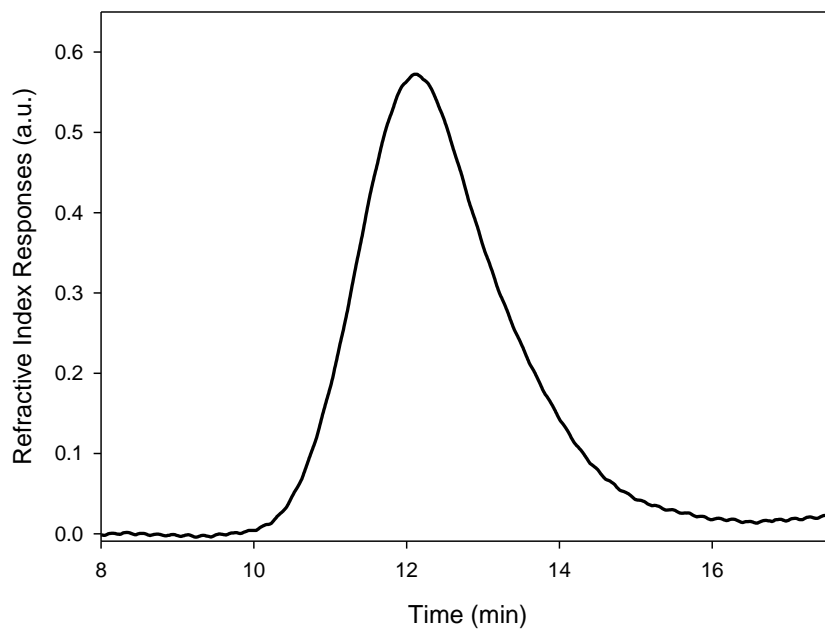


Figure A3.16. GPC of compound **3.6** in DMF.

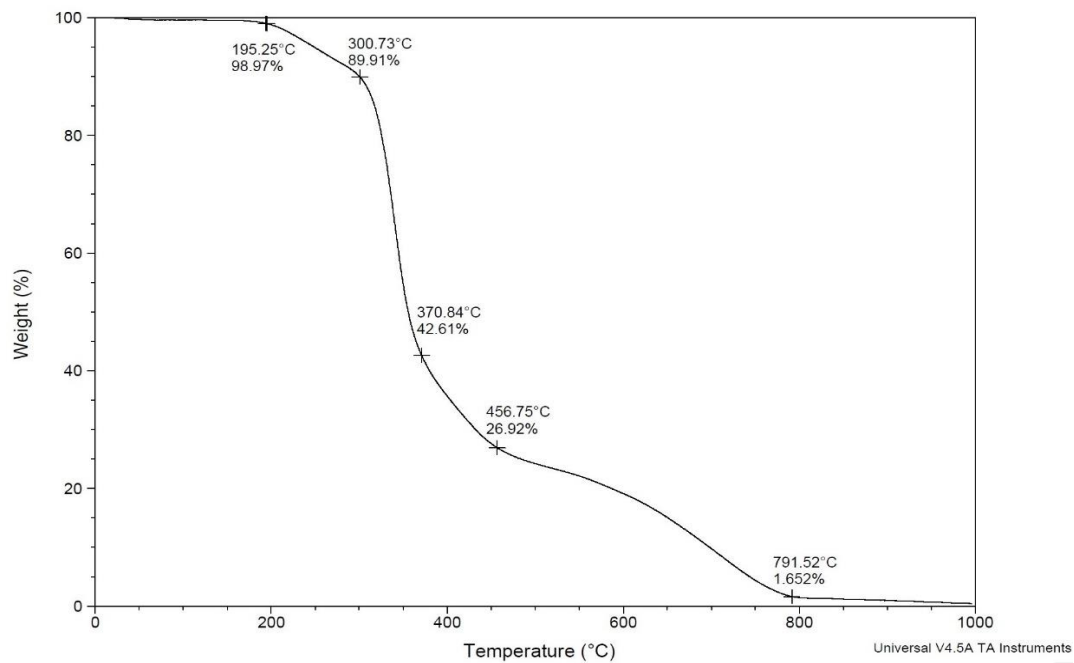


Figure A3.17. TGA of compound 3.6.

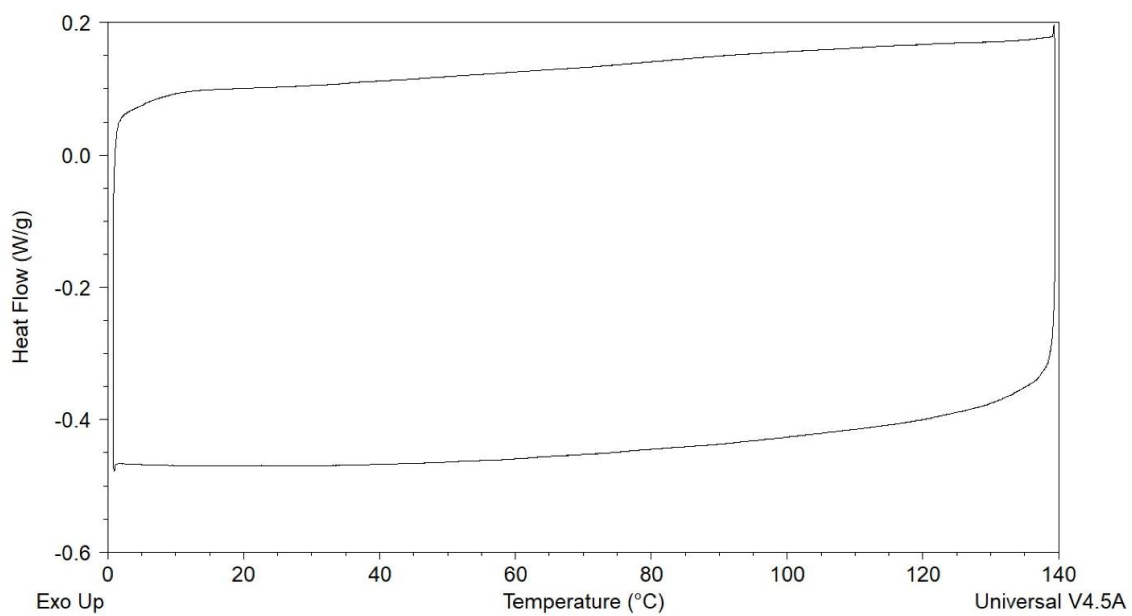


Figure A3.18. DSC of compound 3.6.

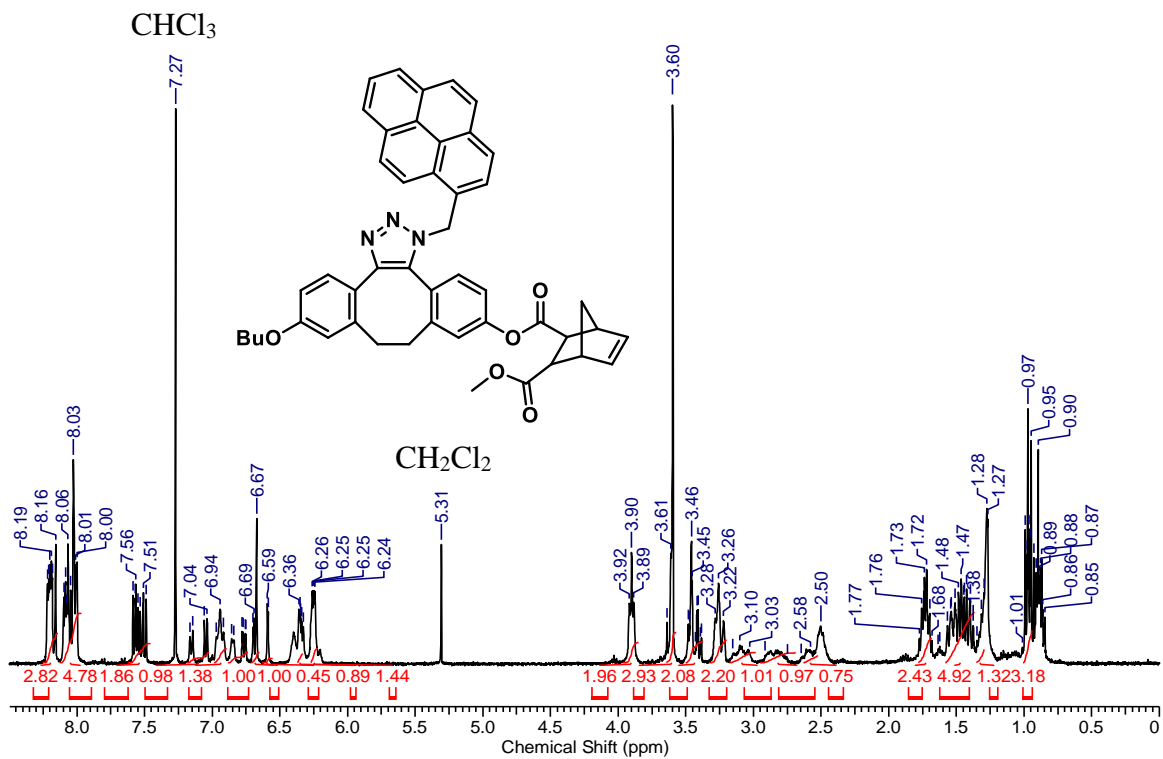


Figure A3.19. ¹H NMR spectrum of compound 3.7.

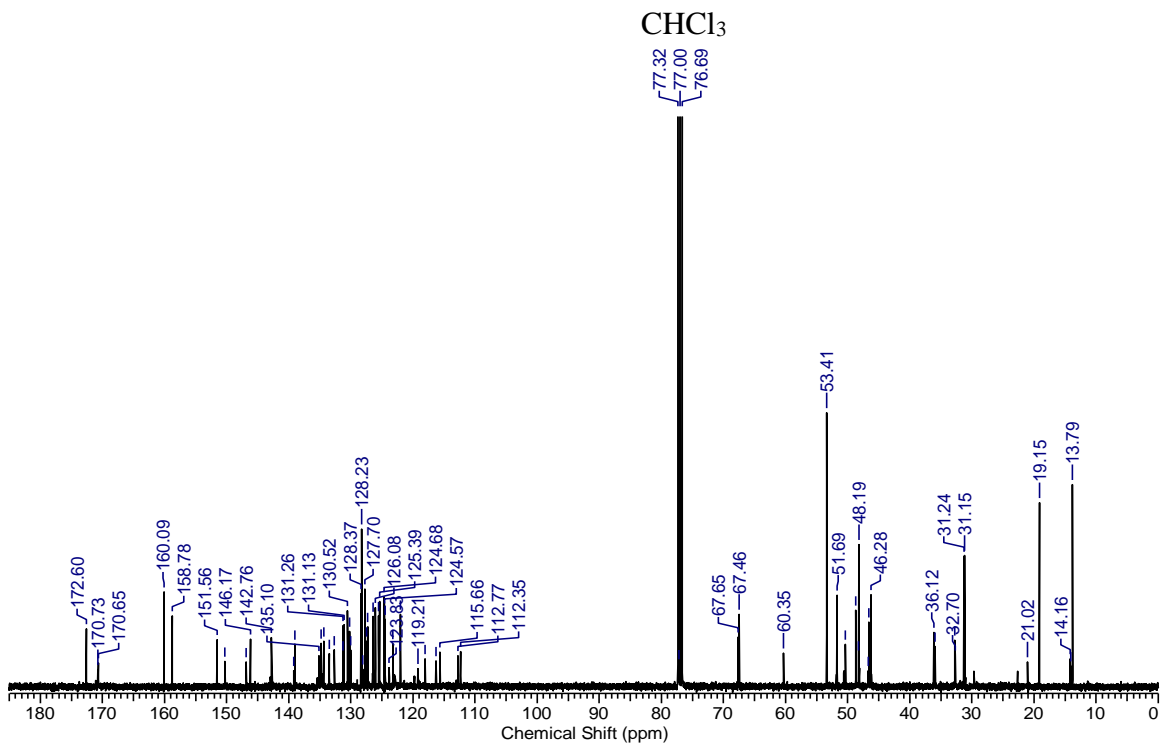


Figure A3.20. ¹³C{¹H} NMR spectrum of compound 3.7.

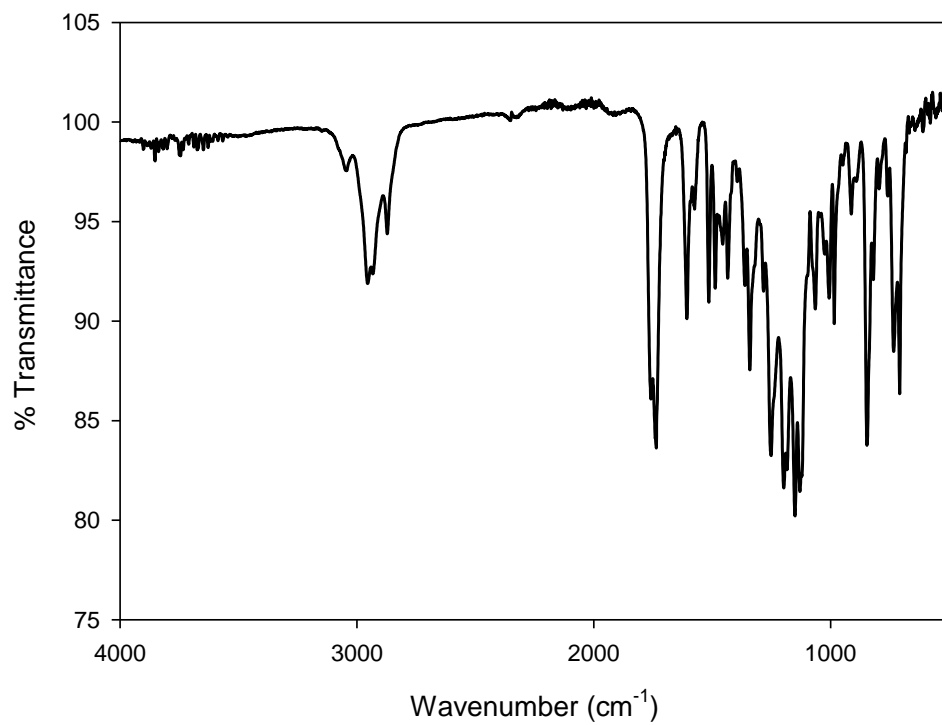


Figure A3.21. IR spectrum of compound 3.7.

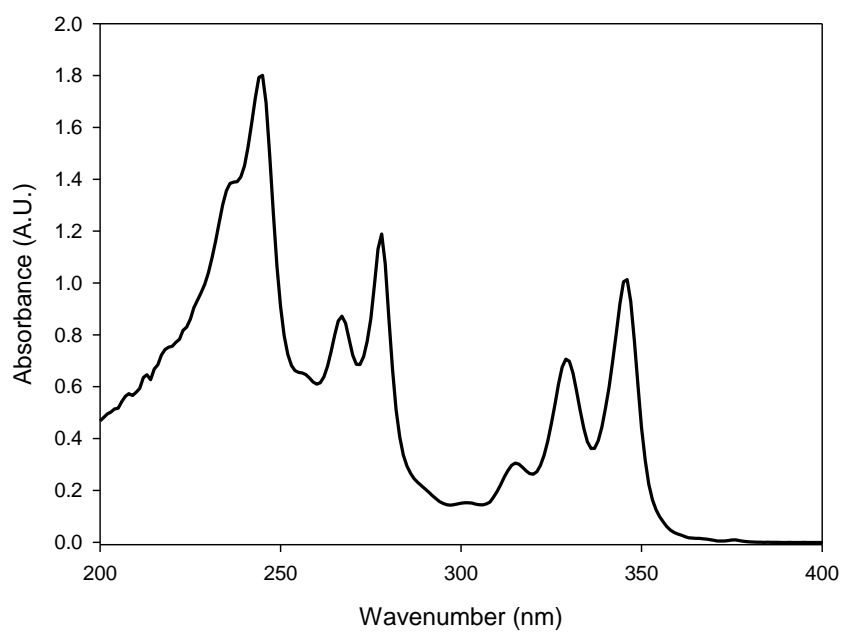


Figure A3.22. UV-Vis spectrum of compound 3.7 in CH₂Cl₂.

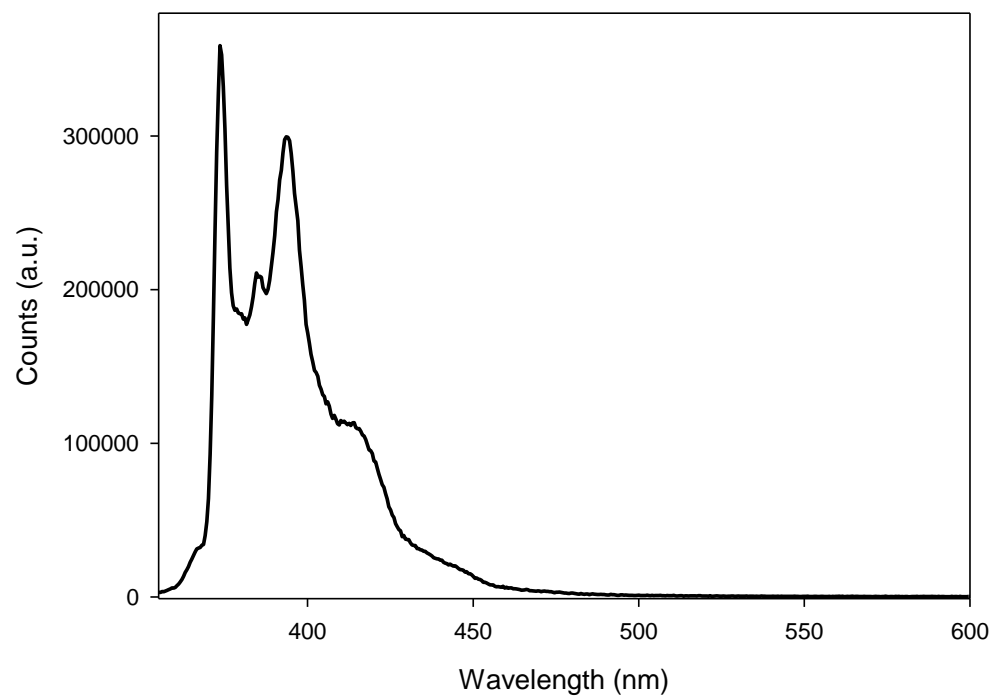


Figure A3.23. Emission spectrum of compound **3.7** recorded in degassed CH_2Cl_2 at 10^{-6} M.

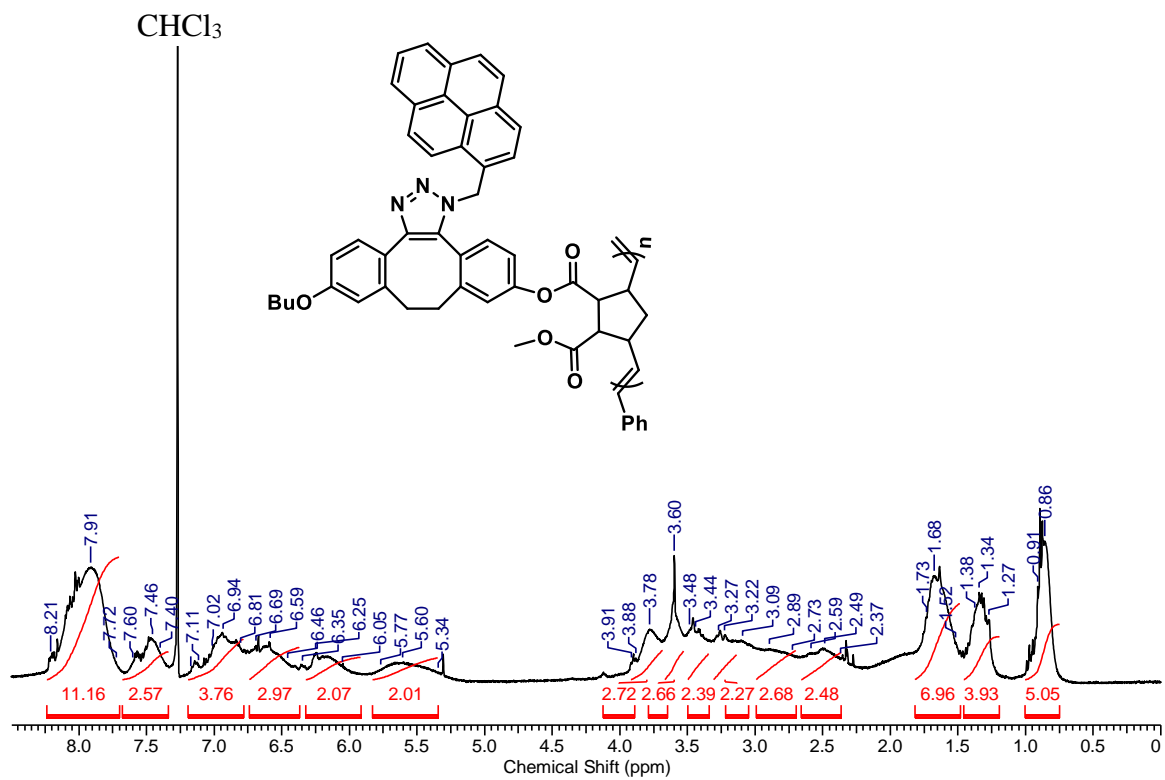


Figure A3.24. ¹H NMR spectrum of compound 3.8.

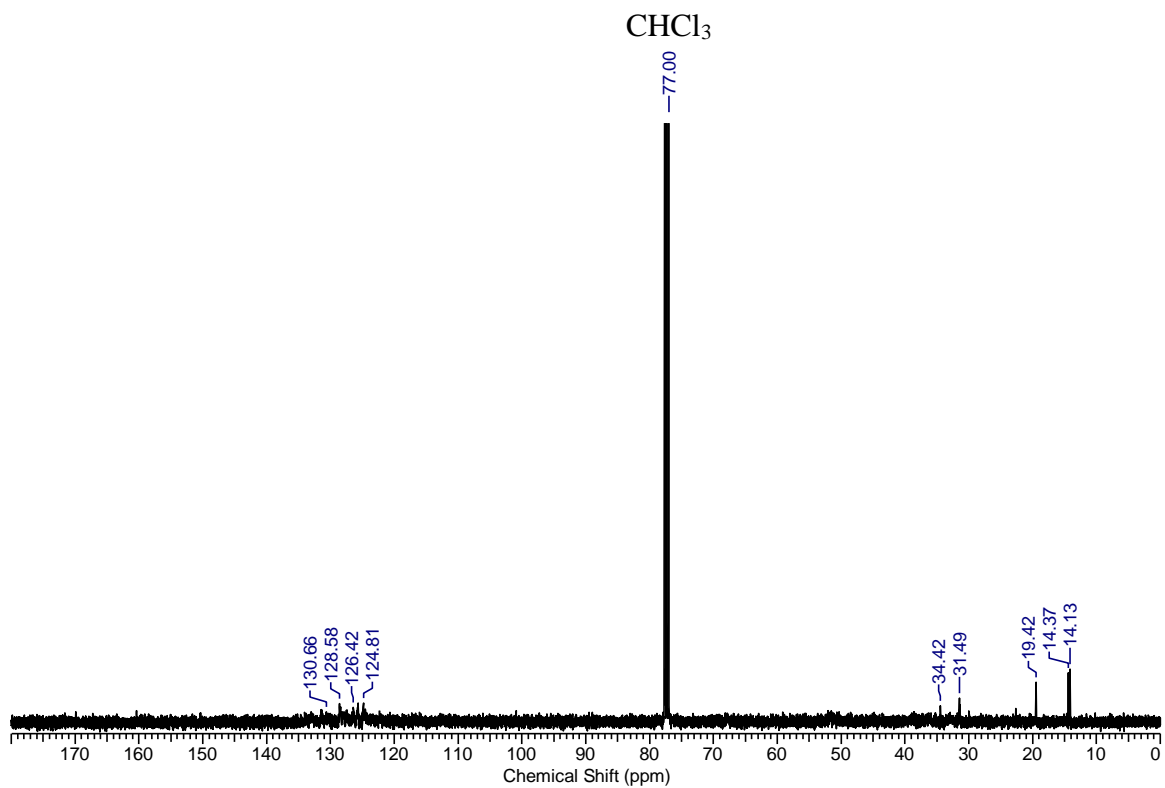


Figure A3.25. ¹³C{¹H} NMR spectrum of compound 3.8.

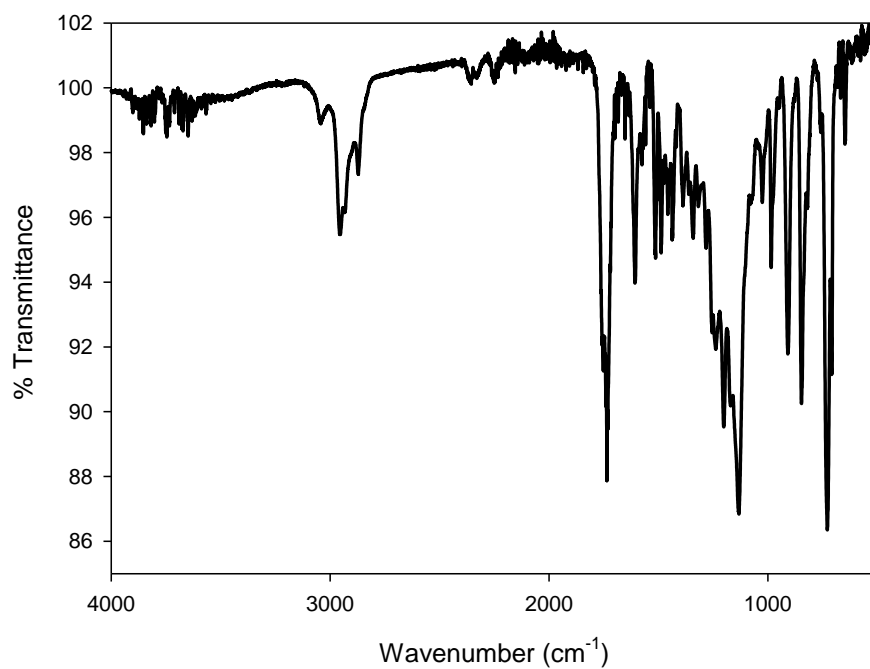


Figure A3.26. IR spectrum of compound 3.8.

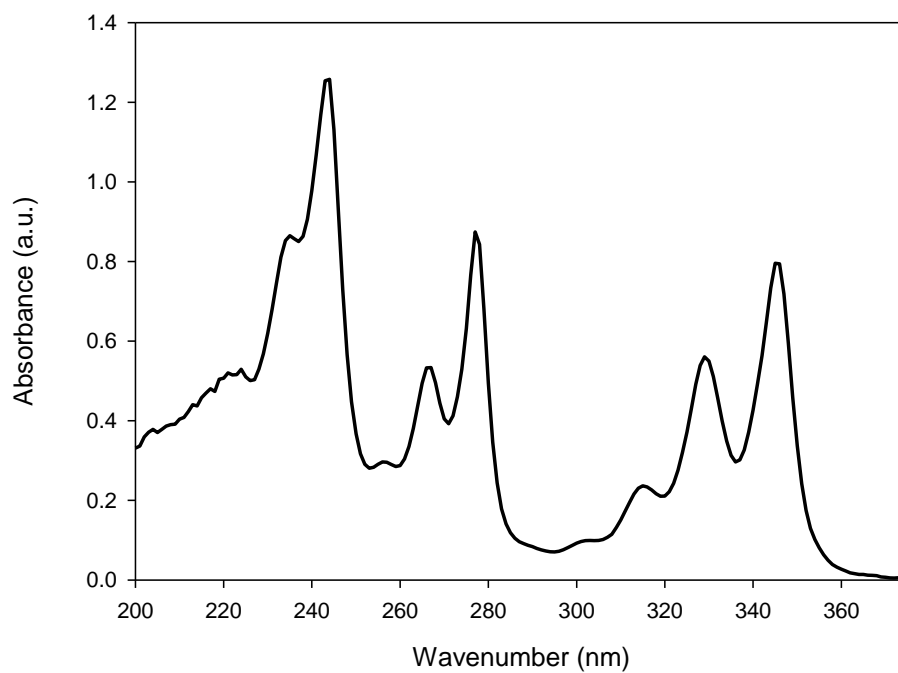


Figure A3.27. UV-Vis spectrum of compound 3.8 in CH₂Cl₂.

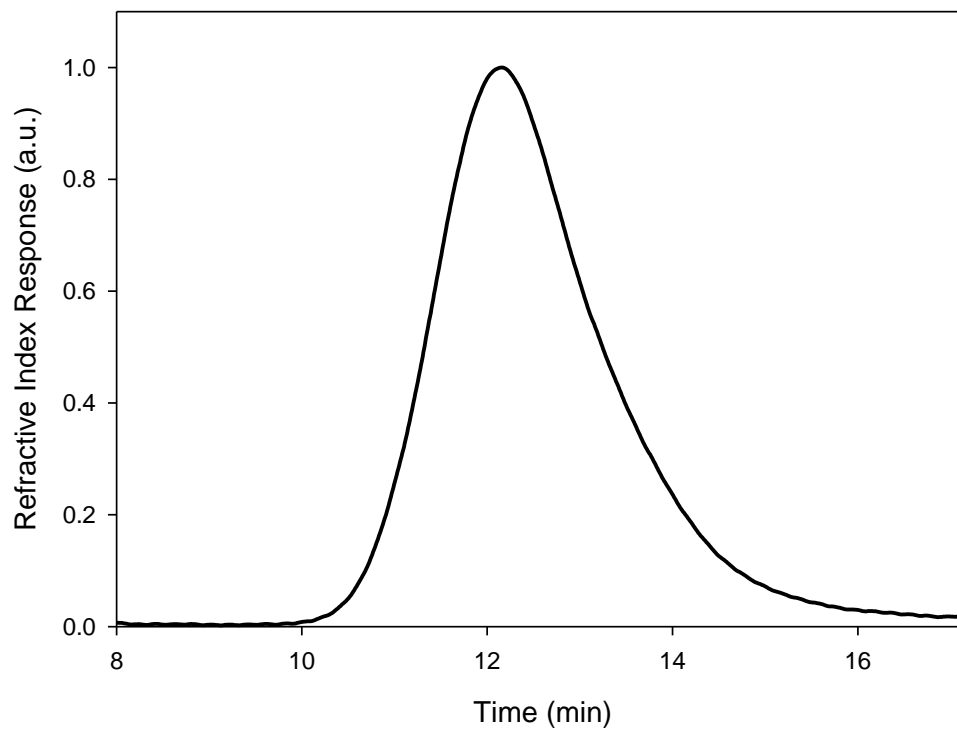


Figure A3.28. GPC of compound 3.8 in DMF.

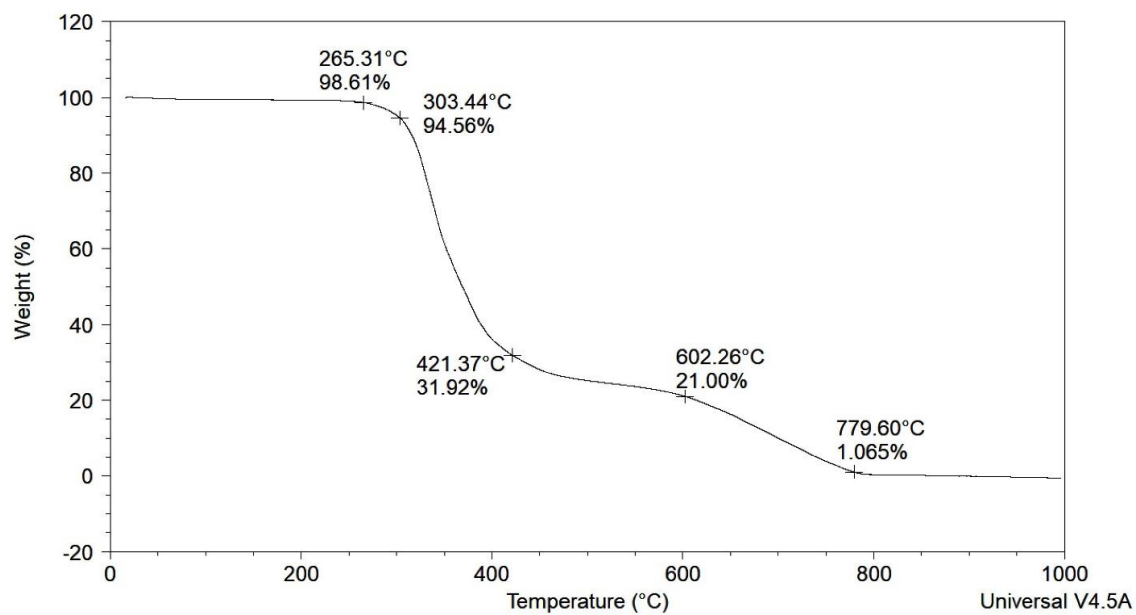


Figure A3.29. TGA of compound 3.8.

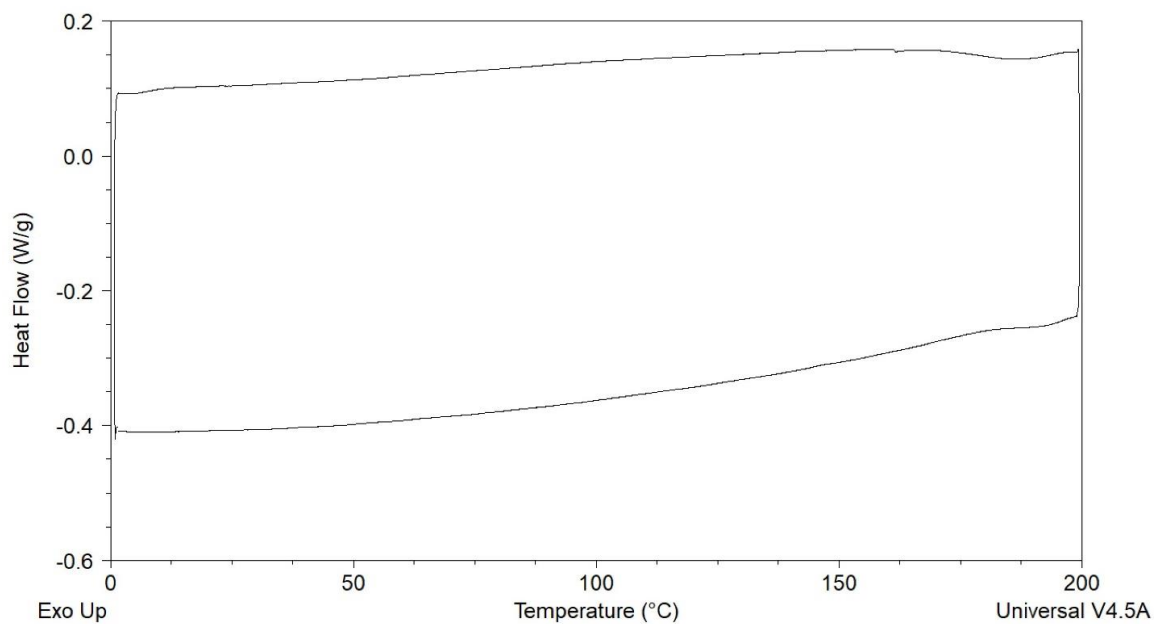


Figure A3.30. DSC of compound **3.8**.

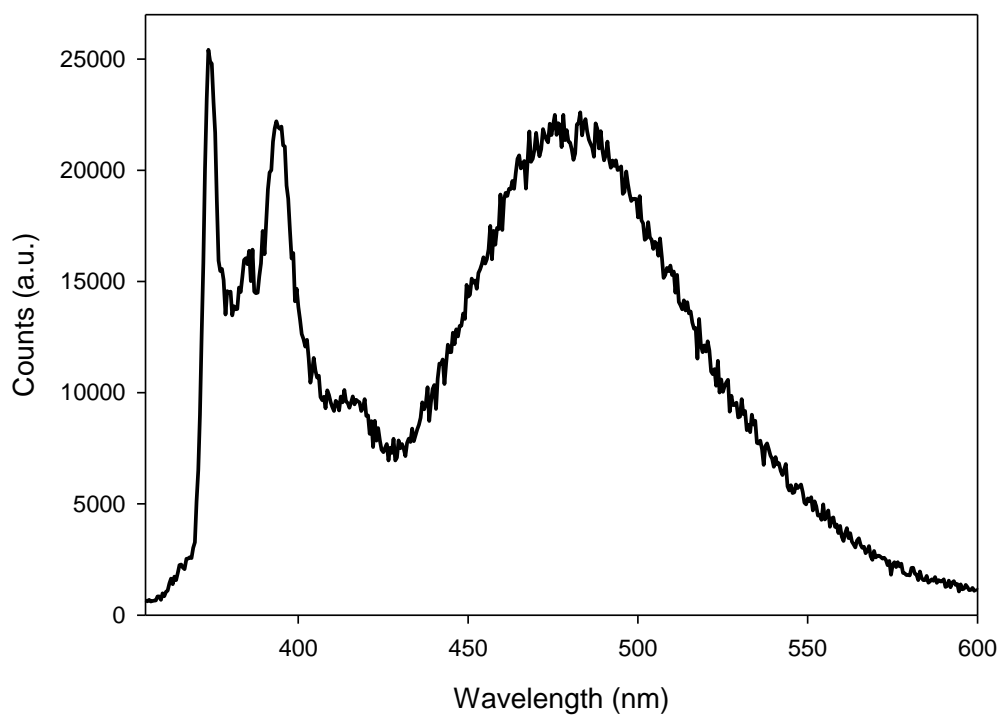


Figure A3.31. Emission spectrum of compound **3.8** recorded in degassed CH_2Cl_2 at 10^{-6} M.

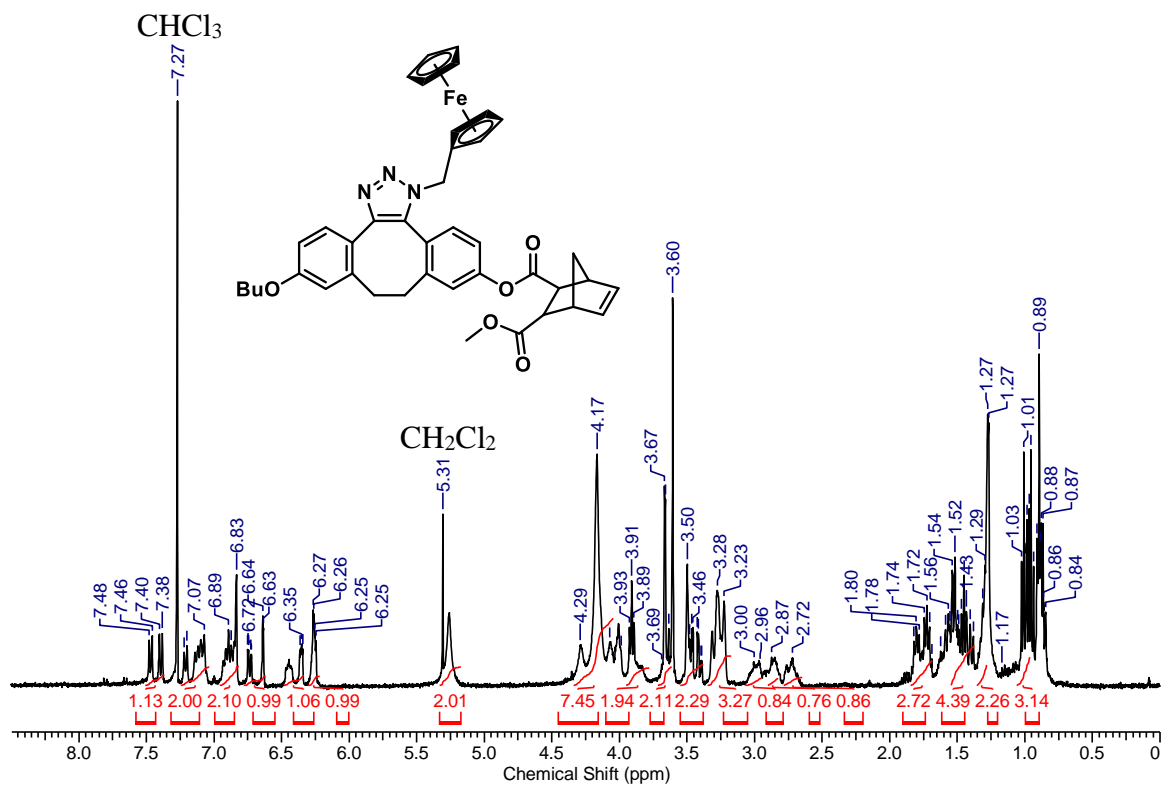


Figure A3.32. ^1H NMR spectrum of compound **3.9**.

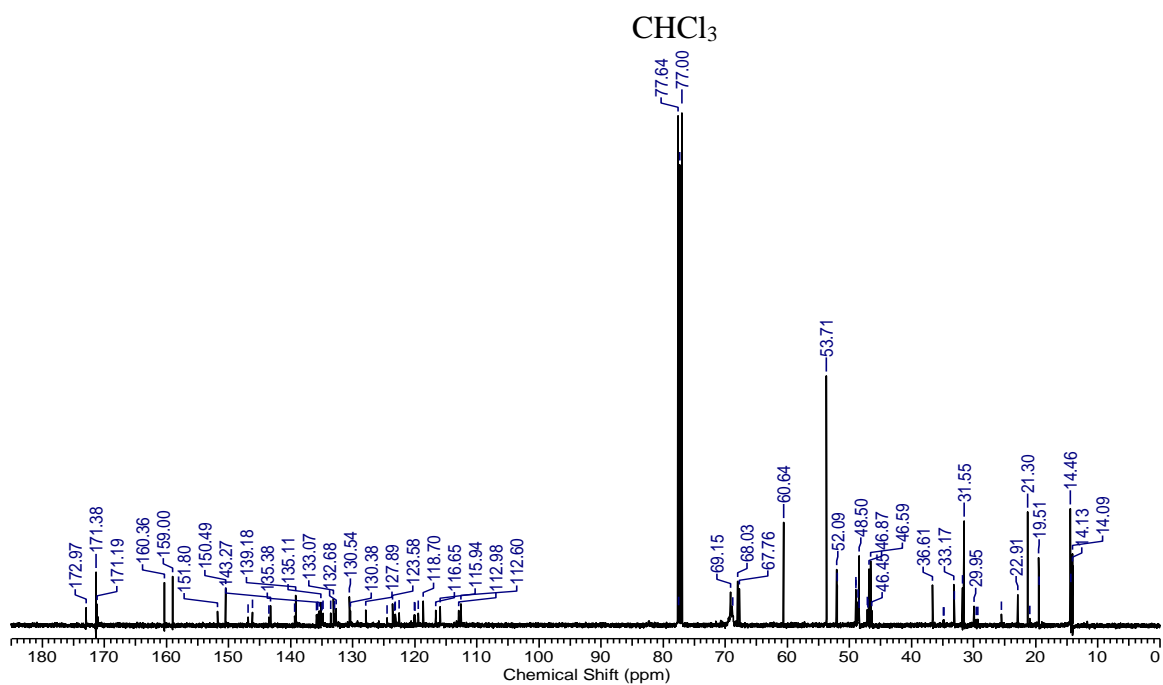


Figure A3.33. $^{13}\text{C}\{^1\text{H}\}$ NMR spectrum of compound **3.9**.

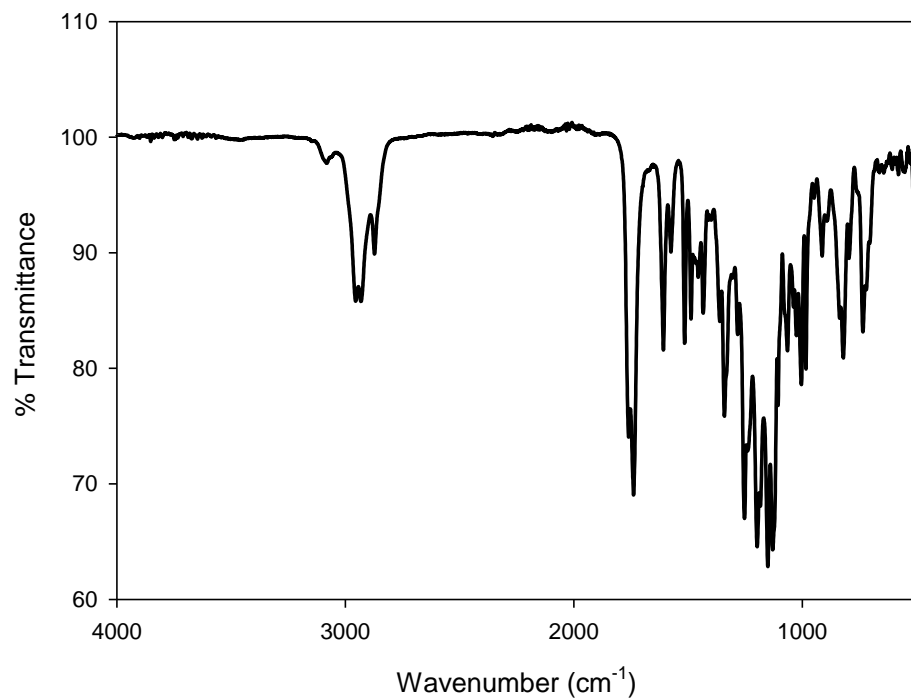


Figure A3.34. IR spectrum of compound **3.9**.

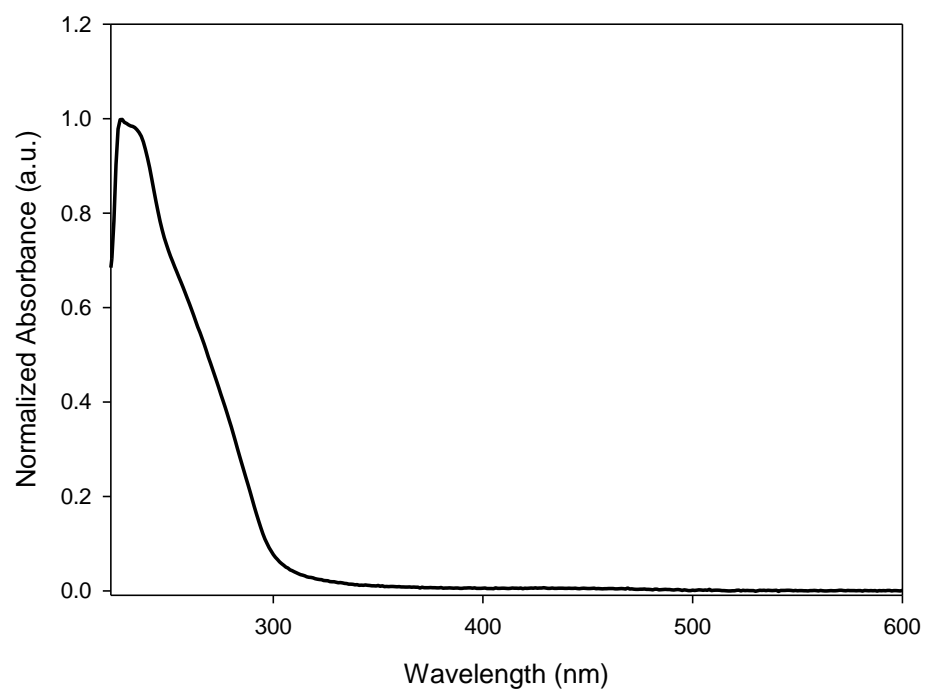


Figure A3.35. UV-Vis spectrum of compound **3.9** in CH₂Cl₂.

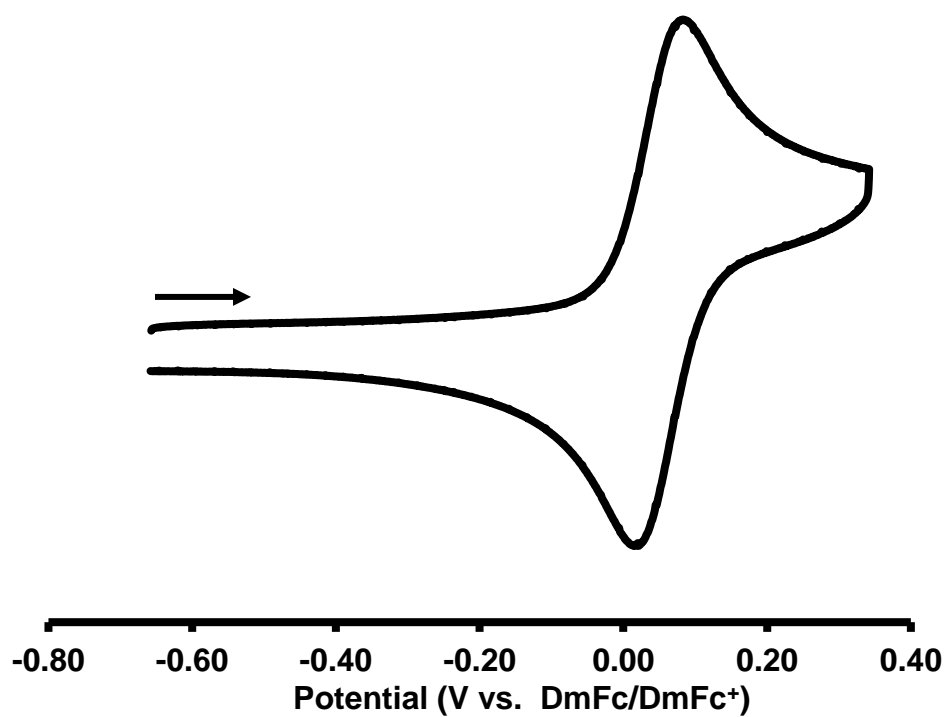


Figure A3.36. CV of compound **3.9** recorded in dry, degassed CH_2Cl_2 containing ~ 1 mM analyte and 0.1 M $[\text{nBu}_4\text{N}][\text{PF}_6]$ as a supporting electrolyte at a scan rate of 250 mV/s. The arrow indicates the scan direction.

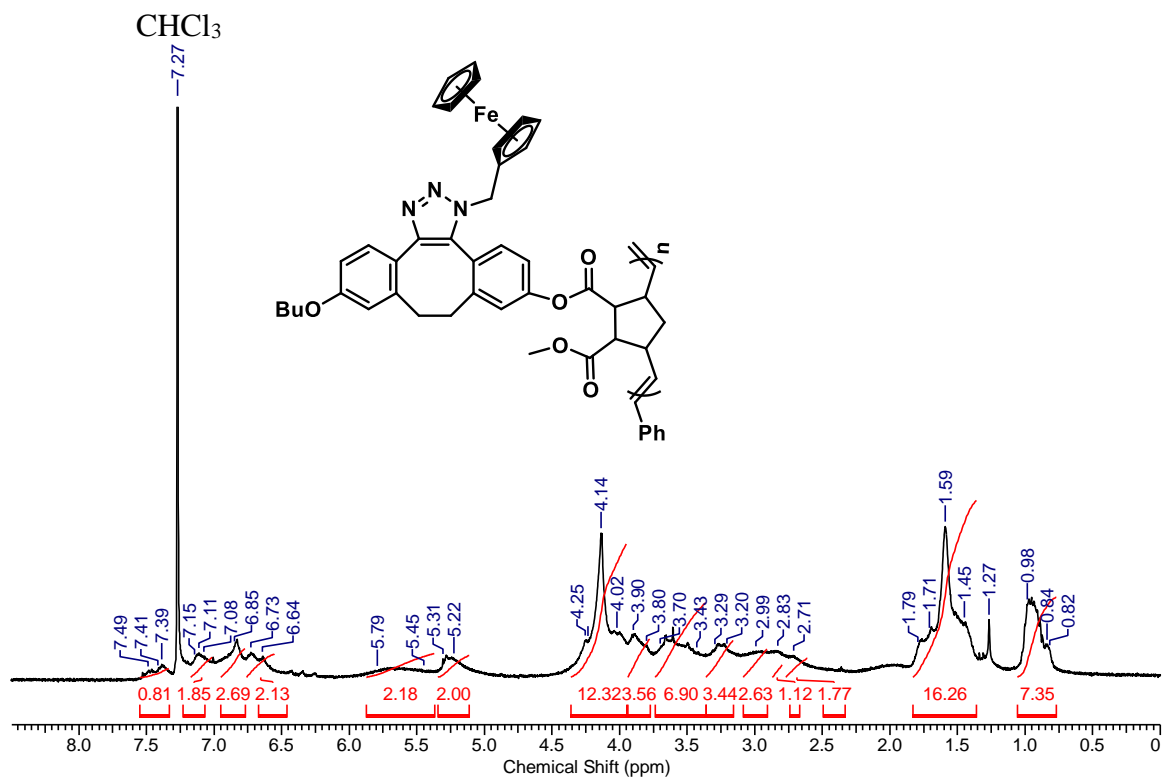


Figure A3.37. ^1H NMR spectrum of compound 3.10.

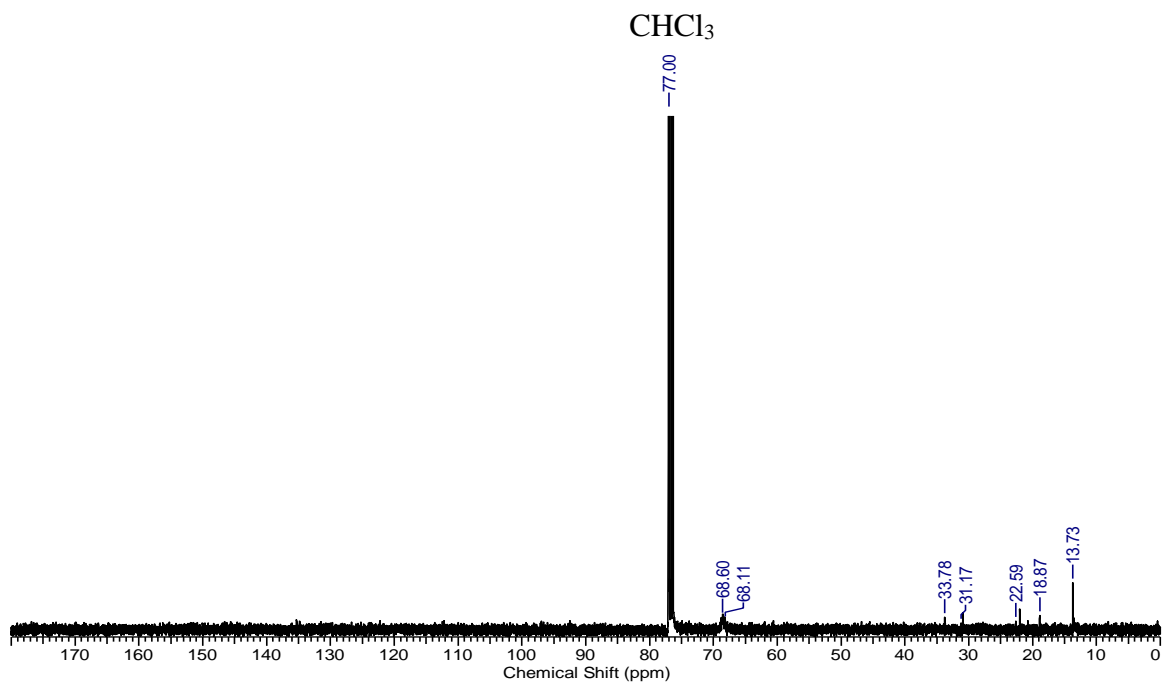


Figure A3.38. $^{13}\text{C}\{^1\text{H}\}$ NMR spectrum of compound 3.10.

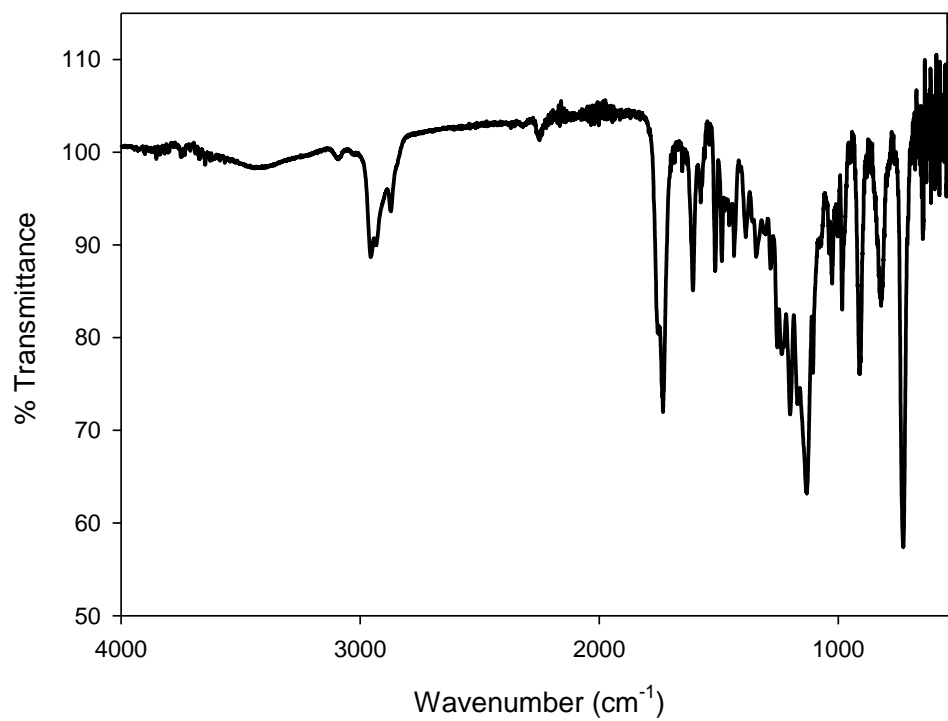


Figure A3.39. IR spectrum of compound **3.10**.

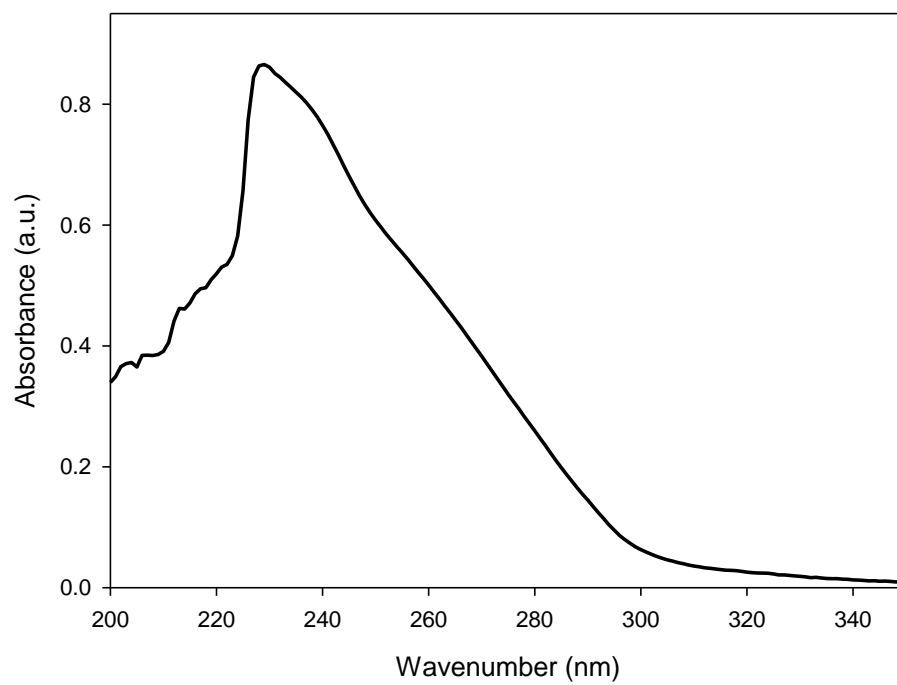


Figure A3.40. UV-Vis spectrum of compound **3.10** in CH₂Cl₂.

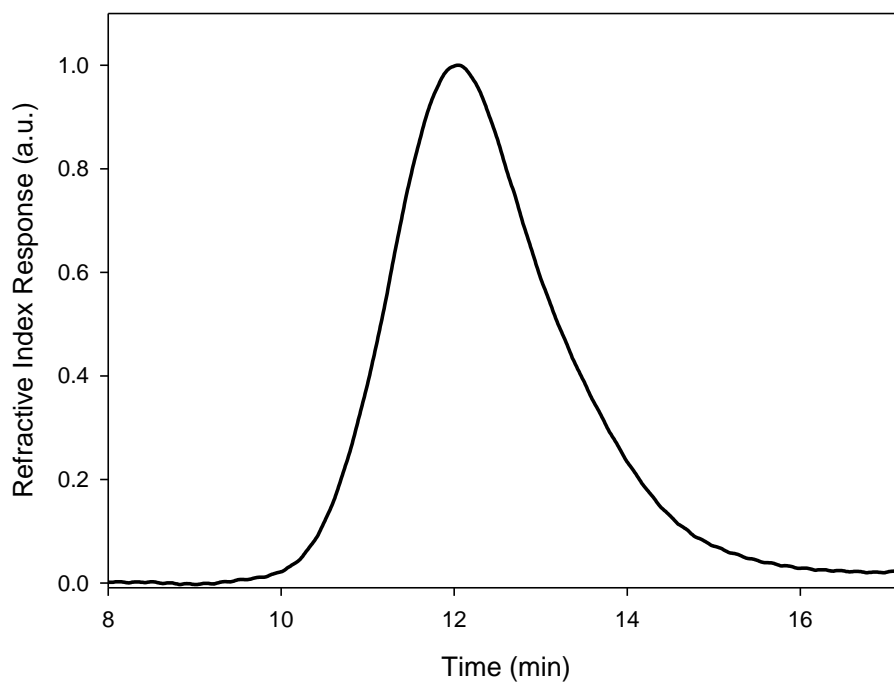


Figure A3.41. GPC of compound **3.10** in DMF.

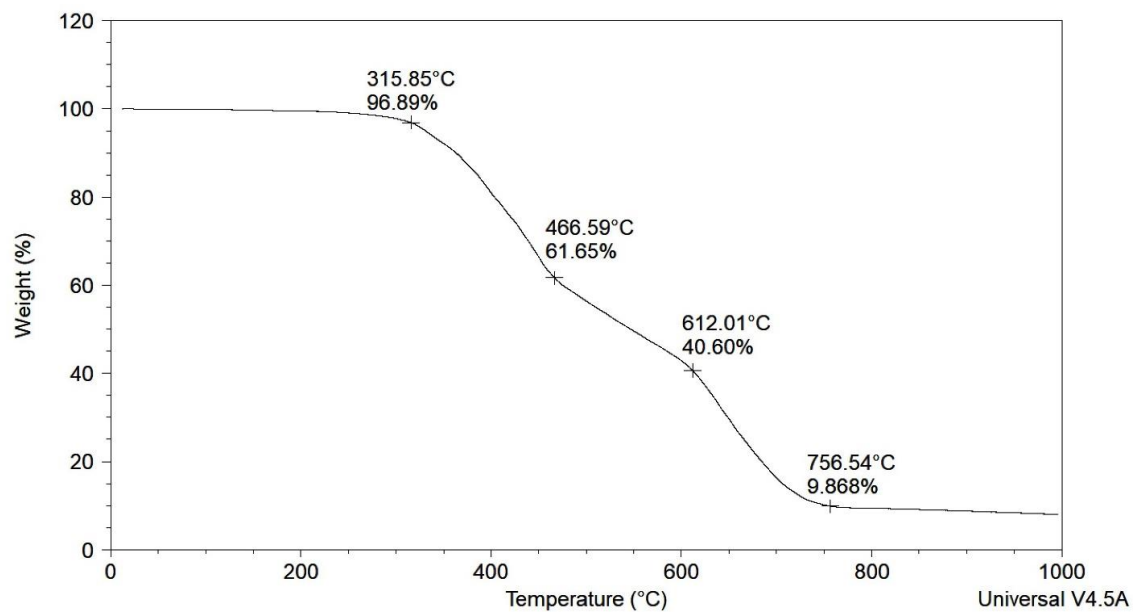


Figure A3.42. TGA of compound **3.10**.

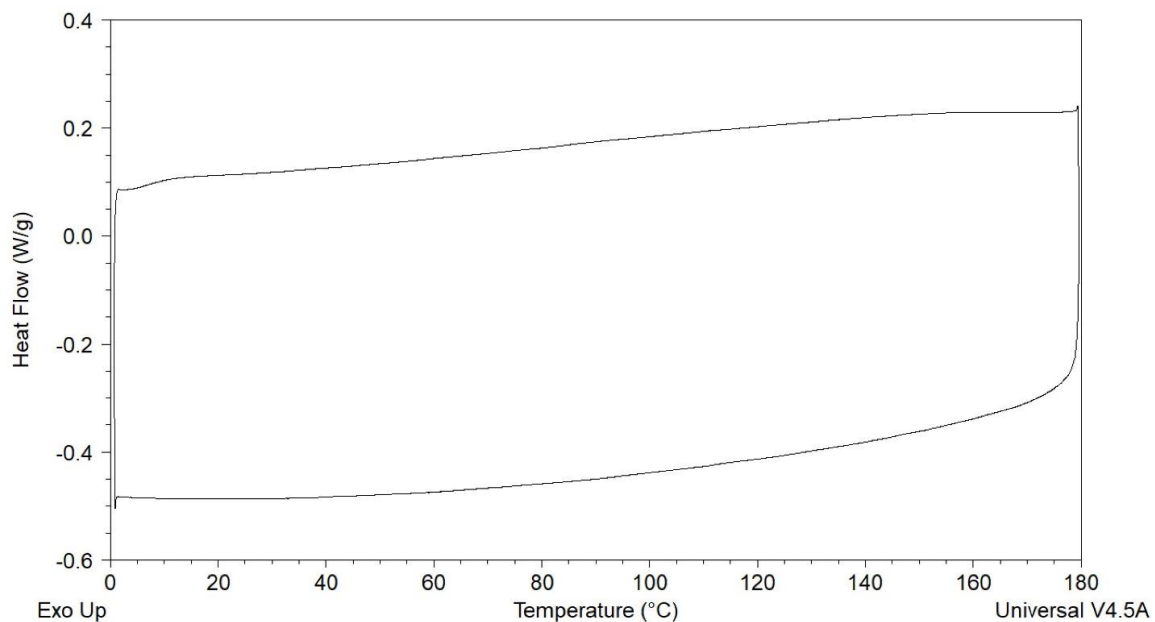


Figure A3.43. TGA of compound **3.10**.

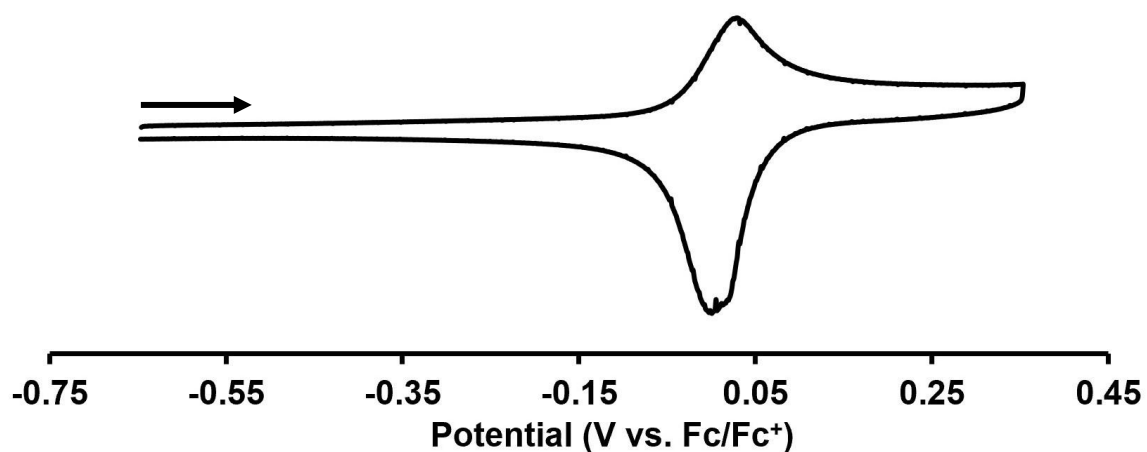


Figure A3.44. CV of compound **3.10** recorded in dry, degassed CH₂Cl₂ containing ~ 1 mM analyte and 0.1 M [nBu₄N][PF₆] as a supporting electrolyte at a scan rate of 250 mV/s. The arrow indicates the scan direction.

Curriculum Vitae

Post-Secondary Education – The University of Western Ontario

M.Sc. (Chemistry) September 2017 – Present

B.Sc. – Honours Specialization in Chemistry – Awarded April 2017

Work Experience

TA duties: 2213A, 2223B,

Research Experience

Summer Research Student – 05/2017 to 08/2017

- Supervisor: Dr. Mark Workentin

Undergraduate Research Thesis Course – 09/2016 to 04/2017

- Supervisor: Dr. Mark Workentin and Dr. Joe B. Gilroy

Presentations (Presenting author underlined)

1. Poster Presentation (1st place prize) (Canadian): Vasdev, R.; Luo, W.; Novoa, S.; Gilroy, J.B.; Workentin, M.S. Ring Opening Metathesis Polymerization of a Cyclopropanone Masked Strained Alkyne: Towards a Photo-Activated Bioorthogonal Clickable Functional Polymer, 45th Ontario-Quebec Physical Organic Minisymposium, Waterloo, ON, Canada, September 11 – September 12, 2017.
2. CSC talk (Canadian): Vasdev, R.; Luo, W.; Gilroy, J.B.; Workentin, M.S. Strategies for the Preparation of Functional Pendant Group Polymer Materials via Click Chemistry, 101 Canadian Chemistry Conference and Exhibition, Quebec City, QC, Canada, May 29 – June 5, 2019.

Course Work

- Fall 2017: Chem 9503R - NMR I (86)
Chem 9507Q - Chemical Communications (87)
- Winter 2018: Chem 9533T - Nucleic Acids Chemistry (85)
Chem 9603S – NMR II (87)
- Fall 2018: 9657 (pass)